# Assessment of Urban Landscape Structure And Dynamics using Spatial Metrics : A Case of Adama Town

Name: Efrem Guesh Kidanu

A Thesis Submitted to Program of Geomatics Engineering

School of Civil Engineering and Architecture
Office of Graduate Studies (OPS)
Adama Science and Technology University

Adama, Ethiopia
January, 2020

# Assessment of Urban Landscape Structure And Dynamics using Spatial Metrics : A Case of Adama Town


Name: Efrem Guesh Kidanu

Advisor: Daniel Alemayehu (PhD)

Co-Advisor: Dejene Tesema (Msc)


A Thesis Submitted to Program of Geomatics Engineering


School of Civil and Architecture Engineering

Office of Graduate Studies

Adama Science and Technology University


Adama, Ethiopia

January, 2020

## Approvals of the board of Examiners

We, the undersigned, members of the Board of Examiners of the final open defense by Efrem Guesh have read and evaluated his/her thesis entitled “ASSESSMENT OF URBAN LANDSCAPE STRUCTURE AND DYNAMICS USING SPATIAL METRICS: A CASE OF ADAMA TOWN” and examined the candidate. This is, therefore, to certify that the thesis has been accepted in partial fulfillment of the requirement of Degree of Masters in Geoinformatics Engineering.

| | | |
|---|---|---|
| Advisor | Signature | Date |
| Co-Advisor | Signature | Date |
| Chairperson | Signature | Date |
| Internal Examiner | Signature | Date |
| External Examiner | Signature | Date |

# Declaration

I hereby declare that this MSc Thesis is my original work and has not been presented for a degree in any other university, and all sources of material used for this thesis have been duly acknowledged. This Thesis has been submitted in Partial Fulfilment of the Requirement for Degree of Masters in Geoinformatics Engineering at Adama Science and Technology University and adopted at the university library to be made available to borrowers under rules of the Library.

Name: Efrem Guesh Kidanu

Signature: __________

This MSc Thesis has been submitted for examination with my approval as thesis advisor.

Name: Daniel Alemayehu (PH. D)

Signature: __________

## Advisor's approval sheet

To: Geomatics Engineering department

Subject: Thesis Submission

This is to certify that the thesis "ASSEEESSMENT OF URBAN LANDSCAPE STRUCTURE AND DYNAMICS USING SPATIAL METRICS: A CASE OF ADAMA TOWN" submitted in partial fulfillment of the requirements for the degree of Master's in Geoinformatics Engineering, the Graduate program of the department of Geomatics Engineering, and has been carried out by Efrem Guesh Id. No A/pr15314/10, under our supervision. Therefore, we recommend that the student has fulfilled the requirements and hence hereby he can submit the thesis to the department.

| | | |
|---|---|---|
| ___________________________ | __________ | __________ |
| Name of major Advisor | Signature | Date |
| ___________________________ | __________ | __________ |
| Name of Co-Advisor | Signature | Date |

## ACKNOWLEDGEMENT

First and foremost, I would like to thank the Almighty God for giving me the courage, patience and determination for the completion of my thesis work. Next, my heartfelt appreciation and gratitude go to my advisors Dr. Daniel Alemayehu and Mr. Dejene Tessema for their constructive comments and guidance throughout the different phases of this thesis work. I am also grateful to all the instructors and staff members of the Geomatics Engineeering Department.

Finally, my thanks go to all of my family members and my friends for their encouragement and support in all related aspects of issues for achiving my goal.

## TABLE OF CONTENTS

CONTENTS Pages

## LIST OF TABLES

## LIST OF FIGURES

## ABBREVIATIONS

| | |
|---|---|
| CSA | Central Statistical Authority |
| DEM | Digital Elevation Model |
| DN | Digital Number |
| DSS | Decision Support System |
| EMA | Ethiopian Mapping Agency |
| ENVI | Environment for Visualization of Image |
| ERDAS | Earth Resource Data Analysis System |
| ETM | Enhanced Thematic Mapper |
| GIS | Geographic Information System |
| GPS | Global Positioning System |
| Ha | Hectare |
| ITCZ | Inter Tropical Convergence Zone |
| LULC | Land Use Land Cover |
| MSS | Multi Spectral Scanner |
| NASA | National Aeronautics and Space Administration |
| NMA | National Meteorological Agency |
| RGB | Red Green Blue |
| RS | Remote Sensing |
| TM | Thematic Mapper |
| UN | United Nations |
| USGS | United States Geological Survey |
| UTM | Universal Transverse Mercator |
| WGS | World Geodetic System |

# Abstract

*Landscape structure and its dynamics is essential for the monitoring and assessment of ecological and environmental consequences of urbanization and associated urban sprawl. Unplanned urbanization and its impacts on natural resources including basic needs has necessitated the investigations of landscape dynamics, urban sprawl and spatial patterns of urbanization. Adama Town is undergoing rapid changes in the last 3 decades especially in the last decade and needs assessing the urban landscape dynamics to lessen the impacts of unplanned urbanization. So, the current study focusses on achieving the status and dynamics of land use land cover, landscape pattern, spatial pattern of urbanization and urban sprawl. The temporal and spatial dynamic pattern of urbanization and landscape pattern of the study area considering the spatio temporal data for the three decades within 2 km buffer from the Town boundary using FRAGSTATS Software environment. The time series of zonal analysis with spatial metrics were used for describing, quantifying and monitoring the spatial configuration of urbanization at landscape and class level. This study indicated a significant increase of urban built-up area during the last three decades. Landscape metrics indicates the coalescence of urban areas that occurred during the rapid urban growth from 2010 to 2019 indicating the clumped growth at the center with simple shapes and dispersed growth in the periphery (2km buffer with convoluted shapes). The results with landscape-level metrics showed that urbanization in Adama Town has resulted in the increment of the number of patches, patch density (PD) and landscape shape complexity and landscape connectivity. The general pattern of the increasingly urbanized landscape was found to be compositionally more diverse, geometrically more complex, and ecologically more fragmented. In addition, the current study confirmed that the increasing urbanization in the study area resulted in a patch density increment and shape complexity and landscape connectivity decrement. An integrated approach of remote sensing, GIS and spatial metrics with gradient and zonal analysis was applied to identify the trends of LULC changes, landscape dynamics, urban sprawl and spatial pattern of urbanization that occur as human invasions transform the landscapes. This study helps regional land use planners to identify and understand the changes in the urban Landscape structure and its dynamics.*



*Key words; land use land cover, urban landscape, urban sprawl, spatial metrics, FRAGSTAT*

CHAPTER ONE

# 1. INTRODUCTION

## 1.1 Background

Rapid urbanization is quite challenging, as the world's urban population increased from 30% in 1950 to 50% in 2000 and expected to increase to 65% by 2050 (Brockerhoff, 2000; Division, 2000). The increasing urbanization is caused by a rising population and the tendency of migration that affected the landscape ecology of an area, travel patterns, resource consumption, lack of air quality, water availability, increased travel cost, time and water discharge (Tewolde & Cabral, 2011).

The population of Ethiopia is more than 110 million and with an annual growth rate of 2.3%, the second largest population in Africa (Fenta et al., 2017). The urban population growth rate is 4.2%, which is higher compared with the average rate (2.2%) for developing countries (UN, 2014). The rapid urban population growth coupled with the economic development led to rapid and unplanned urban expansion and getting affected the landscape structure at all geographic scales (Herold et al., 2005).

Urban landscape structure is a complex variety of biological and physical patches within a matrix of infrastructure, human organizations, and social institutions characterized by composition and configuration (Tewolde & Cabral, 2011). Urban landscapes structure become increasingly disaggregated and complex with human invasion over time (McGarigal and Marks, 1994). According to Zipperer et al.(2000), understanding the change of patterns, processes and their interactions in heterogeneous Landscapes will help to accurately quantify the LULC pattern of the Landscape and its temporal dynamics.

The spatial patterns of landscape transformation through time are undoubtedly related to changes in land uses and land cover. Landscape changes are diverse which are influenced by regional policies, agriculture intensification and urbanization (Calvo-Iglesias et al, 2009). Temporal LULC analyses with spatial metrics are useful to quantify the spatial patterns of landscape dynamics and urbanization (Ramachandra et al., 2012c; Bharath et al., 2012) which helps to know the urban phenomena thorough attributes like patch shape, contagion, epoch, edge etc. This provides valuables insights to the inherent spatial structure over time with growth pattern. It can be said that the current urban landscape includes dynamic and flexible relationships layering, congestion and the landscapes interpenetration make an unbounded and undefined spatial-temporal urban continuity which is difficult to differentiate (de Wit, 2016).

Remote sensing has the potential to provide additional information about the links between land use and infrastructure change and a variety of social, economic and demographic processes. Remotely sensed images are cost-effective and are often used as input to analyze urban sprawl, whereas GIS techniques are used to extract impervious (built-up) area from the satellite images (Jat et al., 2008). GIS techniques in combination with statistical techniques are now used in many urban sprawl studies. Landscape metrics are commonly used tools in the field of landscape ecology to understand landscape characteristics (pattern and structure), changes in landscape and complexity of landscape structure. Landscapes are dynamic systems which are changing continuously due to increasing human interactions. In addition, in landscape metrics, landscape structure and changes are evaluated using different quantitative indices that are calculated on the basis of shape, size, pattern and extent of a landscape.

Adama Town has experienced rapid development especially over the past three decades following the rise to power of the current Ethiopian government in 1991. Adama Town expansion has posed serious threats to the farmers and the natural environment as the surrounding farmlands and nearby rural communities become part of the city's expansion zones. However, the extent and spatial characteristics of the Town expansion and its effect on the Landscape structure is not well-documented and the proposed plan was not confirmed with the existing land use.

This research is therefore, initiated to assess the spatio-temporal dynamics of urban Landscape structure of Adama Town for the past three decades (1990–2019) using multi-temporal Landsat data and spatial metrics. The aims of this study were fourfold: (I) to quantify LULC change; () to quantify the Landscape dynamics of the study area; (III analyze urban sprawl dynamics and (IV) to analyze the spatial pattern of urbanization.

## 1.2 Statement of the Problem

Urban growth has been the focus of contemporary researches, due to its associated social, economic and environmental (Riitters et al., 1997), especially in developing countries where unplanned growth is a common scenario (Bajracharya, 2015). Likewise, urbanization in Ethiopia, particularly in Adama city is swift (Bulti and Assefa, 2019) with remarkable unplanned developments (Bulti and Sori, 2019). Sustainable urban development planning demands scientific understanding of complex urban growth patterns and processes, which poses higher demand for information related to the dynamic process of urban expansion. In this regard, understanding urban sprawl in a space-time context and examining its multi-temporal changes become necessary (Mahamud et al., 2016). Many researchers gave different definition about urban sprawl; sometimes the definitions tend to mix characteristics with the causes, consequences, or impacts. Lack of a single clear, accurate, full and quantitative definition of urban sprawl as the major problem relating to urban sprawl (Bhatta, 2010; Inostroza et al., 2013; and Bhatta, 2010).

The presence of urban sprawl and lack of attention about it are the main challenge in Adama Town. Hence, the current study focuses on examining the urban landscape structure with special emphasis on urban sprawl and its dynamics with urban population growth for providing baseline information on future urban planning of the Town.

## 1.3 Research Question

1. What is the dynamics of urban landscape structure in Adama Town between 1990 and 2019?
2. What is urban sprawl dynamics of Adama Town from 1990 to 2019?
3. Are there significant differences in sprawling pattern in different directions across the Town?

## 1.4 Objective

### 1.4.1 General Objective

The objective of this study is to assess the urban landscape structure and dynamics using spatial metrics for Adama Town.

### 1.4.2 Specific Objective

- To analyze the land use/ land cover and landscape dynamics of Adama Town
- To analyze the dynamics of urban sprawl
- To detect the spatial pattern of urbanization across the Town between 1990 and 2019

## 1.5 Significance of Study

1 For Urban planners; the results of this study are useful in feature planning.

2. For Researchers: in similar field of study, the present study can serve as reference material.

3. For Town administrations: this study can provide a very important information to manage the existing urban sprawl problems and take appropriate take appropriate management measures.

## 1.6 Scope of Study

The study is delimited to cover Adama Town due to the availability of Spatio-temporal imagery from 1990 to 2019 that can be studied using spatial metrics.

CHAPTER TWO

# 2. LITERATURE REVIEW

## 2.1. Land Use and Land Cover Dynamics

Land Use and Land Cover Change detection provides a proper background for environmental planning and urban management analysis. However, detecting land use/cover isn't easy. Comparative analysis using classification operation enables us to detect the trend of land use/ land cover changes in different times (Inostroza et al., 2013)

### 2.2.1 Pre-processing

Preprocessing function involves operations that are normally required before data analysis and extraction of data. These are grouped into radiometric and geometric corrections. Radiometric correction includes correcting the data for sensor irregularities and unwanted sensor or atmospheric noise (Dadras et al., 2014) while geometric correction algorithms conduct the correction sequentially and use the ground control points in higher-level processing.

### 2.2.2 Image Classification

Image classification refers to the task of extracting information that is processed in computer vision that can be digitally identified and classify an image according to its visual content.

According to Duda et al. (2011), supervised classification is an important and human-based classification for multi-temporal images classification and detects class information in the satellite images with similar pixels are used as 'training samples' in Maximum Likelihood algorithm.

### 2.2.3 Post Classification Techniques

One of the most important applications of spatiotemporal data is to detect the changes for the same object between different seasons and different years. The process by which variation in an object at different times or changes that occur in LULC are checked and identified over a certain number of years is known as change detection (Duda et al., 2001; Tewolde and Cabral, 2011). The post-classification technique is one of the best types of change detection which involves the independent production and subsequent comparison of spectral classifications for the same area at two different time periods.

Tewolde and Cabral. (2011), detected LULC changes using spatiotemporal data. In other words, the post-classification-comparison technique, using independent thematic classifications of images for two different time periods, can generate different maps with 'from–to' change information that is easy to interpret.

### 2.2.4 Accuracy Assessment

The accuracy assessment aims to determine the degree of the classified data. Accuracy assessment methods evaluate the performance of classifiers (Huang et al., 2010). This is done through a comparison of kappa coefficients and the computation of overall accuracy assessment through a confusion matrix. Accuracy assessment and Kappa coefficient are common measurements used to determine the efficiency of the classification of images (Belay et al., 2019). A couple of methods that quantitatively evaluate separability of training areas are in use.  The more important in the sampling of test areas representative, the better uniform and consistent Land Cover and Land Use were selected in the neighbourhoods of training sites. Conducting preprocessing (Radiometric and geometric correction) using supervised classification, a study from China reported an overall accuracy assessment of 88.10% and 0.85 kappa statistics during 1990 and overall accuracy of 86.63% and 0.846 kappa statistics during 2015 (Ramachandra et al., 2012). Similarly, Rai et al. (2018) analyzed land use and land cover changes using remote sensing and GIS in North-East Turkey. The study stated an overall accuracy of classification image was 84,4% in1976 and that of the image dated 2000 was 87,1% and the Kappa coefficient was 82.3% and 83,6%.

Again, similar researches were conducted in Ethiopia using remote sensing and GIS techniques with post-classification techniques. Thus, the results showed that an increase in fallow land and built-up area, while decreasing in vegetation and bare land.

The vegetation and bare land were converted to fallow land and built-up areas (Belay et al., 2019; Gebregergis, et al., 2016; Reis, 2008; Tolessa, et al., 2016).

## 2.3 FRAGSTATS Analysis

FRAGSTATS was designed to be as versatile as possible and developed to quantify landscape structure (Tolessa et al., 2016). This software platform offers a comprehensive choice of landscape metrics and it is used for quantifying landscape structure at class and landscape-level which has been previously demonstrated widely (McGarical and Marks, 1995; MacLean and Congalton, 2015). Two separate versions of FRAGSTATS exist one for vector images and the other raster images. The vector version is an Arc/Info AML that accepts Arc/Info polygon coverages. The raster version is a C program that accepts ASCII image files, 8- or 16-bit binary image files, Arc/Info SVF files, ERDAS IMAGE files, and IDRISI image files with spatial grain or resolution of the grid to be > 0.001 m. Both versions of FRAGSTATS generate a similar array of metrics, including a range of area metrics, patch density, size and variability metrics, edge metrics, shape metrics, core area metrics, diversity metrics, and contagion and interspersion metrics. The raster version also computes several nearest neighbor metrics. Landscape metrics calculated by FRAGSTATS is described in terms of its ecological application and limitations.

According to Kumar, et al. (2018), FRAGSTATS was used to quantify the Landscape spatio-temporal dynamics and LULC changes occurred during the 9 years-period (2001-2009) covered by the three hyperspectral images in the typical Mediterranean in central Greece. Six landscape indices were used namely NP, PD, LPI, MESH and ENN at patch and class level. The area provided information to explore the proportion of LULC categories and perimeter-indices helped to understand the role of the edges. The longer the edge of a patch to a given area, the more complex the shape which means patch stability can be judged from an ecological perspective. The choice of these landscape metrics was used based on the scale of analysis as well as the knowledge of the study area and grid attributes mainly the cell size was 30 m and patch neighbors were supported by 8 Cell Rule. Edge depth was also considered with a buffer zone of 100 m to calculate the inner undisturbed area (core area) of the patch as explained (Singh et al., 2017). Similarly, many researchers on FRAGSTATS used to quantify landscape metrics at class and landscape level (Ramachandra et al., 2012; Sudhira, et al, 2004; Tolessa et al., 2016).

Table 2. 1: The Landscape metrics used in this study area.

| S/N | Spatial metrics | Formula | Range |
|---|---|---|---|
| 1 | Largest Patch | LPI = (100)<br>a ij = area (m2) of patch ij | 0 ≤ LPI≤100 |

| | | | |
|---|---|---|---|
| | Index (LPI) | A= total landscape area | |
| 2 | Percentage of Like Adjacencies (PLADJ) | PLADJ = <br>Where, gii = number of like adjacencies (joins) between pixels of patch type<br>gik = number of adjacencies between pixels of patch types i and k | 0<=PLADJ<=100 |
| 3 | Landscape Shape Index (LSI) | LSI = (ei/min ei)<br><br>Where, ei =total length of the edge (or perimeter) of class i in terms of a number of cell surfaces; includes all landscape boundary and background edge segments involving class i. min ei=minimum total length of the edge (or perimeter) of class i in terms of number of cell surfaces. | LSI>1, Without Limit |
| 4 | Normalized Landscape Shape Index (NLSI) | LSI =<br><br>Where, si and pi are the area and perimeter of patch i, and N is the total number of patches. | 0≤NLSI<1 |

| | | | |
|---|---|---|---|
| 5 | Clumpiness | CLUMPY = for Gi < Pi &Pi <5, else<br><br>Gi =<br><br>gii =number of like adjacencies between pixels of patch type gik =number of adjacencies between pixels of patch types i and k. Pi =proportion of the landscape occupied by patch type (class) i. | -1≤CLUMPY ≤1. |
| 6 | Cohesion | | 0≤cohesion<100 |
| 7 | Patch density (PD) | f (sample area) = (Patch Number/Area) * 1000000 | |
| 8 | Number of Urban Patches (NPU) | NP = n<br>NP equals the number of patches in the landscape. | Number of Urban Patches (NPU) |
| 9 | Perimeter-Area Fractal Dimension (PAFRAC) | aij = area (m2) of patch ij.<br>pij=perimeter (m) of patch ij.<br>N= total number of patches in the landscape | 1≤PAFRAC≤2 |
| 10 | Aggregation index (AI) | AI =<br><br>gii =number of like adjacencies between pixels of patch type | 1≤AI≤100 |

| | | | |
|---|---|---|---|
| | | Pi= proportion of landscape comprised of patch type. | |
| 11 | Interspersion and Juxtaposition (IJI) | IJI = -<br>eik = total length (m) of edge between patch types<br>E = total length (m) of edge in landscape, excluding background<br>m = number of patch types (classes) present in the landscape. | 0≤ IJI ≤100 |
| 12 | Splitting index (SPLIT). | S = Where, S = the 'effective mesh number' of a network ø' | |
| 13 | Shannon's Diversity Index (SHDI) | SHDI = | SHDI ≥ 0, without limit |
| 14 | Contagion index (CONT) | | 0 < CONTAG <100 |
| 15 | area-weighted mean patch fractal dimension (FRAC_AW) | si=area patch i; pi= perimeter patch i;<br>N=total nr of patches<br>[1;2] | Ranges between 1 &2:<br>1: simple shapes<br>2: complex shapes |

## 2.4 Urban Landscape Structure and Dynamics

### 2.4.1 Landscape Metrics

“Landscape metrics” refers exclusively to indices developed for categorical map patterns. Landscape metrics are algorithms that quantify specific spatial characteristics of patches, classes of patches, or entire landscape mosaics (Huang et al., 2009).

**(1) Patch level,** which defines the individual patches as the area provides metric information to characterize the spatial character and context for individual patches in the landscape. patch metrics will serve as a reference for the calculation of landscape metrics.

**(2) Class level,** which uses data of the patches that belong to the same land-use type. Class indices individually quantify the quantity and spatial configuration of each patch type and thus provide a means to quantify the level and fragmentation of each patch type in the landscape (Mc. Garical, 2012).

**(3) Landscape-level**, defines the entire landscape, the full extent of the data. Of primary interest is the pattern of the landscape mosaic, the spatial character and distribution of patch (Mc. Garigal, 2012). Landscape metrics can be interpreted more broadly as landscape heterogeneity indices because they measure the overall landscape pattern.

Landscape metrics can be grouped into two general categories: those that quantify the composition of the map without reference to spatial attributes, and people that quantify the spatial configuration of the map, requiring spatial information for their calculation (Gustafson, 1998; Mc. Garigal and Marks, 1995). The composition is definitely quantified and refers to features related to the variability and abundance of patch types within the landscape, but without considering the spatial character, placement, or location of patches within the mosaic. Because composition requires the integration of overall patch types, composition metrics are only applicable at the landscape-level. There are many quantitative measures of landscape composition, including the proportion of the landscape in each patch type, patch richness, patch evenness, and patch diversity (Gustafson, 1998; McGarigal and Marks, 1995). The landscape metrics are grouped into the levels of heterogeneity however they were further grouped to the aspect of landscape pattern.

<u>Area and Edge metrics</u>: This group of metrics represents a loose collection of metrics that deal with the size of patches and the amount of edge created by these patches. Although these metrics could easily be subdivided into separate groups or assigned to other already

recognized groups, there is enough similarity in the basic patterns assessed by these metrics to include them under one umbrella. The area of each patch comprising a landscape mosaic is perhaps the single most important and useful piece of information contained in the landscape.

Shape metrics: The interaction of patch shape and size can influence a number of important ecological processes. Patch shape has been shown to influence inter-patch processes like ligneous plant colonization and may influencing animal foraging strategies (Forman and Godron 1986). However, the first significance of shape in determining the character of patches during a landscape seems to be associated with the 'edge effect'.

Core area metrics: Core area is defined as the area within a patch beyond some specified depth-of-edge influence (i.e., edge distance) or buffers width. Like patch shape, the first significance of the core area in determining the character and performance of patches during a landscape appears to be associated with the 'edge effect'.

Contrast metrics: Contrast refers to the magnitude of difference between adjacent patch types with respect to one or more ecological attributes at a given scale that are relevant to the organism or process under consideration. The contrast between a patch and its neighbourhood can influence a number of important ecological processes

Aggregation metrics: Refers to the tendency of patch types to be spatially aggregated; that is, to occur in large, aggregated or "contagious" distributions. This property is additionally often mentioned as landscape texture. We use the term "aggregation" as an umbrella term to explain several closely related concepts: 1) dispersion, 2) interspersion, 3) subdivision and 4) isolation. Each of these concepts relates to the broader concept of aggregation, but is distinct from the others in subtle but important ways, as follows.

Diversity metrics; Diversity measures have been used extensively in a variety of ecological applications. They originally gained popularity as measures of plant and animal species diversity. There has been a proliferation of diversity indices and that we will make no plan to review them here. FRAGSTATS computes 3 diversity indices. These diversity measures are influenced by 2 components--richness and evenness.

Choosing metrics involves a number of considerations. Firstly, the objectives of the study, spatial characteristics of the system and ecological processes under investigation determine which metrics to use (Mc. Garigal and Marks, 1995). Secondly, landscape metrics were chosen on the basis of the literature review. In China by comparing classified satellite images from 1988, 2002, and 2007. They quantitatively analyzed spatiotemporal changes in land use and landscape pattern using GIS, remote sensing (RS), and 11 landscape pattern metrics. The study showed increased cropland, built-up area, and aquaculture area and a decreased orchards, woodland, and beach area during 1988–2007. In addition, 64.3% of newly-expanded cropland was from woodland; and 34.8% newly-expanded built-up area from cropland, 27.2% from woodland, and 20.4% were converted from beach area. Further, there was 45.1% and 29.4% increased newly-expanded aquaculture from the beach and water body areas, respectively. The analysis of landscape pattern metrics indicated a fragmentation of the landscape, with more complex landscape pattern structure over the last 20 years within the Louyuan Gulf region. The two main driving forces that contributed to dynamic changes in land use and landscape pattern in the last two decades in Lou yuan were urbanization and policy developed to transfer beach/seawater areas.

Similarly, (Mc.Garigal, 2002) studied in Quantifying land use/land cover spatio-temporal and landscape pattern dynamics from Hyperion using SVMs classifier and FRAGSTATS in central Greece covering between 2001 and 2009. The study used 6 spatial metrics for quantifying the landscape pattern dynamics. With the MESH, LPI and AREA (as area-related metrics), with the NP, PD and ENN (as patch density and distance related metrics). Largest changes occurred just in case of conifer forests because the trajectory of the dates is often considered large on both axis: magnitude of the changes was the biggest decrease among all land cover types regarding both PCs. Changes of urban areas were the smallest. Trends were distinguished as monotonously decreasing (conifer forest) monotonously increasing (heterogeneous agricultural areas, bare rocks), transitional ones (changes were different along the two axis: broadleaved forests, urban areas, transitional woodland/scrubland) and when there was no trend (sclerophylls' vegetation). Conifer forests have a decreasing trend. The effective mesh size (Lamine et al., 2018), which is an indicator of subdivision characteristic of a landscape (Jaeger, 2000) Largest Patch Index (LPI) and the mean area (AREA) decreased in the investigated period, number of patches (Haregeweyn et al., 2012), patch density (PD) also decreased. Consequently, the mean distance of the nearest neighbouring patch (ENN) increased. This process indicates a fast fragmentation process that can be considered as the most detrimental process in the area as these forests play an important role in the sustaining the biodiversity.

## 2.5 Urban Sprawl

Urban sprawl dynamics was analyzed considering some of the causal factors. The rationale behind this is to identify such factors that play a significant role in the process of urbanization. The causal factors that are responsible for sprawl include population density and urban growth. To identify the sprawl within the study area, a careful comparison of urbanized area expansion and population dynamic using Shannon's entropy has been done. Shannon's entropy was calculated from the spatial metrics for each direction (n is the total number of direction (i.e., n = 8)

The Entropy may range from 0 to log n, indicating a compact distribution of considered phenomenon (urbanization) for values closer to zero and a dispersed distribution for values closer to log n indicating the occurrence of urban sprawl (Benson et al., 1995; Turner et al., 1989).

### 2.5.1 Urban Sprawl in Ethiopia

Ethiopia is one of the most populous country in Africa. An estimate puts the country's population figure close to 110 million (Fanta et.al., 2017). Urban population growth in Ethiopia is estimated at 6% which is a much higher figure compared to others countries (Fanta et.al., 2017).

The high social problem still prevails in large Towns of the country like Adama Town. The country is one of the least urbanized areas in the Third World. Its economy almost entirely depends on agriculture although production and food provision are low due to bad weather conditions and lack of effective technology. In addition, almost 80 per cent of the population practices only agriculture and animal rearing as a means of livelihood. The rapid urban expansion, a characteristic of many developing countries, is occurring in many parts of Ethiopia, whereby rural villages near towns are being incorporated into the urban sprawl. The changes in the consumption and production behaviors of subsistence farm households in the villages, along with the absence of markets, particularly for labor and land, can result in the rural-urban livelihood transition being far from smooth. Like most developing countries, serious rural to urban migration is a common phenomenon. Ethnic conflicts are common phenomena driving people from their villages. Shanty towns are emerging in different parts of cities, especially the capital, and are the only choices for the majority of the city dwellers that are poor. Additional population increase in bigger Towns is accommodated by crowding of existing houses. Rather than new construction developments, existing houses are often extended or divided illegally. The need for housing is not integrated with the need to prevent horizontal expansion and hence saving the land. Formal and informal settlements are stretching out horizontally from the central Town in all directions. The land is ineffectively used; new developments are planned on virgin land usually leapfrogging from cores. Generally, sprawl and land misuse in Ethiopia is a result of population pressure (both from natural births and migration), poor land policies, lease system and planning (Huang et al., 2010).

### 2.5.2Types of Urban Sprawl

Different scholar's urban sprawl was classified in different types. According to Batty et al. (2003), the type of sprawl found in North America and Europe differs. In North America development is not contiguous but spread out, whereas in Europe the density is higher but the form is more evenly equally scattered across the region, thus leaving more open spaces.

Therefore, the urban sprawl will be classified into the following five types, which are classified in terms of the degree of compactness, dispersion or 'scatteration' (Galster et al., 2001).

(1) Compact contiguous development: sprawl forms gradually around the urban area, not creating patches, and mainly has a high density.

(2) Strip or linear development: the urban expansion along with infrastructural works or rivers, the expansion is continuous but scattered, leaving agricultural and natural land open.

(3) Poly-nucleated nodal development: several smaller towns are agglomerated; the sprawl is discontinuous, with much lower density than the traditional settlement, physically separated from the urban city of which it sprawled. Creating new 'larger' agglomeration of towns separately from each other

(4) The scattered sprawl development: uncoordinated discontinuous development away from the historic central core, creating open and vacant land between new built-up areas.

(5) Leapfrogging development: is the development that leapfrogs over existing barriers. Residents and service providers must pass by vacant land on their way from one developed use to another.

### 2.5.3 Drivers of Urban Sprawl

Cities in the world are still growing, although populations in the world are not reproducing themselves sufficiently (declining fertility rates) and the urbanization has diminished with respect to the 1950s (Weijers, 2012). In addition, he stated that there are several key forces acting as centrifugal forces which make cities expand outside their borders (deeper into the suburbs and rural areas). People demand more and more living space, whereas they still want to enjoy the amenities of a city.

Sprawl and land misuse in Ethiopia are a result of population pressure, poor land policies, lease system and planning and regional imbalance. Christiansen et al. (2011), conducted a literature review to identify the driving forces behind urban sprawl in Europe. He classified the drivers of urban sprawl into four categories: economy, society, transport, and policy.

**(A) Socio-Economy**

Globalization is one of the drivers behind urban sprawl. This may draw people to the cities and concentrate activities. Logically this will go along with increased pressure on the land, which can be a driving force of urban sprawl. The increased accessibility makes urban sprawl in the newly accessible areas possible (Christiansen et al., 2011). According to Dennis Weijers. (2012), microeconomic level market failure one of the driving factor of urban sprawl.

**(B) Society**

Mostly, Population growth can be considered the primary cause of urban sprawl. The global population has doubled over the past 40 years with remarkable shifts in geographical distribution. Africa especially Ethiopia has grown in the fastest rate. Asia, by far the populous region, has more than doubled in size (to over 3.6 billion), as has Latin America and the Caribbean. In contrast, the population of Northern America has grown by only 50 per cent, and Europe's has increased by only 20 per cent and is now roughly stable (Weijers, 2012). Another driver for sprawl is the housing preference of people and the characteristics of residential areas. According to previous researches, low crime rates and a quiet neighbourhood are the most important reasons for people to move to peripheral areas. The city characteristics such as lots of traffic, noise, and pollution, can lead to the feeling of insecurity. Also being close to the rural areas and nature are factors which pull people to the peripheral areas. In cities, there is usually a lack of green spaces (in general), facilities to the sport, and playgrounds. Expensive smaller homes are also pushing people away from the city. Also, the individual income is a factor that relates with housing preference. People with high incomes have more housing possibilities; this, however, can lead to social segregation. Another force of urban sprawl is the second homes. Another factor which makes sprawl possible is the flexibility of work. Technology, internet for example, made it possible to work outside the office (Christiansen et al., 2011).

**(C) Transportation**

The linkage between sprawl phenomenon and the use of private vehicles and its consequent has a negative effect on traffic congestion and air pollution. Sprawl is usually defined as a condition of poor accessibility, followed by the massive use of private vehicles. With the advent of the automobile, the action radius of people increased significantly. Companies do no longer have to establish their businesses along with transportation nodes of railway stations and ports, and people do no longer have to live 'close' to work. The automobile made urban sprawl possible. Because of the urbanization and the increasing population in cities, more roads were needed. Roads are a driver of urban sprawl, in making new areas accessible. Previous researches also show that there is a strong correlation between car dependency and density. Denser cities show less car use than urban sprawl areas with a low density (Christiansen et al., 2011).

**(D) Policy**

Policy failure or regulation failure can be a driver of urban sprawl. Public authorities decide how land development should be managed. If there is little or no regulation and/or policy concerning land development, sprawl can virtually be unlimited. Municipalities may not perceive urban sprawl and low-density built-up areas as undesirable as municipalities precise densification negatively. Coordination problems on physical planning are also a driver of urban sprawl. Another driver behind urban sprawl is the land use and the building types. High density and high utilization of housing will reduce development pressure. However, if a great part of the city is occupied with parking lots, the costly ground which could be used for housing or industry will be occupied, leading to land shortage which may result in urban sprawl (Christiansen et al., 2011).

## 2.6 Effects of urban sprawl

There is a division between the place of sprawl (origin) and the location of its impact (destination). When sprawl takes place at the periphery of a certain locality it could have its direct or indirect impact on other parts of the same locality, within its border or on a neighbouring community. Generally, there are two conflicting ideas about the consequences or effects of sprawl. Some argue that it is harmful and stress measures that should be taken to combat it while, others support and even encourage it.

### 2.6.1 Positive Sides of Sprawl

Sprawl is not always seen as harmful. Some organizations and planners saw sprawl as a sign of economic vitality and not as an ecological threat. They also stress the primary advantage of sprawl, which is decentralization of employment to different parts of a city. They argue that car culture enables people to commute shorter distances at any time and own bigger homes. In addition, it is not healthy for people to live in areas with increased densities and smaller square meters of space per individual household as this creates psychological and health problems. Therefore, their recommendation is for people to live in bigger plots with their own green spaces away from city centers and work areas.

### 2.6.2 Negative Sides of Sprawl

All sprawl leads to loss of limited resource in the land. Over the years, sprawl has directly contributed to the degradation and decline of natural habitats such as wetlands, woodlands and wildlife. It also reduces farmland and open spaces. Water use and energy consumption will be increased. Sprawl leads to land-use patterns which are unfavourable to the development of sustainable transport modes and hence increase the use of a private car that in turn result in increased trip lengths, congestion, increase in fuel consumption and air pollution. In general, it is a threat to ecology. Even though automobile and truck engines have become far cleaner in recent decades, motor vehicle emissions are still the leading sources of air pollution. As homes and businesses spread further and further apart, local governments are forced to provide for widely spaced services and infrastructure leading to higher costs and increased tax burden.

- Decrease livability due to lack of walkability or bike ability and increased traffic
- Lack of maintenance and renewal investments in downtown areas, urban neighbourhoods, and the inner ring of suburbs around a central City resulting in gradual declines of areas where street and utility infrastructure already exists
- Loss of variety in housing choices as mass-produced housing predominates

- The Concentration of poverty leading to an even more bleak future and desperate choices

## 2.7 Measuring Urban Sprawl

Researchers tend to measure urban sprawl on either a metropolitan scale as mostly used in the U.S. or on smaller scales of towns or neighbourhoods, mostly used in. Urban sprawl can be measured in different ways according to different researchers. For example; urban sprawl is a multidimensional phenomenon that requires a different set of measures for each dimension. Most sprawl measures suggested in the literature can be divided into five major groups: growth rates, density, spatial-geometry, accessibility, and aesthetic measure.

### 2.7.1 Growth Rates

In terms of growth rates, urban sprawl is defined as a condition in which population growth rates in the suburbs are higher than inside the central city (Jackson, 1985). Another popular growth-rate measure is the “Sprawl Index” (SI) or “Sprawl Quotient” which can be defined as the ratio between the growth rate of built-up areas and the population growth rate in a certain area. A quotient higher than 1 implies urban sprawl.

### 2.7.2 Density

There are various types of densities and many ways and scales to measure it. Density is defined as the ratio between the amount of a certain urban activity and the area on which it exists. The urban activity can be defined as the number of residential units, a number of residents, or employees. This is the most popular sprawl measure that best represents the phenomenon.

### 2.7.3 Spatial-Geometry

This constitutes the largest group of measures. There are numerous geometric measures, most of which have been adopted from ecological research (Turner, 1989; Mc. Garigal and Marks, 1995) or from fractal geometry (Torrens and Alberti, 2000; Herold and Menz, 2001). Geometric and ecological measures quantify two main characteristics of the urban landscape: configuration and composition. Configuration refers to the geometry of the urban built-up area, and composition to its level of heterogeneity. An urban area will be considered sprawling as long as its geometric configuration is irregular, scattered, and fragmented and its land-use composition more homogenous and segregate (Haregewoin, 2005). Some common measures in this category are leapfrog or continuity (Galster et al., 2001), measure of circularity, fractal dimension and Mean Patch Size (MPS). All of these authors quantified the level of scatter and fragmentation of the urban landscape. The percentage of different land-uses quantifies its level of heterogeneity (McGarigal and Marks, 1995). In these types of measurements, two indicators that can be used for the determination of the determination of the composition and configuration, can be seen deeply.

**(A) Land Use and Land Cover Change Analysis**

Change detection refers to the study of identifying changes of the state of an object (phenomenon) in time. Different time steps will be used to identify changes, by making use of different multi temporal data sets of an area, which can be done with remotely sensed data Change detection is successfully applied in the following applications; land use change analysis, monitoring shifting cultivation, assessment of deforestation, study of changes in vegetation phenology, seasonal changes in pasture production, damage assessment, and other environmental changes.

(B) **Landscape Metrics**

Landscape metrics are used to describe and quantify the structure of urban landscapes (the composition and arrangement) and the spatial relationships (Walz, 2011). The pattern of a landscape is expressed by the "size, shape, arrangement and distribution of individual landscape elements. The reason for using metrics in spatial analysis is to record the structure of an urban landscape quantitatively on the basis of area, shape, edge lines, diversity and topology-descriptive mathematical ratios" (Walz, 2011).

Landscape metrics are quantitative measures of spatial structures and patterns which can be used to describe urban sprawl. The landscape metrics will be subdivided into three levels of measurements.

These indexes are a collection of unit-less metrics that quantify and analyze landscape patches on the basis of geometric shape, complexity and compactness. The landscape metrics are grouped into the levels of heterogeneity which are further grouped in to the aspect of landscape pattern.

### 2.7.4 Accessibility

Sprawl is defined as a condition of poor accessibility followed by the massive use of private vehicles. Accessibility can be quantified by measuring road length, road areas, and the traveling times of households. Another way to measure accessibility is to calculate the fractal dimensions of road networks (Benguigui, 1995). Some ecological measures are useful to measure accessibility like “Mean Proximity Index” (MPI).

### 2.7.5 Aesthetic Measures

Urban sprawl is often considered a boring, homogenous form of development. Being subjective by definition, it is difficult to measure and quantify the aesthetics of sprawl(Ashkenazi & Frenkel, 2008). However, several recent studies have attempted to define archetypes of urban development or sprawl, such as residential sprawl or strip-malls sprawl, and to compare various landscapes to those archetypes.

Ashkenazi and Frenkel, (2008), studied on landscape structure dynamics in Maysor city with 3 km buffer using spatial metrics and Shannon entropy from 1973 to 2009. The study result reveal that the city is experiencing the sprawl in all directions as entropy values are closer to the (log (n). Lower entropy values of 0.007 (NW), 0.008 (SW) during 70’s shows an aggregated growth as most of urbanization were concentrated at city center. While, the region practiced dispersed growth in 90‟s reaching to the threshold value of 0.452 (NE), 0.441 (NW) in 2009 during post 2000’s.

The entropy computed for the city (without buffer regions) shows the sprawl phenomenon at peripheries. However, entropy values are comparatively lower when buffer region is considered. Shannon's entropy values of recent time confirm a minimal fragmented and dispersed urban growth in the city. This also illustrates and establishes the influence of drivers of urbanization in various directions.

A thesis conducted on modelling and mapping of urban sprawl pattern by (Ramachandra et al., 2012) using multi temporal Landsat data and Shannon’s entropy in Cairo from 1984 to 2013. A linear regression analysis was conducted with the 31 observations to model the relationship between the increase in built-up area that shows a positive correlation. The results show that urban sprawl 1.4615, 1.6112, 1.8154, 1.8717, 1.9726 and 2.1023 during 1984, 1990, 2006, 2011 and 2013 respectively. This increase in value of entropy indicates increase in dispersion of built-up area, which is an indication of urban sprawl.

Higher value of overall entropy for the whole urban area represents higher dispersion of impervious area which is a sign of urban sprawl. Increase in dispersion is due to new areas being added. The higher values of entropy in outer areas indicate more urban sprawl compared to central Cairo. Distribution is predominantly dispersed in outer areas, whereas it is more compact in areas surrounding central Cairo. the urban sprawl is characterized by an increase in building along the highways and in the periphery. The percentage of an area covered by impervious surfaces such as asphalt and concrete are a straightforward measure of development (Barnes et al., 2011).

## 2.8 Spatial Pattern of Urbanization

Urbanization is the physical growth of urban areas with the increase in population either by migration or amalgamation of peri-urban areas into cities (Effat and El Shobaky, 2015). Urbanization is the increase in the proportion of total population or area in cities or towns. Urban areas have a very high ecological footprint as urban expansions are associated with problems such as destruction of vegetation, changes in local and global climate and the environmental factors in and around the region (Ramachandra et al., 2012a). Unplanned urbanization has led to a disaggregated growth in the region, evident from the dispersed growth in peri-urban areas with the higher consumption of land and without basic amenities and infrastructure.

Landscape metrics was applied extensively to describe the structures of urban land-use classes and for explaining the drivers of urbanization (Huang et al., 2007). Ramachandra et al. (2013), conducted a study on "Analysis of spatial patterns of urbanization using geoinformatics and spatial metrics in Hyderabad, India" using spatio temporal data and spatial metrics from 1975 to 2009. Nine landscape metrics were used in order to analyze the spatial pattern of urbanization of Hyderabad. Gradients close to the center of city showed a decreasing number of patches indicating the process of clumping or aggregation of urban patches at the city center. NW and NE directions show a significant increase of urban patches in all gradients. The increased number of patches in the buffer region indicates sprawl due to intense urbanization at the central area of the city. All other metrics (area, shape, edge and compactness) indicate a similar trend.

## CHAPTER THREE

### 3. MATERIALS AND METHODS

### 3.1 Study Area Description

This study was conducted in Adama Town. Adama Town is located about 100km South East of Addis Ababa along the main road to Harer, bounded between 8° 26'N and 8°38'N latitude and 39° 12' 15 E and "39°21' 15" E longitude. It is located at an average altitude of 1620 m above sea level. East Shewa zone, in which Adama Town is located, forms part of the mid-central plateau. It is found on a nodal location along main national and regional transport lines from the capital Addis Ababa to other important towns. The Town is divided into four sub Cities and 19 Kebeles following the main Addis Ababa – Harar Road in the east-west direction, the Assela road to the south and the 1st avenue to the north.

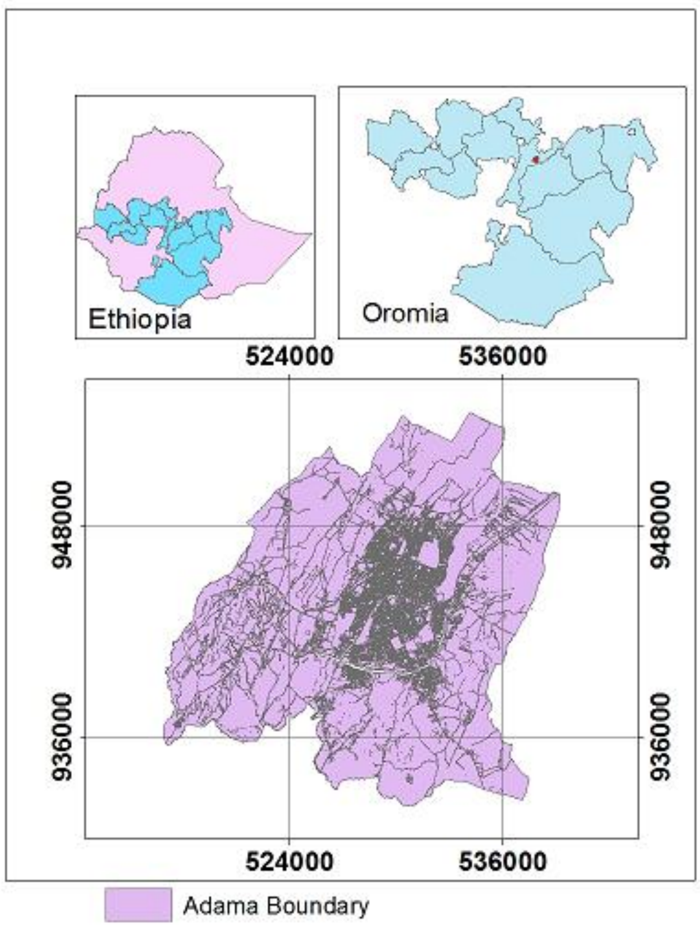


Figure 3. 1: Location of the Study Area

### 3.1.1 Demographic Characteristics of Adama Town

The 1994 national census reported Adama Town had a total population of 127,842 of whom 61,965 were males and 67,877 were females with an area of 29.86 square kilometers. Based on the 2007 census conducted by the central statistical agency of Ethiopia (CSA) it had 220,212 and increased over the population recorded in the 1994 census, of which 108,872 were manes and 111,340 were females. In recent (2014-2017) central statistical agency of Ethiopia projected the total population was  308,506 from this 151,266 were Mans and 157,260 were Females. From 1994 to 2007 census, the growing population size is 92,370 i.e. the annual increment is 5.56%. And also, from 2007 to 2014 the increment population is 88314. This implies that the population is increasing at a rate of 5.72%. While, the annual population growth rate of Adama town in 1990 was 4.6% and reached to 104,464 and in 2000, 2010 and 2019 was 164,716, 260,203 and 429,266 respectively.

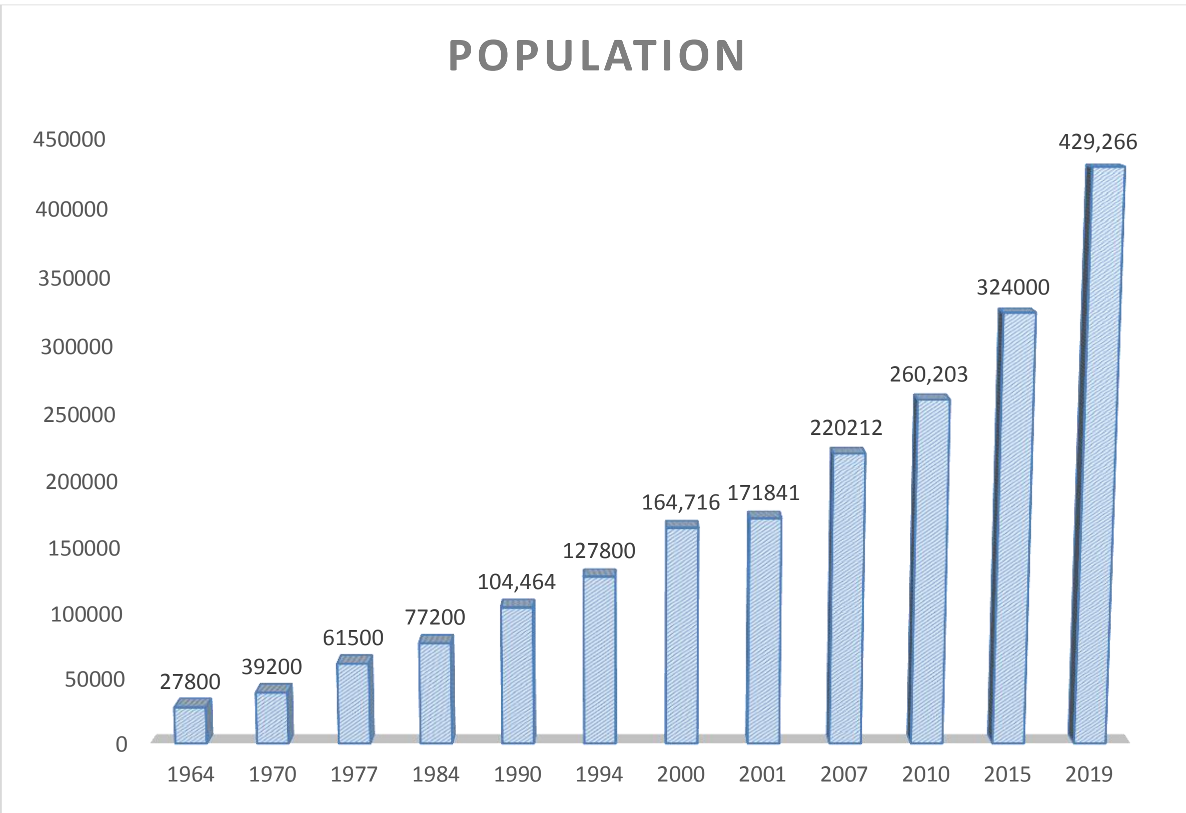


Figure 3. 2: Population of Adama Town (1964-2019) [Source: Adama Town Municipality]

## 3.2 Data and Its Sources

In the present study, Landsat data of four different years were used to identify changes in Land use and Land cover, landscape pattern and spatial pattern of urbanization of Adama town. The first image dates back to 19th January 1990 Landsat (4-5) thematic mapper, the second image dates 20th January 2000 Landsat (4-5) thematic mapper was used, the third image dates back to 15th January 2010, Landsat (7) Enhanced thematic mapper(ETM+) and the fourth image was taken during the end of Jan 2019 Landsat (8) Operational Land Imager (OLI). All these data were chosen because of their clear appearance, which means that shadows of clouds and haze do not impair the image. Moreover, a very narrow time span between all images (i.e., within January) was preferred to minimize phonological variations as recommended by MEINEL et. al. (1997), new structural plans of Adama town were collected for boundary mapping and field survey were taken, Ancillary data from Adama town administration and census of Adama were used. During field survey, ground control points were collected using GPS.

Table 3. 1: Data source and its use

<table>
<tr><th>Data</th><th>Source</th><th>Resolution</th><th>Purpose/Year</th></tr>
<tr><td>Landsat 4-5 TM</td><td rowspan="3">https://earthexplorer.usgs.gov/</td><td rowspan="3">30m*30m</td><td rowspan="3">1990, 2000, 2010 and 2019<br>For land use and land cover analysis</td></tr>
<tr><td>Landsat 7 ETM+</td></tr>
<tr><td>Landsat 8 OLI</td></tr>
<tr><td>Google Earth Image</td><td>Google earth</td><td></td><td>For accuracy assessment</td></tr>
<tr><td>Census Data</td><td>Adama Municipality</td><td></td><td>1994, 2002, 2007 and 2014</td></tr>
<tr><td>GPS data</td><td>Field and Google earth</td><td>Number</td><td>For accuracy assessment</td></tr>
<tr><td>The Master plan of Adama Town</td><td>Adama municipality</td><td>1:50,000</td><td>To generate boundary map</td></tr>
</table>

## 3.3 Materials used

### 3.3.1 Softwares Used

The ERDAS IMAGINE 14 software packages was used to process and classify the Landsat images and for GIS purpose ARC GIS 10.5 was applied, for extraction and preparing for different maps (LULC, Built up….). The public domain of FRAGSTATS version 4.2.1 package was used to calculate the Landscape pattern indices (Table3.2).

Table 3. 2: Softwares and their Use

| **Softwares** | **Version** | **Purposes** |
|---|---|---|
| ERDAS IMGINE | 2014 | Used for image classification, accuracy assessment, AOI extraction |
| GPS | Garmin | For GCP collection |
| FRAGSTATES | 4.2.1 | Used for calculation of spatial metrics |
| Arc GIS | 10.5 | For preparing maps etc. |
| SPSS | 26.0 | For statistical data |
| Microsoft office word | 13 | For documentation |

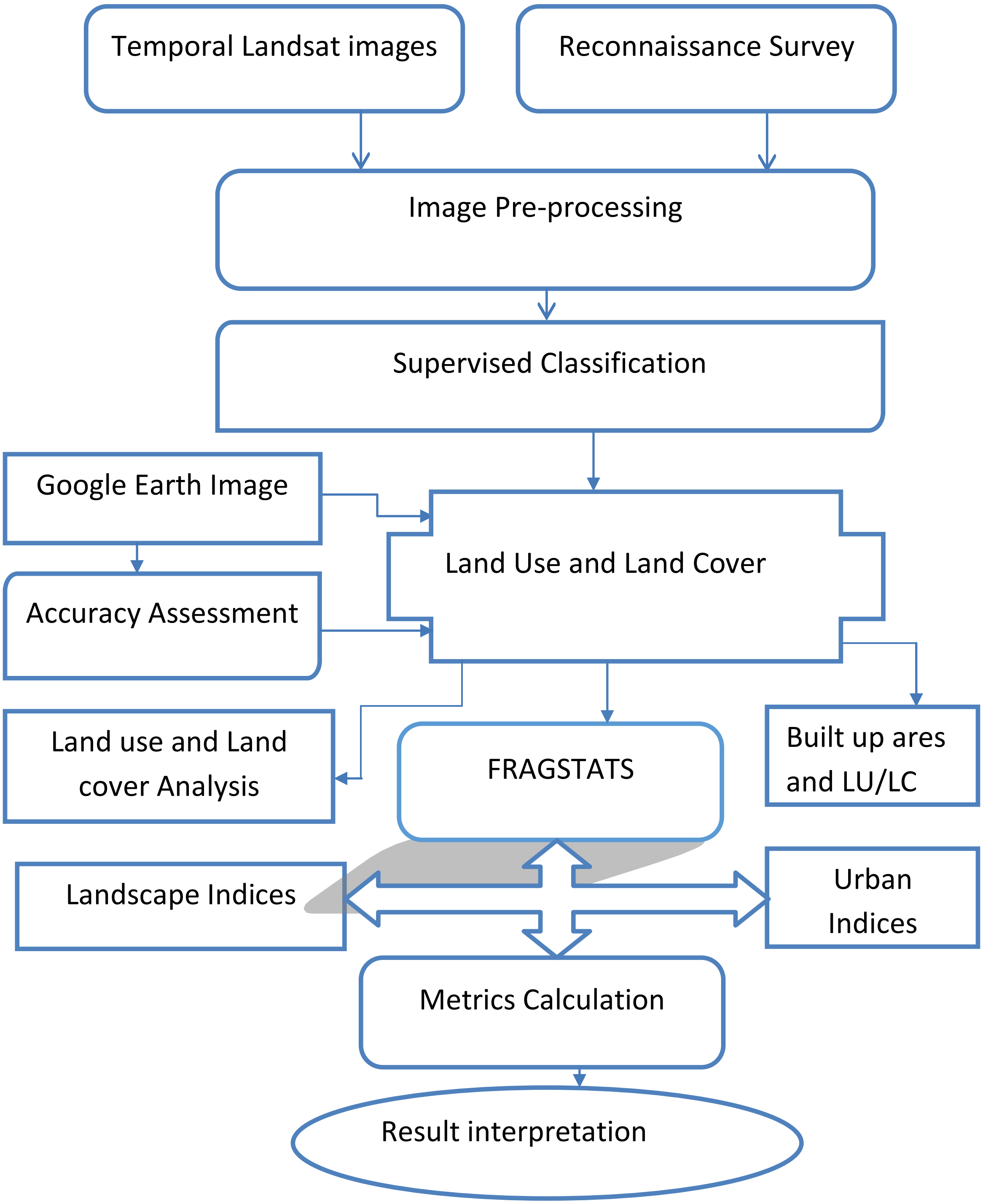


Figure 3. 3: Flow Chart of the research work

# CHAPTER FOUR

# 4. DATA ANALYSIS, RESULTS AND DISCUSSION

## 4.1. Land use and Land cover Dynamics

The LULC dynamics is the most important factor for changes affecting global and ecological system as stated (Ramachandra et al., 2013; Bray and Islam, 2012). The land cover and land use changes significantly affect key aspects of earths system functioning for example in contributing for global climate warming, as well as impact soil degradation, local and regional climate change (Srivastava et al., 2012).

In the current study, for preparation of LULC classification some steps were followed. These are: pre-processing, image classification, post classification and accuracy assessment.

### 4.2.1 Image Pre-processing

Landsat data of four different years were acquired from USGS earth explorer. The first image dates back to 19th January 1990 with Landsat (4-5) thematic mapper, the second image dates 20th January 2000 with Landsat (4 -5) thematic mapper, the third image dates back to 15th January 2010, with Landsat (7) Enhanced thematic mapper (ETM+) and the fourth image was taken during the end of Jan 2019 with Landsat (8) Operational Land Imager (OLI). All images have 30m spatial resolution. The data were chosen on the basis of their clear appearance, which is free from cloud and haze. Moreover, a very narrow time span between all images (i.e., within January) was selected to minimize phonological variations of suggested by Meinel et. al. (1997), in which a new structural plan of Adama Town was collected for boundary mapping. Ancillary data from Adama Town administration and census of Adama Town were also used. During field survey, ground control points (GCPs) were collected using hand held GPS. All the images between (1990, 2000, 2010 and 2019) were stacked using Layer Stack Tool and the stacked layers were geo-referenced using GCP to transform the existing coordinate system to UTM_WGS 84 datum zone 37 north. All the images were subsetted using Subset Tool to mask to the study area coverage (AOI) using the administrative boundary

**Image Enhancement**

Pre-processing of satellite images prior to image classification and change detection is essential. Due to spatial, spectral, temporal and radiometric resolution constraints, the complexity of physical environment cannot be accurately recorded by normal remote sensing sensors.

Prior to conducting further image enhancement techniques, the band combinations (FCC) for each image were conducted on RGB color combination basis as 4,3,2 (1990, 2000, and 2010) and 5,4,3 (2019) respectively. Histogram Equalization and Pan-sharpening Techniques were used to improve the image contrast for better discrimination of land use land cover classes in ERDAS IMAGINE and ArcGIS software environment.

4.2.3 **Image Classification**

Image classification refers to the task of extracting information that is processed in a computer that can classify an image according to its visual content Kaeli et al. (2015). Supervised classification is an important and human based classification for multi-temporal image classification and detects class information in the satellite images and similar pixels are used as training samples. Based on the detailed examination of Google Earth Image of the study area (see Annex-2), six land use land cover classes were defined as built up, bare land, fallow land, vegetation, agriculture and water bodies.

In this study, Land use Land cover classes were classified using supervised classification and Maximum Likelihood algorithm using ERDAS IMAGINE 14 software packages for all images during three decades. The classification of images was based on examining the reflectance for each pixel and making a decision about the signature it resembles accurately. For obtaining more accurate LULC classes, for one class 20 consistent training samples were selected. Prior ground verification knowledge is essential to recognize the pattern of land use and land cover classes during supervised image classification and the classification system were developed as per Jansen et al. (2001) classification algorithm. Google Earth and data collected during field trips (training sites/ground control points using GPS) served as reference data. The accuracy of the images was checked and the overall accuracy and kappa statistics (Table 4.5) were deemed satisfactory for land use change analysis. Finally, the generated LULC maps for the year 1990, 2000, 2010 and 2019 as shown in Fig.2.4.

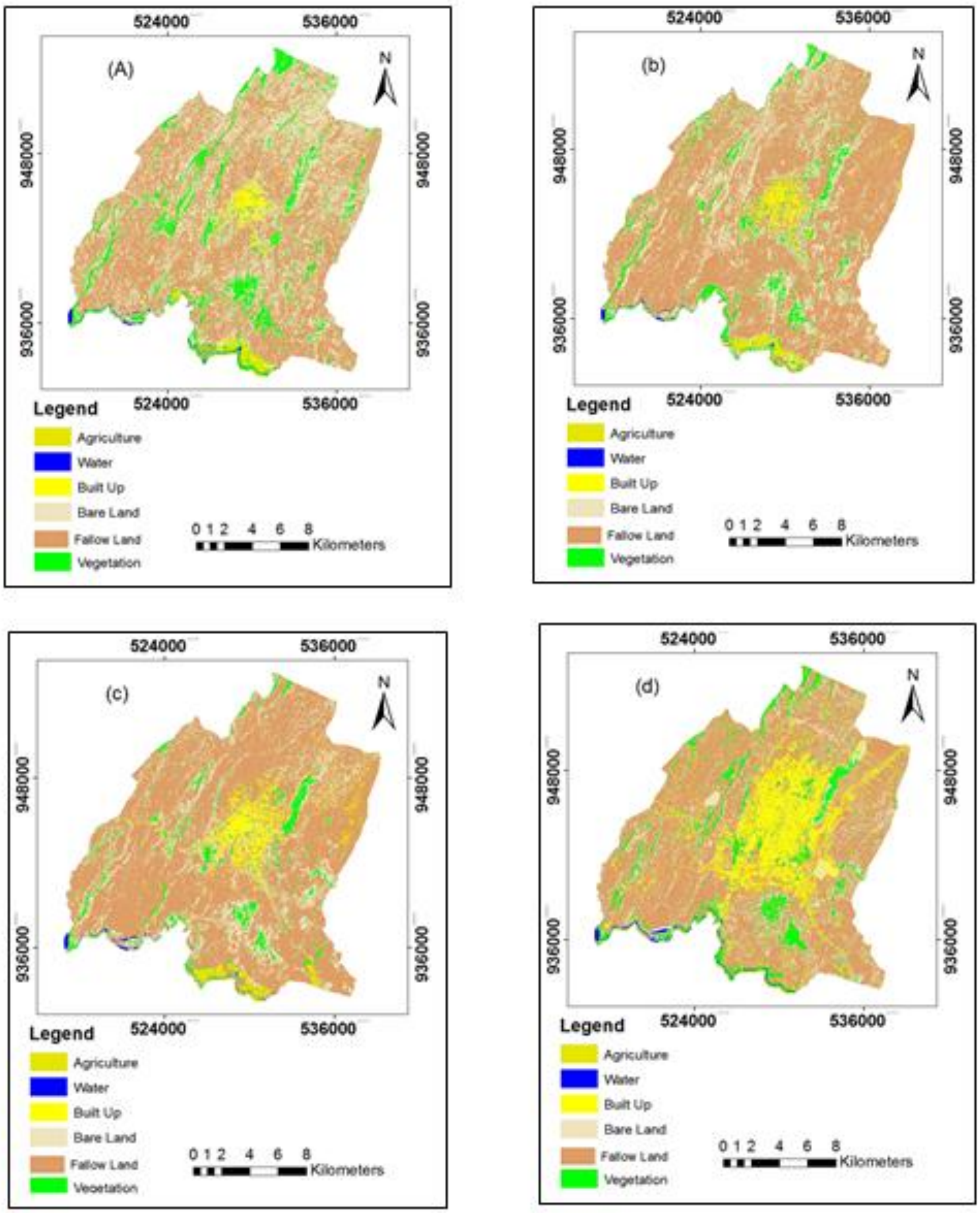


Figure 4. 1: LULC map of Adama Town during (a)1990, 2000(b), 2010(c) and 2019(d)

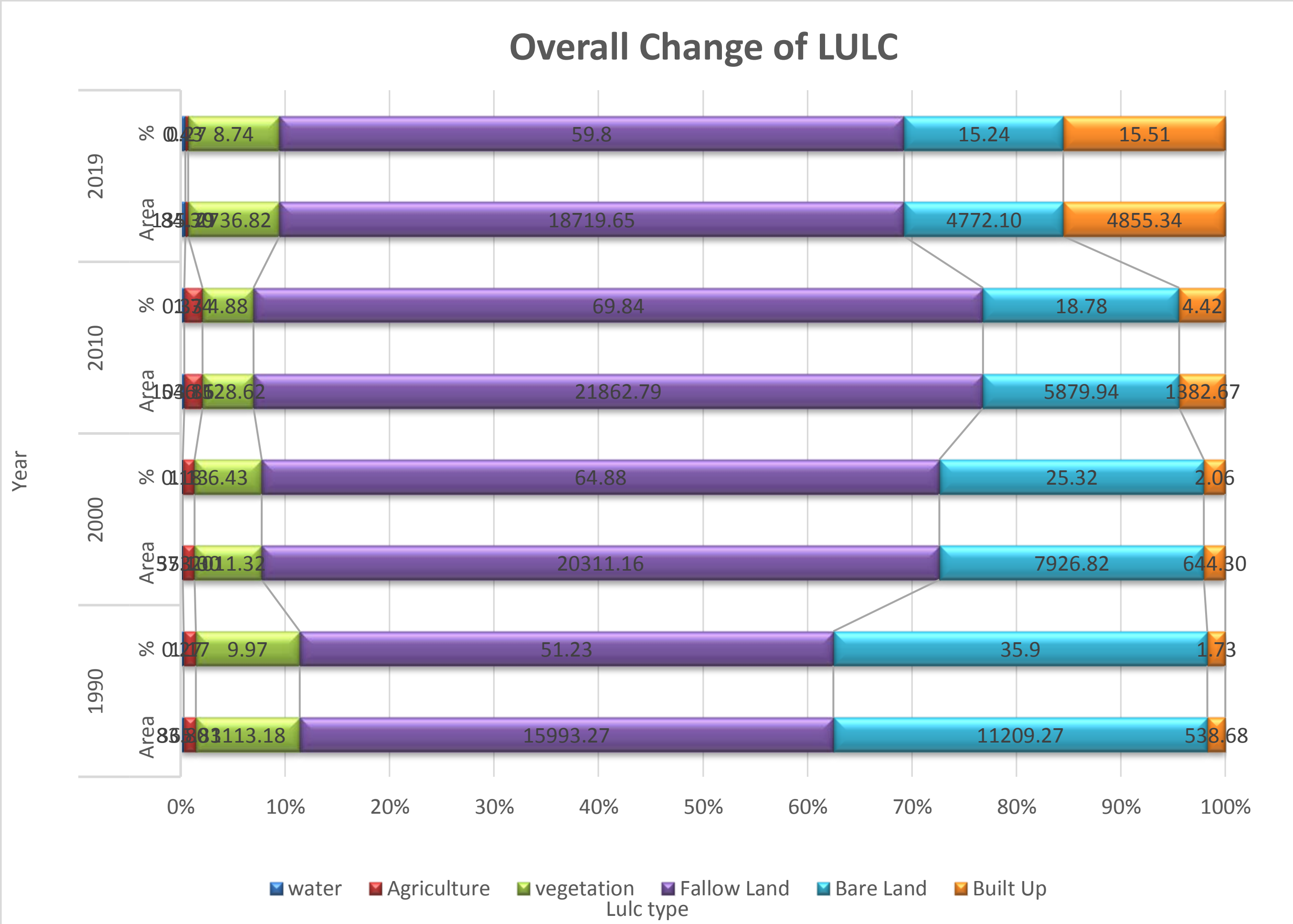


Figure 4. 2: the proportion of area for each class type in the landscape

The above figure (4.2) shows that the LULC during 1990 fallow land and bare land accounts for 15993.27 ha (51.23%) and 11209.27 ha (35.9 %) ha of the total area of the Town respectively , followed by vegetation cover and built up area accounting about 3113.18 ha ( 9.97% ) and 3638.1 ha (23.1%) respectively. During 2000, the highest category was covered by fallow land 20311.13 ha, sharing 64.88% of the total area and followed by bare land containing (7926.82 ha, 25.32%) and vegetation cover sharing 2011.32 ha (6.43%). The remaining land cover was built up (644.30 ha, 2.06%), agricultural land (353.30 ha, 1.13%), water bodies (57.10 ha, 0.18%) as shown in (Table 4.1 and Fig. 4.1). In addition, in 2010 the fallow land area was the highest coverage (21862.79 ha, 69.84%) followed by bare land (5879.94 ha, 18.78%), vegetation area was minimum during the study period (1528.62 ha, 4.88%), the built area has showed the highest increment post-2000 and reached (1382.68 ha, 4.42% of the total area), the vegetation cover of Adama Town was minimal during this period and decreased to 1528.62 ha (4.88%) while, agriculture and water bodies to 546.12 ha (1.74%) and 103.86 ha (0.33%) respectively (Fig 4.2). During 2019 the result of Land Cover and Land Use classification shows the highest category of the land was covered by fallow land (18719.65 ha/ 59.80%) and it is followed by Built-up area (4855.34 ha/ 15.5%) and bare land (4772.10 ha, 15.2%), while vegetation, agriculture and water bodies were 2736.82 ha (8.74%), 84.30 ha (0.27%) and 135.79 ha (0.43%) respectively (Table 4.1 and Fig 4.2).

The relative change of LULC of the study area was calculated between (1990-2000, 2000-2010 and 2010-2019) and the annual rate of change for each class of LULC was calculated using the following formula proposed by (Puyravaud, 2003).

$$r = \ln (A2/A1)/\Delta T \qquad \text{Equation 4.1}$$

Where r is the change for each class per year, A1 is the class area of the first year and A2 is the class area of the second year and ΔT is the difference in time. The relative change of the LULC of the study in three decades are shown in Table 4.1.

Table 4. 1: LULC annual rate of changes of the landscape of the study area

| LULC Type | Area Diff(a-b) | Change rate(a-b) % | Area Diff(b-c) | Change rate(b-c) % | Area Diff(c-d) | Change rate(c-d) % |
|---|---|---|---|---|---|---|
| Vegetation | -1101.86 | -4.40 | -482.70 | -2.70 | 1208.2 | 6.50 |
| Built Up | 105.62 | 1.80 | 738.70 | 7.60 | 3472.67 | 14.00 |
| Water | -26.70 | -3.84 | 46.76 | 6.00 | 31.93 | 3.00 |
| Bare Land | -3282.45 | -3.500 | -2046.88 | -3.00 | -1107.83 | -2.30 |
| Agriculture | -12.51 | -0.30 | 192.82 | 4.40 | -461.82 | -20.80 |
| Fallow Land | 4317.89 | 2.40 | 1551.63 | 0.70 | -3143.14 | -1.70 |

NB: a – 1990, b = 2000, c = 2010 and d = 2019

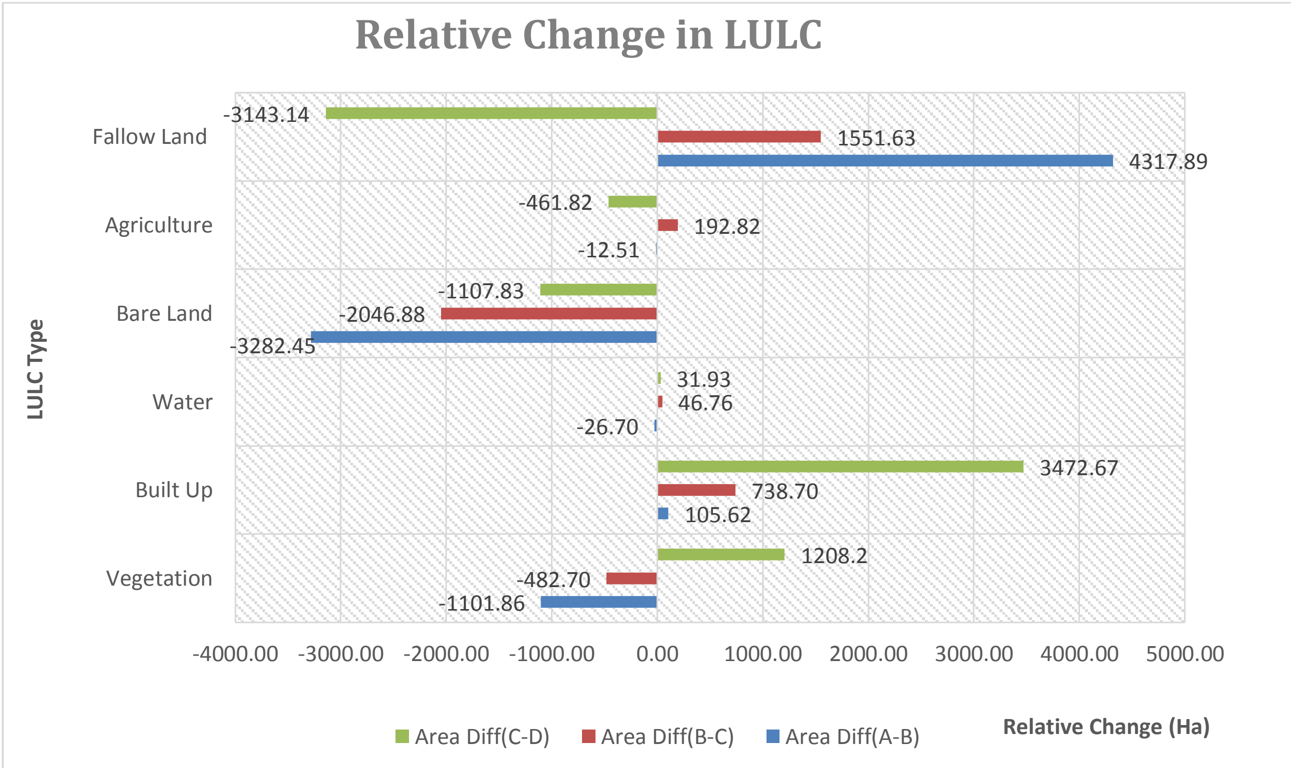


Figure 4. 3: Relative change in LULC

The analysis of the result shows that a significant continuously decreased in the vegetation cover of the town from 1990 to 2000 by 4.40% while during the third period vegetation cover of the Town showed a progressive increase with 6.5% annual rate of change (Table 4.1) as the government gives attention to climate change reduction strategies.

An increasing rate of change for fallow land was observed by 2.4% and 0.70% in the year range between (a-b) and (b-c) respectively while in (c-d) the rate of change for fallow land decreased by 1.70%. Other significant increasing annual rates of change were observed in built-up area by 1.80%, 7.60% and 14.00% in the first period (a-b), in the second period(b-c) and in the third- period respectively (c-d) (Table 4.1). This is because of population and urban growth.

Then rate of change of bare land decreased in all the study period by 3.5%, 3.00% and 2.30% respectively. A declining overall annual rate of change for the total vegetation by 0.22% and 0.27% for the first and second-periods were observed respectively. The rate of change in agricultural land decreased in the first and third period 0.30% and 20.80% respectively, while between (b-c) increased by 4.40 % (Table 4.2).

The relative change in Land Use and Land Cover of Adama Town (Fig. 4.2) was assessed based on data presented in Table 4.1. The changes showed some irregular pattern in this area from 1990 to 2019. Land cover change from 1990–2000 showed negative changes in most of the categories. This means about 1101.86 ha of vegetation cover had decreased in 1990–2000 period and in 2000–2010 data showed a decreased value to 482.7 ha, while in the third period the vegetation cover showed a positive increase 1208.20 ha. However, bare land, showed a negative change during the study period; whereas the relative change of built-up area showed a positive change in all the three-time periods to 105.62 ha, 738.70 ha and 3472.67 ha respectively as indicated in Fig 4.2 and Table 4.2. Similarly, the relative change in follow land has shown increment in the first and second periods to 4317.89 ha and 1551.63 ha respectively while in the third period a negative change of 3143.14 ha was shown (Fig 4.2 and Table 4.2). The change in agricultural land was negative during the first and third period by 12.51 ha and 461.82 ha respectively while in the second period the relative change in agricultural land was positive by 192.82 ha. However, the water bodies have the lowest changes in the study period. During the period between "1990-2000", the relative change in the water bodies was negative by 26.7 ha while in the second and third period the changes were positive by 46.76 and 31.93 respectively.

#### 4.2.4 Post Classification Techniques

##### 4.2.4.1 Change Detection

One of the most important applications of spatio temporal data is to detect the changes for the same object between different seasons and different years. The process by which variation in an object at different times or changes that occur in LULC are checked and identified over a certain number of years is known as change detection (Singh, 1989; Tewolde and Cabral, 2011).

In this study, LULC change detection was analyzed using post-classification technique comparison in the Arc GIS software environment by overlaying two land use and land cover classes based up on the classified images between the three-period ranges i.e. 1st period (1990-2000), 2nd period (2000-2010) and 3rd period (2010 - 2019). The Land Use and Land Cover changes were subsequently quantified through change maps and area tabulation summary in terms of area in hectare (Table 4.2 - 4.4).

Table 4. 2: Land-Use and Land-Cover (LULC) change matrix between 1990 and 2000.

| LULC class | Built up | Bare Land | Fallow Land | Water | Vegetation | Agriculture | 2000 |
|---|---|---|---|---|---|---|---|
| Built up | 315.83 | 73.93 | 147.17 | 0.16 | 21.14 | 5.74 | 563.97 |
| Bare Land | 142.56 | 3606.3 | 4931.25 | 9.01 | 498.71 | 5.74 | 9193.57 |
| Fallow Land | 182.84 | 3069.53 | 14419.1 | 8.84 | 277.15 | 54.54 | 18012 |
| Water | 1.91 | 36.79 | 12.9 | 50.4 | 5.97 | 0.6 | 108.56 |
| Vegetation | 13.43 | 1112.11 | 752.21 | 2.08 | 1172.38 | 62.3 | 3114.51 |
| Agriculture | 0.14 | 46.55 | 59.93 | 0.18 | 69.84 | 212.96 | 389.6 |
| 1990 | 656.71 | 7945.21 | 20322.6 | 70.66 | 2045.19 | 341.88 | 31304.91 |

The result in the first period showed that there was a major conversion from vegetation to bare land was 1112.11 ha and from vegetation to fallow land was 752.21 ha. In the same year, a change from fallow land to barren land was 3069.53 ha, from bare land to fallow and to built-up area, and from agricultural land to vegetation. Generally, there is a sharp decrease of bare land and vegetation in this period which is converted to fallow land and built up area.

Table 4. 3: Land-Use and Land-Cover (LULC) change matrix between 2000 and 2010.

| LULC **class** | Built Up | Bare Land | Fallow Land | Water | Vegetation | Agriculture | 2010 |
|---|---|---|---|---|---|---|---|
| Built Up | 460.89 | 81.38 | 118.85 | 1.6 | 3.27 | 0.59 | 666.58 |
| Bare Land | 241.85 | 2477.2 | 4590.0 | 31.81 | 526.41 | 77.68 | 7944.95 |
| Fallow Land | 645.49 | 2542.88 | 16690.7 | 19.49 | 216.38 | 207.43 | 20322.37 |
| Water | 0.09 | 9.56 | 9.96 | 50.49 | 0.63 | | 70.73 |
| Vegetation | 52.5 | 774.47 | 383.49 | 3.65 | 787.92 | 43.24 | 2045.27 |
| Agriculture | 0.41 | 22.35 | 97.6 | 0.97 | 14.64 | 239.06 | 375.03 |
| 2000 | 1401.23 | 5907.84 | 21890.6 | 108.01 | 1549.25 | 568 | 31304.93 |

In the second period, the results show that a major conversion from bare land to fallow land and fallow land to bare land were observed, fallow land to built-up area (645.49 ha), vegetation to barren land (774.471 ha), and bare land to build up (241.85 ha) as shown in Table 4.2 (B). this is due to urbanization.

Table 4. 4 Land-Use and Land-Cover (LULC) change matrix between 2010 and 2019.

| LULC class | Built Up | Bare Land | Fallow Land | Water | Vegetation | Agriculture | 2019 |
|---|---|---|---|---|---|---|---|
| Built Up | 1102.14 | 96.28 | 183.4 | 0.74 | 17.69 | 0.21 | 1400.46 |
| Bare Land | 754.34 | 1421.81 | 2533.9 | 44.53 | 1122.62 | 16.08 | 5893.3 |
| Fallow L | 2890.36 | 2983.56 | 15223.6 | 29.13 | 703.27 | 23.71 | 21853.63 |
| Water | 1.65 | 14.29 | 4.84 | 78.75 | 5.57 | 0.47 | 105.57 |
| Vegetation | 67.89 | 221.9 | 400.81 | 3.84 | 834.33 | 13.84 | 1542.61 |
| Agriculture | 16.64 | 70.54 | 355.81 | 0.77 | 72.59 | 46.67 | 563.02 |
| 2010 | 4833.02 | 4808.38 | 18702.38 | 157.76 | 2756.07 | 100.98 | 31304.89 |

During the third period, another major change from fallow land to bare land (2983.56 ha) and followed by fallow land to the built-up area was also observed. A few areas were converted to agricultural land and water bodies in the study area during this period as indicted in (Table 4.4).

From this land use/land cover matrix, the largest conversion was shown from bare land to fallow land (6931.25 ha). Fallow land and bare land followed by vegetation cover experienced the greatest conversion to other land uses than any other land cover types over the study period although such conversion varies from time to time. Generally, this conversion is due to high population growth and urban growth.

#### 4.2.4.2 Accuracy Assessment

The accuracy assessment aims to determine the degree of the classified data. Accuracy assessment methods evaluate the performance of classifiers (Ramachandra et al., 2012a). This is done through a comparison of kappa coefficients (Congalton et al., 1983) and the computation of overall accuracy assessment through a confusion matrix.

In this study stratified random sampling in ERDAS IMAGINE software was applied. This sampling technique can be a segmentation of the thematic map in to gird or appropriately into the category. A minimum of 20 samples per class to obtain classification accuracies ranging from 80 to 90 as recommended by Richards and De Leeuw (2006), were taken. The selection of a sample from the LULC map can be verified by ground truth data and comparing with Google Earth map see (Table 4.5).

Table 4. 5: Classification accuracy (Kappa statistics and overall accuracy) of the four LULC

| Class Name | 1990 | | 2000 | | 2010 | | 2019 | |
|---|---|---|---|---|---|---|---|---|
| | Pro.Acc (%) | Use.ACC (%) | Pro.Acc (%) | Use.ACC (%) | Pro.Acc (%) | Use.ACC (%) | Pro.Acc (%) | Use.ACC (%) |
| Agriculture | 100 | 80 | 100 | 100 | 100 | 100 | _ | _ |
| Bare Land | 76.47 | 81.25 | 78.95 | 93.75 | 71.43 | 83.33 | 80 | 80 |
| Built up | 85.71 | 100 | 100 | 100 | 100 | 100 | 100 | 77.78 |
| Fallow Land | 88.89 | 80 | 97.14 | 89.47 | 94.44 | 85 | 91.43 | 91.43 |
| Vegetation | 87.5 | 87.5 | 100 | 75 | 100 | 100 | 100 | 100 |
| Water | 100 | 100 | _ | _ | _ | _ | 100 | 100 |
| Overall Acc. | 85% | | 90% | | 86.67% | | 88.33% | |
| Kappa Stat. | 0.8083 | | 0.8156 | | 0.7558 | | 0.8079 | |

The results of the contingency analysis in Table 4.5 showed that the overall classification accuracies of the year 1990 LULC was 85.00% and overall Kappa statistics 0.808, in 2000 the overall accuracy was 90.00% and Kappa statistics was 0.816, in 2010 the overall accuracy was 86.67% and 0.756 Kappa statistics while in 2019 the overall accuracy was 88.33% and 0.808 Kappa statistics. So according to De Leeuw (2006), the kappa coefficient is rated as considerable.

## 4.3 Urban Landscape Structure Dynamics

### 4.3.1 Landscape Metrics

Landscape metrics quantify the pattern of the landscape within the designated landscape boundary only. Consequently, the interpretation of these metrics and their ecological significance requires an acute awareness of the landscape context and the openness of the landscape relative to the phenomenon under consideration. These concerns are particularly important for nearest-neighbor metrics. Based on the four classified LULC images (1990, 2000, 2010, and 2019) and further, the classified images were segmented based on 8 cardinal directions (N, E, S, W, SW, NW, NE and SE). The classified and cropped vector image were converted into raster format in ArcGIS software. Using the extracted cardinal raster image, the landscape pattern metrics were calculated with the help of FRAGSTAT software package. The Spatio-temporal pattern of the landscape is quantitatively described in the following two sections (i.e. landscape level and class levels).

A total of 15 landscape metrics both at class and landscape-level were chosen for this study. These are number of patches (NP), patch density (PD), class per cent of landscape (PLAND), largest patch index (LPI), landscape shape index (LSI), area-weighted mean patch fractal dimension (FRAC_AW), Shannon's diversity index (SHDI), contagion index (CONT), patch cohesion index (COHES), perimeter area fractional dimension (PAFRAC), interspersion and juxtaposition index (IJI), aggregation index (AI), and splitting index (SPLIT). All of these metrics are used to quantify and examine the spatiotemporal changes of landscape compositions and configurations (Landscape structure) for the study area (McGarical and Marks, 2002).

#### *(A) Landscape Metrics at the Landscape Level*

Landscape level indices represent the spatial pattern of the entire landscape mosaic, considering all patch types simultaneously. The indices can be interpreted more broadly as landscape heterogeneity indices and they measure the overall landscape pattern (McGarigal and Marks, 1995).

At the landscape level 8 landscape metrics were used (i.e. number of patches (NP), patch density (PD), largest patch index (LPI), landscape shape index (LSI), area-weighted mean patch fractal dimension (FRAC_AM), Shannon's diversity index (SHDI), contagion index (CONT), patch cohesion index (COHESION).

Table 4. 6: Landscape metrics at a landscape level from 1990 to 2019

| Year | NP | PD | LPI | LSI | FRAC AM | CONTAG | COHES | SPLIT | SHDI |
|---|---|---|---|---|---|---|---|---|---|
| **1990** | 2538 | 8.07 | 39.21 | 40.89 | 1.29 | 44.48 | 98.37 | 5.84 | 1.08 |
| 2000 | 2741 | 8.72 | 62.26 | 36.71 | 1.30 | 50.12 | 98.95 | 2.57 | 0.96 |
| 2010 | 2464 | 7.83 | 68.52 | 29.57 | 1.28 | 53.12 | 98.94 | 2.12 | 0.93 |
| 2019 | 4086 | 13.02 | 57.03 | 39.83 | 1.29 | 41.07 | 98.82 | 2.96 | 1.14 |

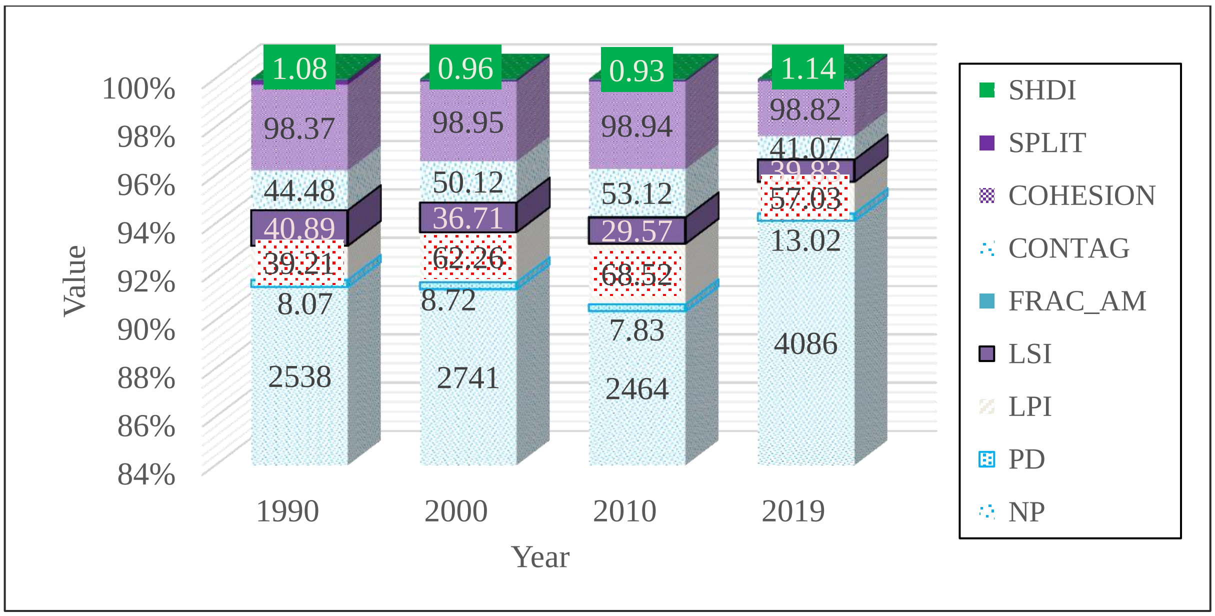


Figure 4. 4: Landscape composition at landscape level between 1990 and 2019

Table 4.4 shows the change in landscape pattern metrics at landscape level between 1990 and 2019. The number of patches increased from 1990 to 2000 (2538 to 2741). Similarly, from 2464 in 2010 to 4086 in 2019, whereas the NP decreased from 2741 in 2000 to 2464 in 2010). Patch density (PD) increased from 8.07% in 1990 to 8.72% in 2000 and after one decade (2000-2010 it decreases to 7.83 %. However, the PD increased from 7.83 in 2010 to 13.02 in 2019. Patch density increases exponentially as the irregularity of patch shape increases; yet, landscape connectivity decreases. These patterns were repeatedly supported for urbanizing landscapes throughout the world (Wu et al., 2011).

This suggests that increasing in NP and PD the urban landscape of Adama Town was fragmented especially from 2010 to 2019, while it was less fragmented during the year from 2000 to 2010.

Landscape shape index (LSI) increased from 39.21% in 1990 to 62.26% in 2000 and a slight increase to 68.52% in 2010, indicating considerable growth within the study area. However, this tendency changed in the second period, when the size of LPI decreased to 57.03%. This is characterized by the appearance of new, dispersed settlements (Araya and Cabral, 2010). Although the city has shown a slower urbanization rate in the third period; this pattern suggested that, the shape of the landscape as a patch mosaic became more irregular with urbanization.

The CONTAGION index increased from 44.48% in 1990 to 50.12% in 2000 and again increased to 53.12% in 2010, but it is reduced from 44.48% in 1990 to 41.07% in 2019. Besides, the largest patch index (LPI) significantly increased from 39.21 in 1990 to 57.03 in 2019.

The patch cohesion index (COHESION) showed a slight increment between 1990 and 2000 (98.37 to 98.95), but a slight reduction in the second and third decade (98.95 to 98.94) and (98.94 to 98.82) respectively. The LSI was maximum in the first period 40.89 (1990). It showed a decrement in 2000 and 2010 from 36.71 to 29.57 respectively, it was yet increased in the last period by 39.83.

Area-weighted mean fractal dimension index (FRAC_AW) showed a very slight increase in the first period (1900–2000), while a slight decrease in the second period (2000–2010) and in the third period (2010–2019). This indicates that shape complexity has become irregular over time and fragmentation processes have strengthened in the first and third period compared to the second period. Accelerated urbanization, including Human activities can result in landscape pattern fragmentation and more complex landscape structure.

Besides, SPLIT metrics substantially decreased from 5.84 in 1990 to 2.57 in 2000, and the decrease in the second period (2000–2010) was smaller than in the first period. Whereas, in the third period (2010–2019) the SPLIT showed a slight increment by 0.83, suggesting that ecological processes strengthened due to human disturbance in recent years. SHDI decrease from 1.08 from 1990 to 0.96 in 2000 and from 0.96 in 2000 to 0.93 in 2010, however SHDI increases from 0.93 in 2010 to 1.14 in 2019 as shown in Table 4.5.

The increase in landscape pattern metrics during the study period because of the fact that fragmentation of the landscape tended to strengthen (Huang et al., 2010) and spatial variability of the landscape increased in Adama Town in the last three decades. Moreover, the landscape pattern structure became more complex, as discerned in the following landscape metric changes from 1990 to 2019. Human activities, including urban expansion and population growth, can result in landscape pattern fragmentation and more complex landscape structure.

**(B) Landscape Metrics at Class level**

The class-level indices have a spatial feature to represent the spatial distribution and pattern as they measure the configuration of a particular patch type. The class level indices act as fragmentation indices because class level metrics provided more comprehensive information on the comparative contributions of individual configuration of a particular patch type (Ramachandra et al., 2013). In the present study, we have calculated the following eight class level metrics using FRAGSTATAS 4.2 software. These are: the percentage of landscape (PLAND), number of patches (NP), patch density (PD), largest patch index (LPI), interspersion and juxtaposition index (IJI), patch cohesion index (COHESION), perimeter area fractional dimension (PAFRAC) and aggregation index (AI).

Results of the time series landscape metrics at class level for the study area.

**Number of Patch:** NP is a type of metrics that describes the growth of particular patches whether in an aggregated or fragmented growth in the region and also explains the underlying urbanization. It ranges from 0 (Clumpiness) to 100 (fragmented). In general, When the number of patches increase the level of fragmentation will also increase and vice versa.

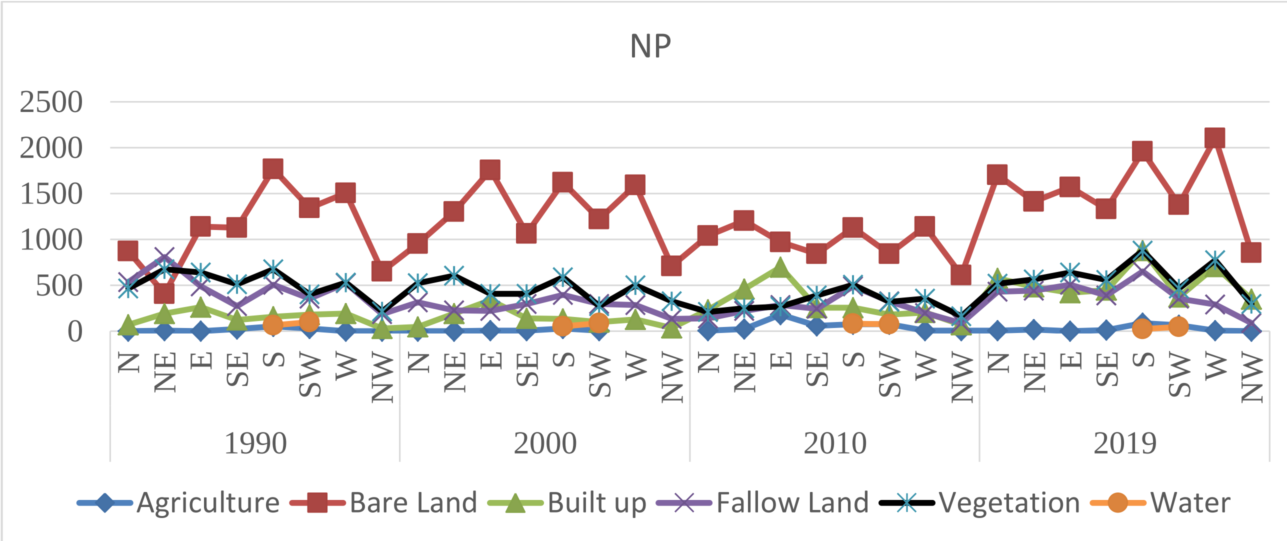


Figure 4. 5: The change of number of patches in eight directions from 1990 to 2019

The number of patches for built-up areas was increased from 159 during 1990 to 182 in 2000 and again increased to 275 in 2010, while in 2019 the NP was drastically increased to 715 about (160%). The maximum number of patches for the urban area was found to be 261 in 1990, 336 in 2000, 701 in 2010 in E direction and 878 in 2019 (S), while minimum NP for urban area were 29 in 1990, 35 in 2000, 74 in 2010 and 349 in 2019 in NW direction. This suggested that, an increase in the number of patches and patch density showed that, it is more fragmented towards disturbance as compared to other classes across the landscape due too many small numbers of patches.

The number of patches for vegetation areas decreased from 785 in 1990 to 745 in 2000 and a gain decreased to 486 in 2010 while in 2019 the NP was drastically increased to 858. The maximum number of patches for vegetation was obtained 674 (NE), 606 (NE), 508 (S) and 881 (S) in 1990, 2000, 2010 and 2019 respectively, while minimum NP for vegetation were obtained 215, 329, 166 and 269 (NW) direction in 1990, 2000, 2010 and 2019 respectively. This suggested that the vegetation areas were more fragmented in the NE and S direction compared to NW direction in the study period due to urban sprawl and as fallow land was more in this direction.

The number of patches for water bodies were minimum compared to other classes. The NP for water body decreased from 51 in 1990 to 40 in 2000 while in 2010 NP increased to 53 and again increased to 57 in 2019. The maximum number of a patch for water bodies were found to be 103, 87, 51, 83 (S) in 1990, 2000, 2019 and 2010 respectively, while minimum NP was observed in all direction except S and SW direction. The number of patches for bare land areas increased from 1067 in 1990 to 1510 in 2000 and decreased to 1320 in 2010, while in 2019 the number of patches increased to 2023. The maximum number of the patch for the bare land area 1768 S, 1759 E, 1204 NE and 1958 S during 1990, 2000, 2010 and 2019 respectively while minimum NP were 406 NE, 708 NW, 613 NW and 858 NW in 1990, 2000, 2010 and 2019 respectively.

The number of patches for agricultural areas increased from 19 in 1990 to 27 in 2000 and again increased to 87 in 2010 while in 2019 the NP decreased to 42. The maximum number of patches for agricultural areas are 54, 29, 87 (S) and 182 E directions during 1990, 2000, 2019 and 2010 respectively while minimum NP for agricultural land 4 and 6 during 2010 and 2019 respectively. While in 1990 and 2000 (W & NW); there is no agricultural land in the year 1990 and 2000 in the direction of W and NW.

The number of patches for fallow land areas decreased from 456 in 1990 to 237 in 2000 and increased to 243 in 2010, while in 2019 the NP increased to 395. The maximum number of the patch for the fallow land area was obtained 818 NE, 396, 489 and 652 in S direction during 1990, 2000, 2010 and 2019 respectively, while minimum NP was 187, 134, 90 and 91 in 1990, 2000, 2010 and 2019 respectively.

Generally, the highest number of patches was scored for bare land followed by vegetation and fallow land especially during 2019 in SE (818) direction. However, the minimum NP was scored for agricultural land 4(W) direction.

This suggested that the bare land followed by vegetation shows that very high fragmented towards disturbance compared to other classes across a landscape (Fig 4.5(a)). While, the agriculture land was aggregated.

**Patch Density (PD):** it is similar with NP but PD gives density about the landscape in analysis, as the number of patches increase so is the patch density.

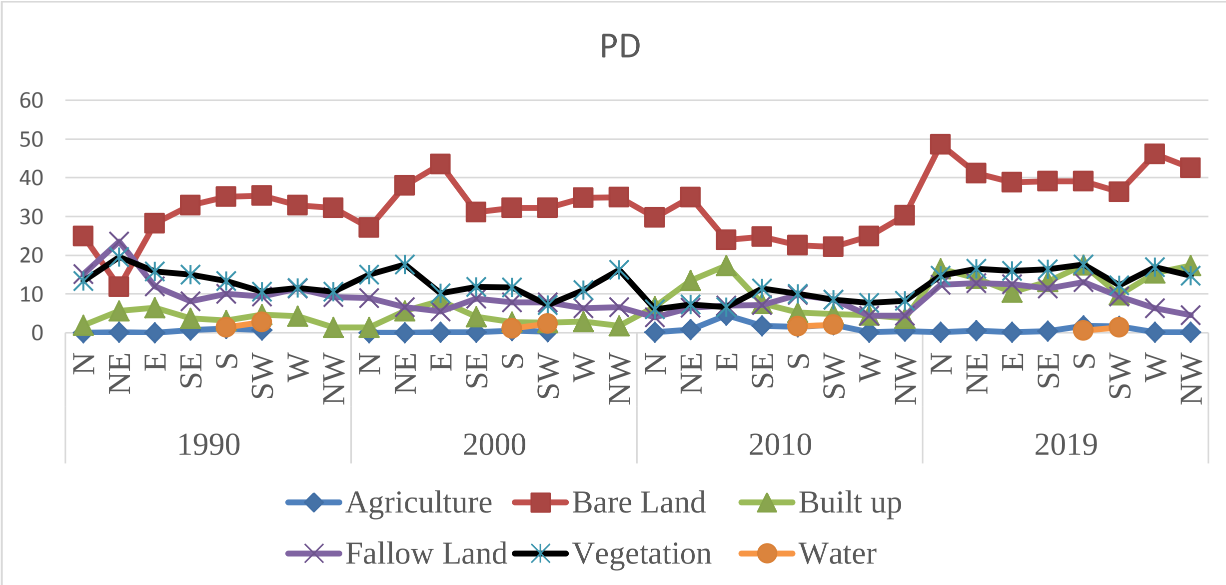


Figure 4. 6: The change of patch density in eight directions from 1990 to 2019

The patch density (PD) for built-up areas increased from 0.51 in 1990 to 0.58 in 2000, 0.87 in 2010 and increased to 2.28 (the highest increment in the study period for PD) in 2019. The maximum PD for built-up area was investigated 35.10 in 1990 (S), 43.13 in 2000 (E), 34.97 in 2010 (NE) and 48.56 in 2019 (N). while the minimum PD for built-up areas were 11.79 in 1990 (NE), 27.12 in 2000 (N), 22.11 in 2010 and 36.27 in 2019.

The patch density (PD) for vegetation areas decreased from 2.50 in 1990 to 2.37 in 2000, 1.55 in 2010 and increased to 2.72 in 2019. The maximum PD for vegetation area investigated 19.58 in 1990 (NE), 17.60 in 2000 (NE), 11.37 in 2010 (SE) and 17.60 in 2019 (S); while the minimum PD scored 10.62 in 1990 (NW), 7.22 in 2000, 6.03 in 2010 (N) and 12.21 in 2019.

The patch density (PD) for fallow land decreased from 1.45 in 1990 to 0.75 in 2000 and increased to 0.77 in 2010 and again increased to 1.26 in 2019. The maximum PD investigated 23.59 NE, 8.74 SE, 9.70 S and 13.03 S in 1990, 2000, 2010 and 2019 respectively. The minimum PD fallow land scored 8.06 in (SE) 1990, 5.48 in (E) 2000, 3.95 in (N) 2010 and 4.50 in (NW) 2019.

The patch density (PD) for bare land increased from 3.39 in 1990 to 4.80 in 2000 and again increased to 6.45 in 2019, while in 2010 PD decreased to 4.20. The maximum PD investigated 35.34 (S) and 35.10 (SW) in 1990, 43.43 (E) in 2000, 34.97 (E) in 2010 and 48.56 (E) in 2019.

The minimum PD bare land was scored 11.79 in (NE) 1990, 27.12 in (N) 2000, 22.11 (S) in 2010 and 36.27 (SW) in 2019.

There is no patch density (PD) for water bodies in all direction except in the S and SW directions with the maximum patch density of observed in the 2.7 in the SW direction during 1990 followed by 2.28 in the same direction during 2000. The patch density (PD) for agricultural land increased from 0.06 in 1990 to 0.09 in 2000, and again increased to 0.28 in 2010 while decreased to 0.13 in 2019. The maximum PD investigated 1.07 S, 0.58 S, 4.49 E and 1.74 S in 1990, 2000, 2010 and 2019 respectively. The minimum PD agricultural land was scored 0.13 W, 0.1 E in 2010 and 2019 respectively.

**Perimeter-Area Fractal Dimension (PAFRAC):** is a patch mosaic which provides an index of patch shape complexity across a wide range of spatial scales (i.e., patch sizes). PAFRAC approaches 1 for shapes with very simple perimeter such as square (indicating clumping of specific class) and approaches 2 for shapes with highly convoluted parameters. PAFRAC determines patch shape complexity across a wide range of spatial scale in class level metrics.

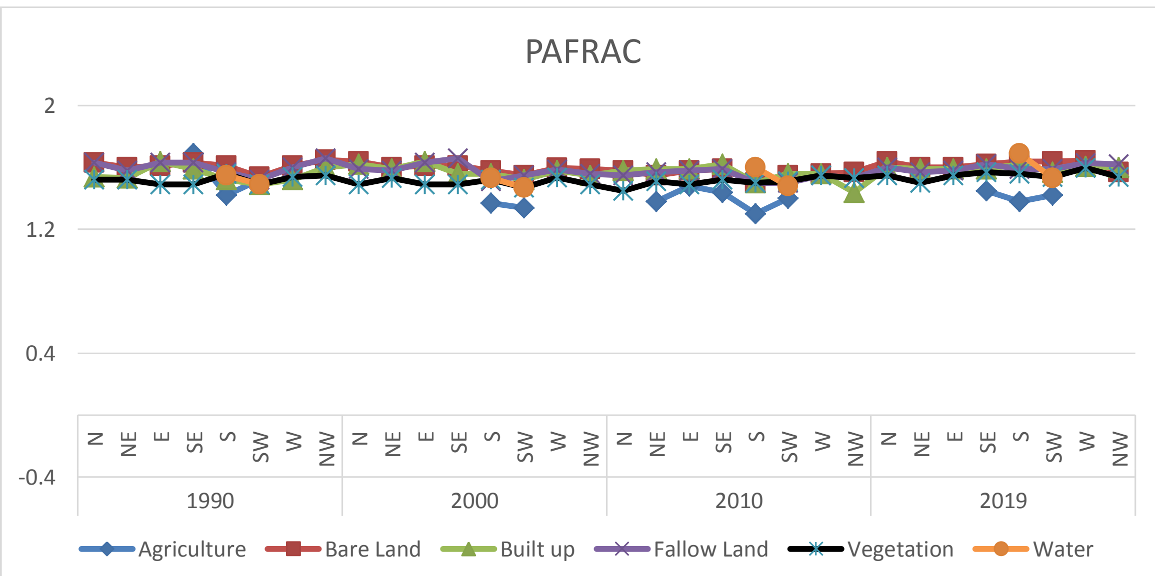


Figure 4. 7: The change of PAFRAC in eight directions from 1990 to 2019

The PAFRAC for the built-up area, shown in the table, increased in the first decade from 1.63 in 1990 to 1.68 in 2000 and increased in the second period to 1.67 in 2010. In the third period, it is similar to the second period for there is no change. The maximum of PAFRAC for the built- up area was 1.64 in (E) direction during 1990 and 2000, 1.62 (SE) in 2010 and 1.57 (W) in 2019. However, the minimum number of PAFRAC investigated 1.49 (SW), 1.52 (SW) and 1.62 (S) during 1990, 2000 and 2019 respectively.  This suggests the shape complexity of the town increases from time to time.

The PAFRAC for the water bodies increased in the first decade from 1.40 to 1.47, but in the second period it decreased to 1.40 but it was increased to 1.63 in the third period. The maximum of PAFRAC values for water bodies were 1.55, 1.53, 1.60 and 1.69 in S direction in 1990, 2000, 2010 and 2019 respectively; whereas the minimum number of PAFRAC investigated in all direction (0) except SW, and S directions in the study period.

The PAFRAC for agricultural land area shown in the table increased in the first decade from 1.43 to 1.45, while in the second period decreased to 1.42 and increased to 1.46 in the third period. The maximum of PAFRAC values for agricultural areas were 1.69 in E direction during 1990; 1.37 (S), in 2000; 1.48 (E) in 2010; and 1.56 (NE) in 2019.  But the minimum number of PAFRAC values were found in S, SE and SW, N, NW and NE directions for 1990, 2000 and 2010, 2019 respectively. This suggested that the shape complexity for agricultural land of the town is simple (not more complex).

The PAFRAC values for the vegetation classes as shown in the table (4.7C) increased in the first decade from 1.58 in 1990 to 1.61 in 2000 and decreased in the second period to 1.58 (2010). In the third period, it increased to 1.61. The maximum PAFRAC values of 1.56 in S direction during 1990 and 1.53 in NE during 2000, 1.55 (W) in 2010 and 1.60 (W) in 2019. But the minimum number of PAFRAC values include 1.49 (SW), 1.47 (SE), 1.45 (N) and 1.50 (N) during 1990, 2000, 2010 and 2019 respectively. This suggested that the shape complexity for vegetation cover of the town is more complex especially during 2000 and 2019 increased from time to time except in 2019 with a value of 1.61.

The PAFRAC for the fallow land area, shown in the table, increased in the first decade from 1.63 in 1990 to 1.68 in 2000 and again increased in the second period to 1.67 in 2010. In the third period it is similar to the second period for there is no change.

The PAFRAC for the bare land area, shown in the table, was almost similar in the study period and ranges between 1.65 and 1.67 in the class level. While in the direction wise the PAFRAC of bare land area shown maximum value of 1.59 in the North (N) and 1.64 in North West (NW) directions but the minimum values were found to be 1.50 in the South and 1.57 in the South-West direction. This suggested that the shape complexity for bare land was stretched with maximum in the N and NW while in the S and SW direction the shape complexity of bare land was minimally stretched.

**The patch cohesion index (COHESION**); measures the physical connectedness of the corresponding patch, and has a close relationship with habitat fragmentation. Patch cohesion increases as the patch type becomes more clumped or aggregated in its distribution; hence, it is more physically connected (Zhang et al., 2004).

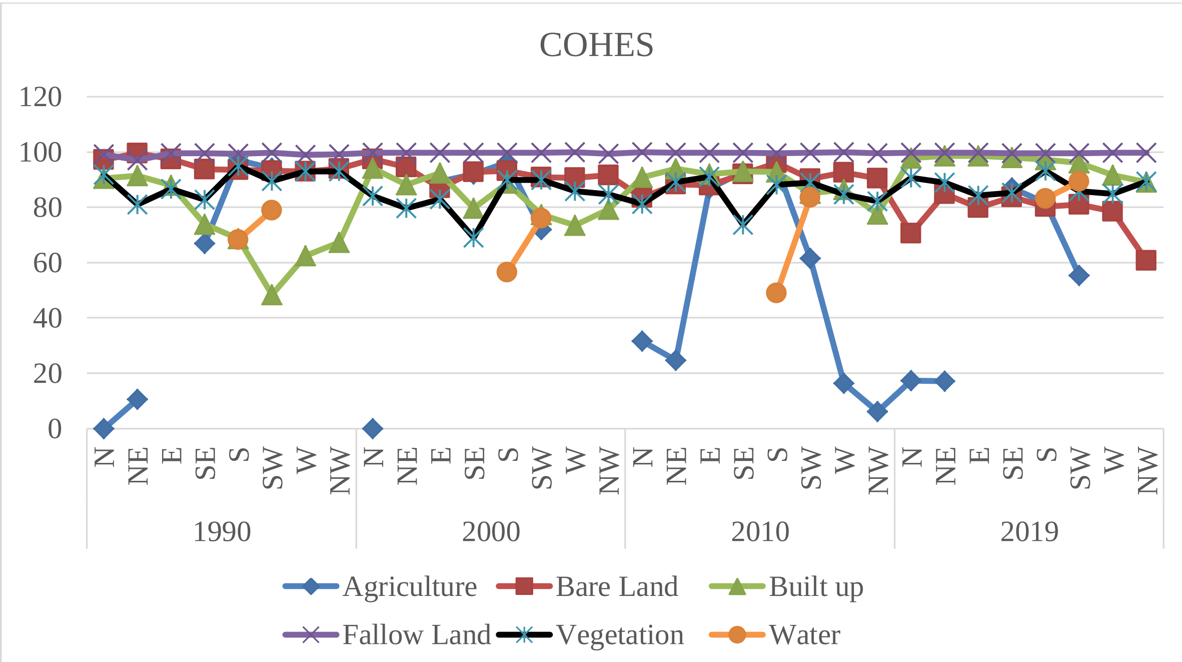


Figure 4. 8: The change of COHESION in eight directions from 1990 to 2019

The cohesion index for the built-up area increased during the study period from 89.36 in 1990 to 92.16 in 2000, 94.49 in 2010 and to 97.75 in 2019. The maximum COHESION index for the built-up areas were found to be 91.46 (NE), 94.20 (N), 93.86 (NE) and 98.57 (E) in 1990, 2000, 2010 and 2019 respectively. The overall study reveals that the year 2019 comprises the maximum COHESION in three decades.

The patch cohesion index (COHESION) for the water bodies decreased from 51.80 in 1990 to 46.14 in 2000, while increased in the second and third period to 54.51 and 62.56 respectively.

The maximum COHESION index for the water bodies were found to be 48.90 in the S and 89.40 in the SW directions but the minimum COHESION index of 0 was scored in all direction except in the S and SW. The COHESION index for vegetation decreased during the study period from 80.81 in 1990 to 71.13 in 2000 but increased to 74.82 in 2010 and again increased to 78.56 in 2019. The maximum cohesion index for vegetation was found 94.90 (S), 89.92 (SW), 91.09 (E) and 93.06 (S) in 1990, 2000, 2010 and 2019 respectively. The overall study reveals that the year 1990, especially in the south direction, comprises the maximum AI in three decades.

The patch cohesion index (COHESION) for the fallow land area increased from 99.41 in 1990 to 99.80 in 2000, again increased to 99.81 in 2010, while decreased to 99.73 in 2019.

The patch cohesion index for the bare land area decreased from 95.90 in 1990 to 89.27 in 2000, again decreased to 84.11 in 2010, and decreased to 65.75 in 2019. The maximum COHESION index for the bare land area were found to be 99.55 (NE), 97.38 (N), 96.00 (S) and 84.93 (NE) in 1990, 2000, 2010 and 2019 respectively. While the minimum values of COHESION were 92.98 W, 86.89 E, 83.49 N and 60.80 NW in 1990, 2000, 2010 and 2019 respectively.

The overall study reveals that the bare land comprises the maximum COHESION index in 1990. This suggested that the bare land was aggregated in its distribution; hence, more physically connected especially in the North and North-West directions compared to other years.

**Largest Patch Index (LPI):** The largest patch index (LPI): at class level computes the percentage of the total landscape are involved inside the largest patch. Independently, it is a straightforward to estimate for dominance (McGarigal and Marks, 2002). LPI equals the percentage of the landscape comprised by the largest patch.

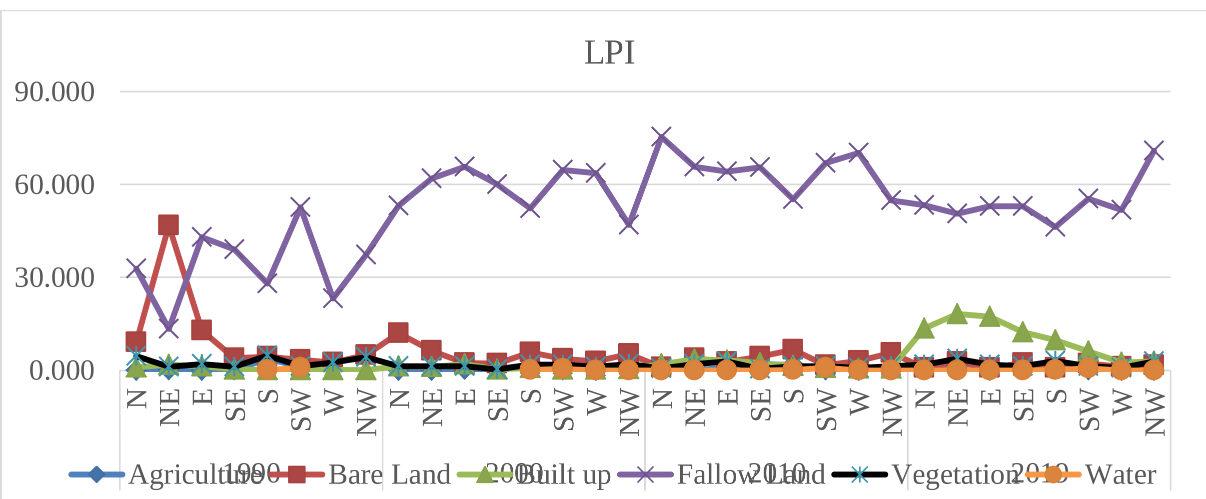


Figure 4. 9: The change of largest patch in eight directions from 1990 to 2019

The LPI for water bodies decreased from 0.1% in 1990 to 0.06% in 2000 but it was increased to 0.1% in 2010 and decreased to 0.08 in 2019. The maximum LPI values were 0.02 and 0.74) in the S and SW direction respectively. While the minimum LPI values were observed in all direction except in the S and SW directions.

The LPI for bare land area were decreased from 10.21% in 1990 to 3.12% in 2000. It also decreased to 1.73% in 2010 and also decreased to 0.31% in 2019. The maximum LPI values were found to be 46.75% (NE), 12.01 (N), 6.60 (S) and 2.60 (NE) direction in 1990, 2000, 2010 and 2019 respectively. But the minimum LPI values were found to be 2.57% (W), 2.15% (E), 1.01% (N) and 0.80 (S) in 1990, 2000, 2010 and 2019 respectively.

The LPI for the built-up area was increased from 1.09% in 1990 to 1.38% in 2000 and again increased to 2.84% in 2010 while during 2019 the LPI for the built-up area was further increased to 11.27%. The maximum LPI values from this analysis include 1.79 (NE), 2.03 (E), 3.57 and 18.22 in NE direction during 1990, 2000, 2010 and 2019 respectively. But the minimum LPI values were 0.07 (SW), 0.24 (W), 0.6 (NW) and 2.47 (W) in 1990, 2000, 2010 and 2019 respectively.

The LPI for vegetation class was decreased from 0.81% in 1990 to 0.28% in 2000, increased to 0.67% in 2010 and increased to 0.69% in 2019. The maximum LPI was investigated 4.77 (S), 2.05 (NW), 2.93 (E) and 3.64 (NE) during 1990, 2000, 2010 and 2019 respectively. While the minimum LPI were found to be 1.17, 0.26, 0.38 (SE) and 0.73 (W) in 1990, 2000, 2010 and 2019 respectively.

The LPI for the fallow land area increased from 39.21% in 1990 to 62.26% in 2000 and again increased to 68.52% in 2010, but it was decreased to 57.03% in 2019. The maximum LPI values were found 52.73 (SW), 65.77 (E), 75.38 (N) and 70.87 (NW) directions in 1990, 2000, 2010 and 2019 respectively. While the minimum LPI values were found to be 13.30 (NE), 46.97 (NW), 54.82 (NW) and 46.33 (S) in 1990, 2000, 2010 and 2019 respectively.

The LPI for the agricultural land area was decreased from 0.65% in 1990 to 0.53% in 2000 and again decreased to 0.45% in 2010 similarly, the LPI was decreased to 0.06% in 2019. The maximum LPI were found to be 3.68% (S), 1.88% (S), 1.86% (S) and 0.36 (SE) during 1990, 2000, 2010 and 2019 respectively.

**Interspersion and Juxtaposition Index (IJI).** According to (McGarical and marks, 1994). IJI measures the extents to which patch types are interspersed. Higher values (IJI=100) result when the urban patch types are well interspersed (i.e., equally adjacent to each other), whereas lower values characterize landscapes in which the patch types are poorly interspersed i.e., disproportionate distribution of patch type adjacencies (IJI=0): IJI is undefined and reported as “NA” in the “base name”. Full file as a dot in the “base name”. Class file if the number of patch types is less than 3.

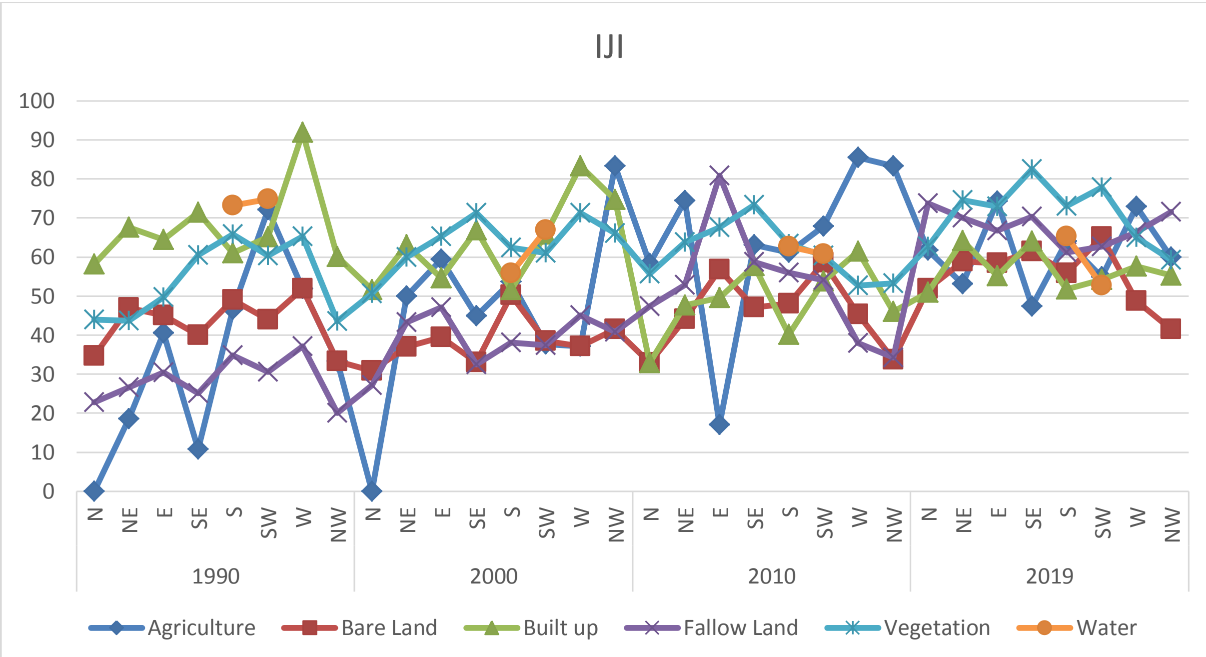


Figure 4. 10: The change of IJI in eight directions from 1990 to 2019

IJI for the water bodies was decreased from 79.19 in 1990 to75.27 in 2000 and again decreased to 72.55 in 2010 while IJI in 2019 was increased to 74.73. The maximum IJI was between 52 and 74.8 in S and SW direction respectively while the minimum IJI values were observed except for the S and SW directions.

IJI for the built-up area was decreased from 61.78 in 1990 to 53.46 in 2000 and again decreased to 49.16 in 2010, while IJI in 2019 for the built-up area was increased to 51.5. The maximum IJI for the built-up area was 91.90, 83.32 and 61.49 in W direction during 1990, 2000 and 2010 respectively and 64.22 (NE) in 2019. While the minimum IJI was 58.15, 51.56, 32.94 and 50.97 during 1990, 2000, 2010 and 2019 respectively. This suggested that the built-up area was poorly interspersed during 2010 and 2019 compared to 1990 and 2000.

The interspersion and juxtaposition index (IJI) for vegetation area was increased from 57.87 in 1990 to 60.37 in 2000 and again increased to 62.17 in 2010 and increased to 69.54 in 2019.

The increasing IJI values during the study periods shows that interspersion between adjacent patches will be increased. The maximum IJI values were 65.84 (S), 71.35 (W), 73.34 (SE) and 82.52 (SE) during 1990, 2000, 2010 and 2019 respectively while the minimum IJI was 43.72 (NE), 50.66 (N), 52.73 (W) and 62.62 (N) during 1990, 2000, 2010 and 2019 respectively. This suggested that the vegetation area was poorly interspersed during 1990 and 2000 compared to other years.

IJI for the fallow land area was increased from 31.18 in 1990 to 38.50 in 2000 and again increased to 54.37 in 2010, while IJI in 2019 for the fallow land area was significantly increased to 99.81. The maximum IJI values were 37.17 (W), 47.05 (E), 80.80 (E) and 73.77 (N) in 1990, 2000, 2010 and 2019 respectively. But the minimum IJI values were 20.08 (NW), 27.18 (N), 34.32 (NW) and 61.13 (S) in 1990, 2000, 2010 and 2019 respectively. This shows that the fallow land area was poorly interspersed during 1990 and 2000 compared to other years. However, during 2010 it was well interspersed (i.e., equally adjacent to each other).

IJI for the agricultural land area was decreased from 64.04 in 1990 to 61.76 in 2000 and again decreased to 52.56 in 2010, while IJI in 2019 for the agricultural land area was significantly increased to 77.34. The maximum IJI values were 72.08 (SW), 59.44 (E), 85.53 (W) and 74.27 (E) in 1990, 2000, 2010 and 2019 respectively. But the minimum IJI values were 17.06 (E) and 47.42 (SE) in 2010 and 2019 respectively. This shows that the agricultural land was poorly interspersed during 2010 compared to other years. However, during 2019 the agricultural land was well interspersed (i.e., equally adjacent to each other).

IJI for the bare land area was decreased from 39.79 in 1990 to 36.16 in 2000, while in the second decade the IJI of bare land was increased to 43.82 and again in the third decade also increased to 51.95. The maximum IJI values were 51.91 (W), 50.22 (S), 58.53 (SW) and 65.18 (SW) in 1990, 2000, 2010 and 2019 respectively while the minimum IJI values were 33.33 (NW), 30.90 (N), 32.96 (N) and 41.49 (NW) in 1990, 2000, 2010 and 2019 respectively. This shows that the bare land area was poorly interspersed during the study period (i.e. not equally adjacent to each other).

**Proportion of Land (PLAND);** PLAND is fundamental measures of landscape composition; specifically, how much of the landscape is comprised of a particular patch type.

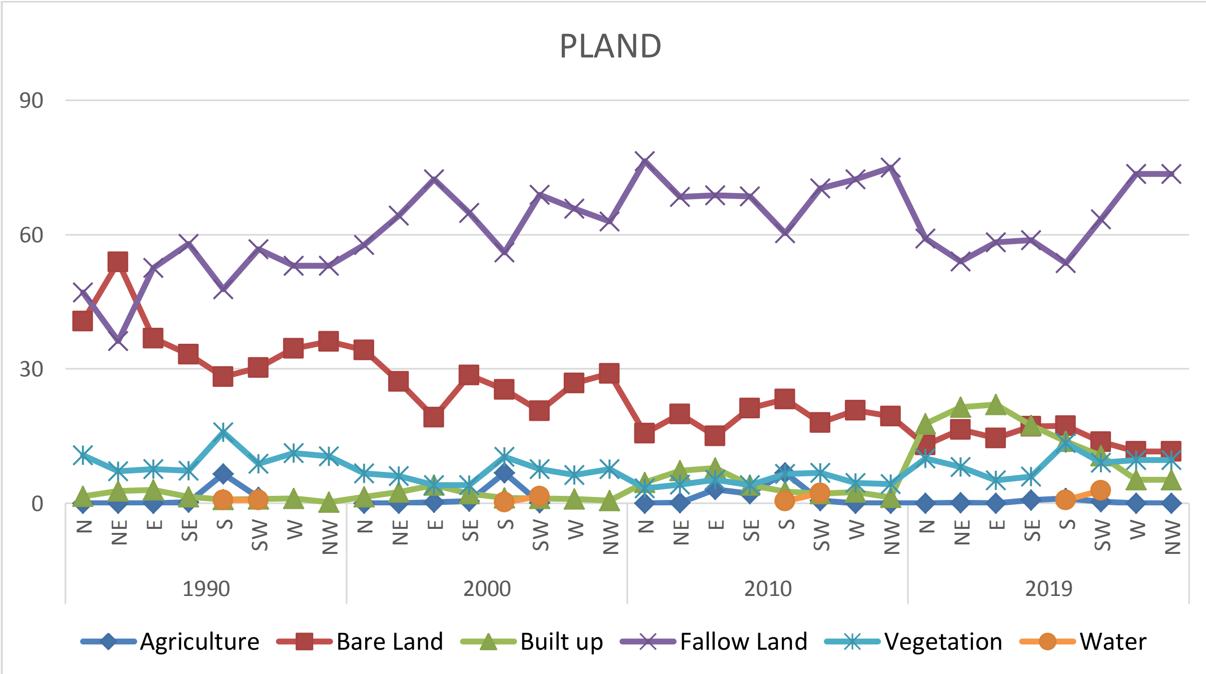


Figure 4. 11: The change of PLAND in eight directions from 1990 to 2019

PLAND for the built-up area of Adama town was increased from time to time especially in the latest decade (2019). The PLAND increases from 1.76% in 1990 to 2.23% in 2000, to 4.37% in 2010, while in 2019 the PLAND was drastically increased to 15.33%. The maximum PLAND values for built-up area were found to be 2.94 (E) in 1990, 4.1 (E) in 2000, 7.21 (NE) in 2010 and 21.44 (NE), while minimum PLAND values were 0.26, 0.56, 1.26 in the NW direction and 5.19 in NW and W during 1990, 2000, 2010 and 2019 respectively.

PLAND for vegetation cover of Adama town was decreased in the first and second period while in the third period the vegetation cover was increased. The PLAND decreases from 9.81% in 1990 to 6.48% in 2000, to 4.84% in 2010, while in 2019 the PLAND was increased to 8.77%. The maximum PLAND for vegetation were 15.79 (S) in 1990, 10.35 (S) in 2000, 6.80 (N) in 2010 and 13.42 (S) in 2019 while the minimum PLAND was scored 7.20 (NE), 4.10 (E & SE), 3.33 (N) and 5.13 (E) direction in 1990, 2000, 2010 and 2019 respectively.

PLAND for fallow land area was increased in the first and second decade except in the third decade (2010_2019). The PLAND for fallow land increases from 51.78% in 1990 to 64.32% in 2000, to 70.64% in 2010, while in 2019 the PLAND was decreased to 59.99%. The maximum PLAND for fallow land area was observed 57.87 (E) in 1990, 72.35 (E) in 2000, 76.46 (N) in 2010 and 73.57 (W & NW), while minimum PLAND was scored 36.22% NE, 62.90% NW, 60.28% S and 53.59% S in 1990, 2000, 2010 and 2019 respectively.

PLAND for the agricultural land area was decreased from 1.24% to 1.19 in 1990 and 2000 and increased to 1.82% in 2010 while in 2019 decreased to 0.33%. The maximum PLAND for the agricultural land area was observed 6.58%, 6.76%, 6.81% and 1.11% (S) in 1990, 2000, 2010 and 2019 respectively. While minimum PLAND was scored 0% in the W and NW direction in 1990 and 2000.whlie the minimum PLAND was scored 0.02 in W direction and 0.01 in E during 2010 and 2019 respectively.

PLAND for the bare land area was decreased time to time during the study period. The PLAND for bare land was decreased from 35.09% in 1990 to 25.56% in 2000 and again decreased to 17.97% in 2010 and 15.03% in 2019. The maximum PLAND for bare land area was observed 53.86% (NE) in 1990, 34.22% (N) in 2000, 23.26% (S) in 2010 and 17.29% (S) and 17.12% (SE) in 2019. While minimum PLAND was scored 28.28% S, 19.24% E, 14.98% E and 13.03% N in 1990, 2000, 2010 and 2019 respectively.

PLAND for water bodies was minimum in the study area and decreased from 0.33% in 1990 to 0.22% in 2000, while in the second and third period, the PLAND of water was increased to 0.37 and 0.55 respectively. The maximum PLAND for water bodies was observed in S and SW direction ranges between (0.25_2.84) in the study period. And minimum in all direction except S and SW direction.

**Aggregation Index (AI)**; gives the similar indication as Clumpiness i.e., it measures the aggregation of the urban patches, ranges from 0 to 100. Values closer to zero indicate disaggregation and values closer to 100 indicate aggregated growth of the urban areas.

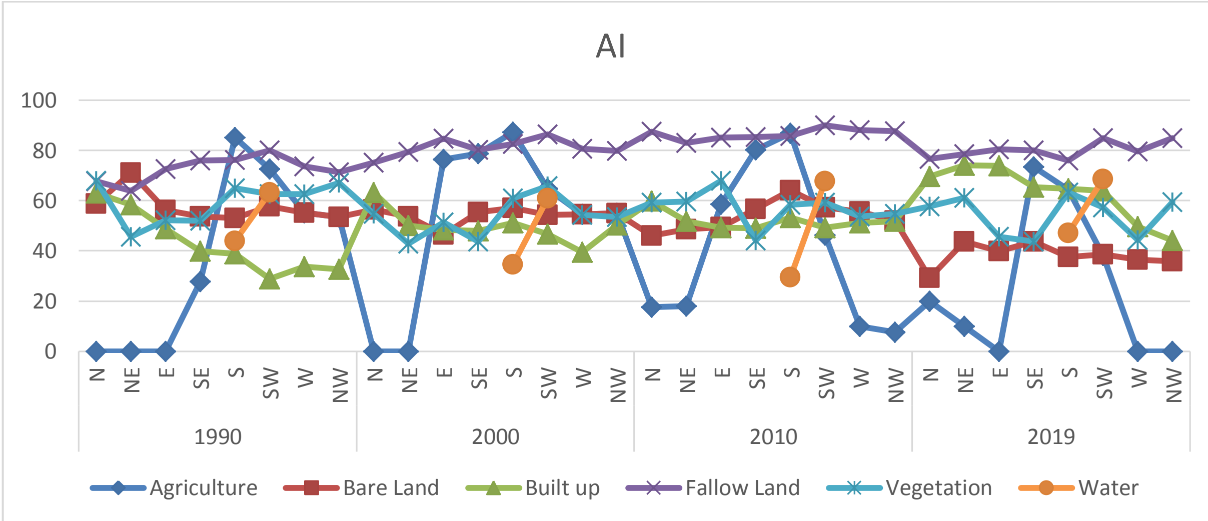


Figure 4. 12: The gradient change of AI in eight directions from 1990 to 2019

The aggregation index (AI) for water bodies was decreased in the first decade from 39.15 in 1990 to 32.26 in 2000, while increased to 41.15 in 2010, while in the third period AI was decreased to 34.73. The maximum value of AI was obtained in SW and S (29.4_68.5) and the minimum AI was obtained (0) in all direction except S and SW direction.

The aggregation index (AI) for bare land was decreased in the first decade from 50.54 in 1990 to 41.89 in 2000 and again decreased to 39.54 in 2010, in 2019 AI was decreased to 74.33. The maximum value of AI was obtained 71.02 NE, 57.08 S, 64.10 S and 43.68 SE &NE directions of the Town during 1990, 2000, 2010 and 2019 respectively. The minimum AI was obtained 53.12 S, 46.42 E, 46.14 N and 29.20 N in 1990, 2000, 2010 and 2019 respectively.

The aggregation index (AI) for built up was decreased in the first decade from 48.51 to 43.44, 1990 and 2000 respectively, while in the second period AI was increased from 43.44 to 48.71 and again increased to 57.30 in 2010 and 2019 respectively. The maximum value of AI was obtained 63.09, 63.16 and 59.87 in N direction of the town during 1990, 2000 and 2010 respectively. While in 2019 the maximum AI was 74.12 in NE direction. The minimum AI was obtained 28.76 SW in 1990, 39.48W in 2000, 48.96 SE in 2010 and 44.14 NW in 2019.

The aggregation index (AI) for vegetation was decreased in the first decade from 45.28 in 1990 to 34.57 in 2000, while in the second period AI was increased to 40.84 in 2010 and in the third period AI was decreased to 40.16. The maximum value of AI was obtained 67.95 (N), 65.88 (S), 59.71 (NE) and 63.23 (S) directions of the town during 1990, 2000, 2010 and 2019 respectively. The minimum AI was obtained 45.59 (NE), 42.93 (NE), 44.06 (SE) and 43.77 (SE) in 1990, 2000, 2010 and 2019 respectively.

The aggregation index (AI) for fallow land was increased in the first decade from 69.09 in 1990 to 76.55 in 2000 and again increased to 83.29 in 2010, while in the third period AI was decreased to 74.33. The maximum value of AI was obtained 80.09, 86.47, 90.10 and 85.01 in SW directions of the Town during 1990, 2000, 2010 and 2019 respectively. The minimum AI was obtained 63.94 NE, 75.23 N, 82.93 NE and 75.90 S in 1990, 2000, 2010 and 2019.

The aggregation index (AI) for agricultural land was increased in the first decade from 69.09 in 1990 to 76.55 in 2000 and again increased to 83.29 in 2010, while in the third period AI was decreased to 74.33. The maximum value of AI was obtained 80.09, 86.47, 90.10 and 85.01 in SW directions of the Town during 1990, 2000, 2010 and 2019 respectively. The minimum AI was obtained 63.94 NE, 75.23 N, 82.93 NE and 75.90 S in 1990, 2000, 2010 and 2019.

## 4.4 Urban Sprawl Dynamics

According to many scholars which are cited in the previous studies, urban sprawl is a complex and multidimensional phenomenon (O'neill et al., 1988; Singer et al., 2005; Ewing et al., 2002; Gulster et al., 2011 and Mubaraka et al, 2011). It is a form of spatial development, mainly found in open and rural lands on the edge of metropolitan areas; it is characterized by low densities, scattered and discontinuous “leapfrog” expansion and segregation of land uses, strip-malls and the massive use of private vehicles.

Urban sprawl was measured using density gradient (population, built up) and Shannon’s entropy.

### 4.4.1 Built-Up Density

Built-up density is the ratio of the urbanized (built-up) area to the total landscape area at any point in time. It simply indicates quantitatively how dense the urban area is, irrespective of the location of urban patches within the administrative boundary.

Table 4. 6: Built up density of Adama Town from 1990 to 2019

| Zone | 1990 | 2000 | 2010 | 2019 |
|---|---|---|---|---|
| N | 0.019 | 0.03 | 0.052 | 0.188 |
| NE | 0.032 | 0.041 | 0.078 | 0.218 |
| E | 0.032 | 0.043 | 0.081 | 0.226 |
| SE | 0.016 | 0.034 | 0.045 | 0.183 |
| S | 0.009 | 0.017 | 0.028 | 0.147 |
| SW | 0.01 | 0.018 | 0.023 | 0.115 |
| W | 0.011 | 0.02 | 0.026 | 0.083 |
| NW | 0.007 | 0.009 | 0.019 | 0.062 |

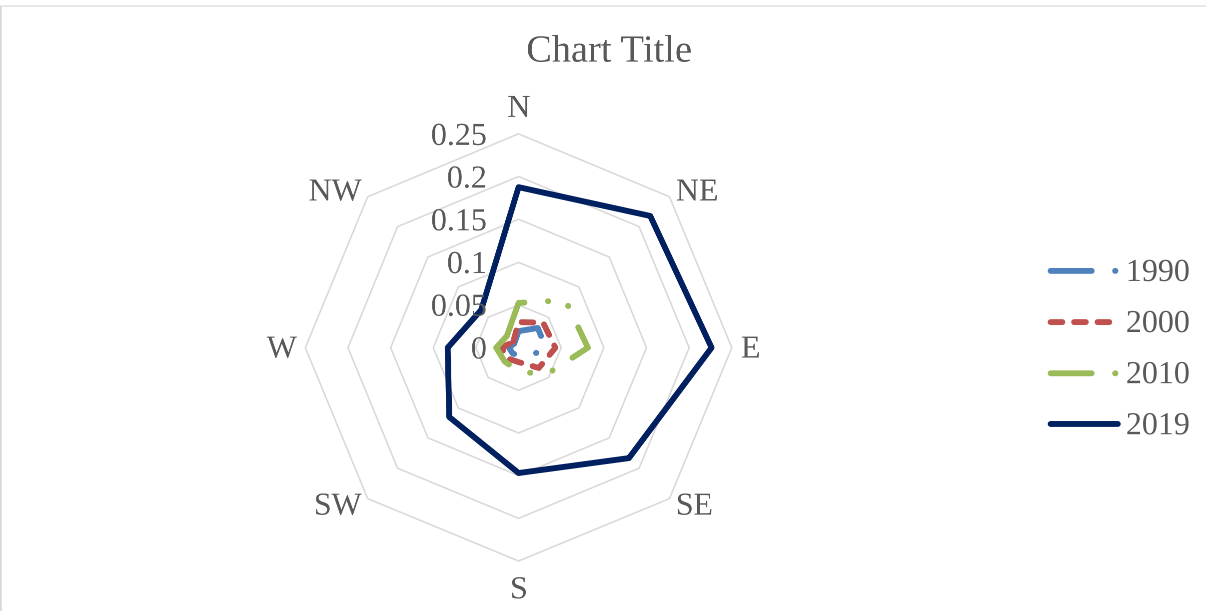


Figure 4. 13:: A spider chart of built-up density of Adama Town

From 1990 to 2019, Adama town showed a high increase in the built-up areas. After 1990, the Central district shows a fairly constant urban density and following a similar pattern. A marked increase in the built-up density was noted from the year 2010 to 2019 especially in the N, E, NE and SE directions. From 1990 to 2010, the urban density has not been changed much except for a considerable increase in all direction except in E direction.

Built up density was minimal and the value ranges from 0.022 (considering 2km buffer) to 0.062 (without buffer) in the North West direction in 1990. There was a sharp growth in the region in almost all direction from 1999 till 2009, maximum value reaching 0.289 in the E direction (considering 2km buffer) and 0.226 (without considering the buffer) (Table 4.6)
From 1990 to 2019, Adama town showed a high increase in the built-up area. After 1990, the Central district shows a fairly constant built-up density compared to fringe zone (2km buffer) and following a similar pattern. From 1990 to 2010, the built-up area density has changed in all directions except in E the direction. A marked increase in the built-up density was noted from the period 2010– 2019 especially in the N, E, NE and SE directions.

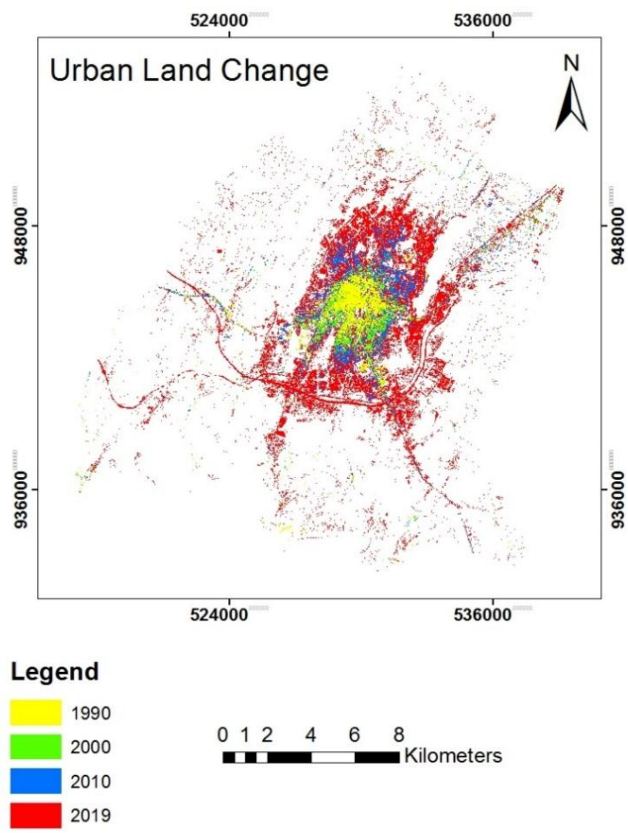


Figure 4. 14:: Built up change map of Adama Town between 1990 and 2019

The total population within the study area was increased by 57.68% between 1990 and 2000, while urbanized areas increased by 19.61%, between 2000 and 2010. The population increased by 57.97% and urban growth by 144.60% between 2010 and 2019; population increased by 64.97% whereas urban growth increased by 251.16%. The comparison clearly indicates that the growth rate of urbanized areas is always higher than the growth rate of population, during all time except in the first decade (Fig 3.2).

Table 4.7: Calculation of Shannon's Entropy for Adama Town

| Zone | Urban area in km^2 | | | | Area of districts km^2 | ) | | | |
|---|---|---|---|---|---|---|---|---|---|
| | 1990 | 2000 | 2010 | 2019 | | 1990 | 2000 | 2010 | 2019 |
| N | 0.717 | 0.727 | 1.923 | 6.928 | 36.893 | 0.077 | 0.077 | 0.156 | 0.314 |
| NE | 1.186 | 1.129 | 2.862 | 7.956 | 36.577 | 0.112 | 0.107 | 0.200 | 0.331 |
| NW | 0.148 | 0.206 | 0.404 | 1.339 | 21.686 | 0.034 | 0.044 | 0.074 | 0.172 |
| S | 0.452 | 0.675 | 1.457 | 7.630 | 51.995 | 0.041 | 0.056 | 0.100 | 0.282 |
| SE | 0.578 | 0.851 | 1.621 | 6.568 | 35.852 | 0.067 | 0.089 | 0.140 | 0.311 |
| SW | 0.383 | 0.467 | 0.908 | 4.606 | 39.927 | 0.045 | 0.052 | 0.086 | 0.249 |
| E | 1.369 | 1.821 | 3.428 | 9.553 | 42.340 | 0.111 | 0.135 | 0.204 | 0.336 |
| W | 0.527 | 0.541 | 1.259 | 3.968 | 47.770 | 0.050 | 0.051 | 0.096 | 0.207 |

The comparison clearly indicates that the growth rate of urbanized areas is always higher than the growth rate of population, during all the time except in the first decade. Shannon entropy analysis was performed based on directions. Shannon entropy computed using temporal data are listed in Table 4.7. Adama is experiencing the highest sprawl in all directions during 2019 as entropy values are closer to the threshold value (log (8) = 0.9). Lower entropy values of 0.034 (NW), 0.041 (S) during 1990 and 0.044 (NW), 0.051 (W) and 0.056 (S) during 2000 shows an aggregated growth as most of the urbanization were concentrated at Town. However, the region experienced dispersed growth in 2019 reaching higher values of 0.336 (E), 0.332 (NE), 0.314(N) in 2019.

The Shannon's entropy computed for the Town (without buffer regions) shows the sprawl phenomenon at peripheries. However, entropy values are comparatively lower when buffer region is considered. Shannon's entropy values of recent time confirmed a minimal fragmented and dispersed urban growth in the city. This also illustrates the influence of drivers of urbanization in various directions.

Table 4. 7: Total Shannon’s entropy

| YEAR | SHANNON'S ENTROPY |
|---|---|
| 1990 | 0.535 |
| 2000 | 0.612 |
| 2010 | 1.053 |
| 2019 | 2.203 |

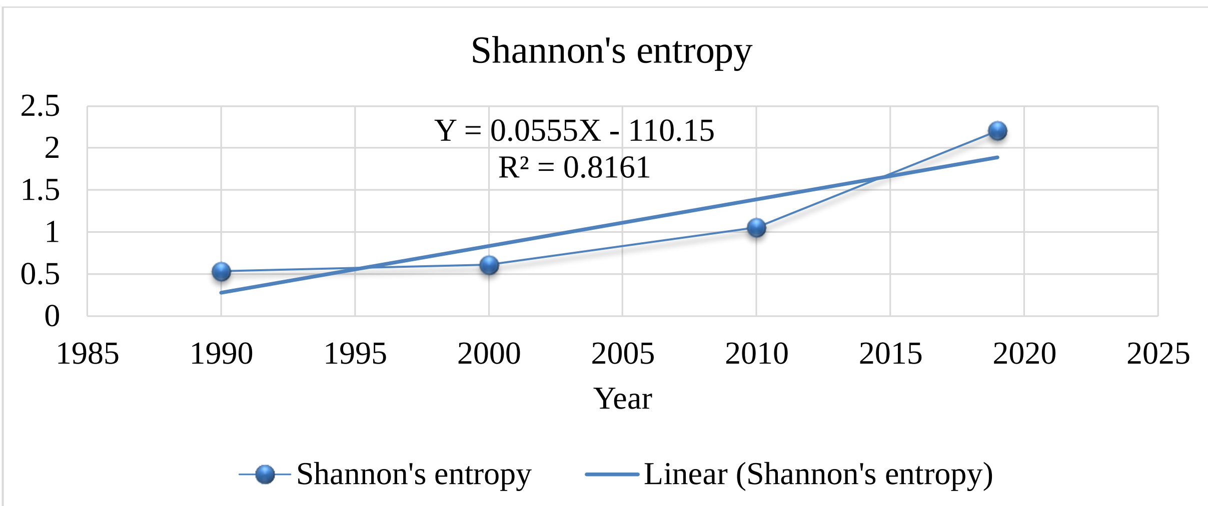


Figure 4. 15: Shannon’s Entropy trend line from 1990 to 2019

Entropy value has increased from 0.535 in the year 1990 to 0.612 in the year 2000. Further, an increase from 0.612 in the year 2000 to 1.053 in the year 2010 and extremely increased to 2.203 in 2019. This increase in the value of entropy indicates an increase in dispersion of built-up area, which is an indication of urban sprawl especially during 2019 Adama was faced to urban sprawl compared to other years. The closer to the upper limit of (log n) i.e. 0.9 the more dispersion is the built-up area in the region. A higher value of overall entropy for the whole urban area represents a higher dispersion of impervious area which is a sign of urban sprawl (O'neill et al., 1988). Increase in dispersion is due to new areas being added. Hence it can be concluded that Shannon’s entropy is a useful and effective tool for identifying the urban sprawl phenomenon in terms of dispersion of the impervious (built-up) area.

The difference in entropy between two different periods of time can also be used to indicate the change in the degree of dispersion of land development or urban sprawl (Sudhira et al. 2004).

$\Delta Hn = Hn\,(t + 1) - Hn\,(t)$

$\Delta Hn = Hn\,(2000) - Hn\,(1990) = 0.612 - 0.535 = 0.077$

$\Delta Hn = Hn\,(2010) - Hn\,(2000) = 1.053 - 0.612 = 0.441$

$\Delta Hn = Hn\,(2019) - Hn\,(2010) = 2.203 - 1.053 = 1.150$

To understand the dynamics of urban sprawl, it is necessary to analyze the increase in built-up areas and population growth.

Table 4. 8: Rate of Urban Growth in Adama in 1990, 2000, 2010 and 2019

| POP1 | POP2 | POP3 | POP4 | Population growth rate | | |
|---|---|---|---|---|---|---|
| 1990 | 2000 | 2010 | 2019 | R=ln(P2/P1)/T *100 | R=ln(P3/P2)/T *100 | R=ln(P4/P3)/T *100 |
| 104464 | 164716 | 260203 | 429266 | 4.55% | 4.57% | 10.64% |

According to the first official census in 1990, the population of Adama Town was 104,464. During 1990–2019-time interval, land development and other economic plans in Adama encouraged a great number of people to migrate to urban areas. During 2000 the population of Adama was 164716. After 2015 population revolution and a considerable number of people migrated from village and rural areas to Towns see table 4.8. The annual population growth rate in this city was 4.55% between 1990 and 2000, 4.57 between 2000 to 2010 and 10.64 between 2010 and 2019. Population became 260,203 in 2019 with annual population growth rate equal to 10.64%.

Table 4. 9: Rate of Population Growth in Adama in 1990, 2000, 2010 and 2019

| URB A(U1) | URB A(U2) | URB A(U3) | URB A(4) | URBAN Growth Rate | | |
|---|---|---|---|---|---|---|
| 1990 | 2000 | 2010 | 2019 | R=ln(U2/U1) | R=ln(U3/U2) | R=ln(U4/U3) |

| | | | | | | |
|---|---|---|---|---|---|---|
| | | | | /T*100 | /T *100 | /TT 100 |
| 538.68 | 644.30 | 1382.67 | 4855.34 | 1.79% | 7.64% | 13.96% |

The horizontal rate of increase in built-up areas mentioned in (Table 4.9) is considered the independent factor Y for the simple linear regression analysis. The Population annual growth rate was considered the dependent factor X. A linear regression analysis was conducted with the 4 observations to model the relationship between the increase in built-up area as the dependent variable (Y) and the independent variable population growth (X).

Data was available for the period between 1990 and 2019 and the urban area growth rate (Y) as well as population annual growth rate for the period between 1990 and 2019. A positive linear correlation exists and the linear regression equation is Y= 1.5229X- 2.2343. The multiple R = 0.878 and the coefficient of determination (co-variance) R square = 0.7714 and the adjusted R square is 0.543 with the standard error of 4.115. This shows that population growth have a significant role in the sprawl phenomenon, as can be understood from the positive correlation coefficients (Effat and El Shobaky, 2015)Table 4.10.

Table 4. 10: An APA style correlation of urban growth and population growth

| | ***Population Growth*** | ***Urban Growth*** |
|---|---|---|
| **Population Growth** | 1 | |
| ***Urban Growth*** | 0.878 | 1 |

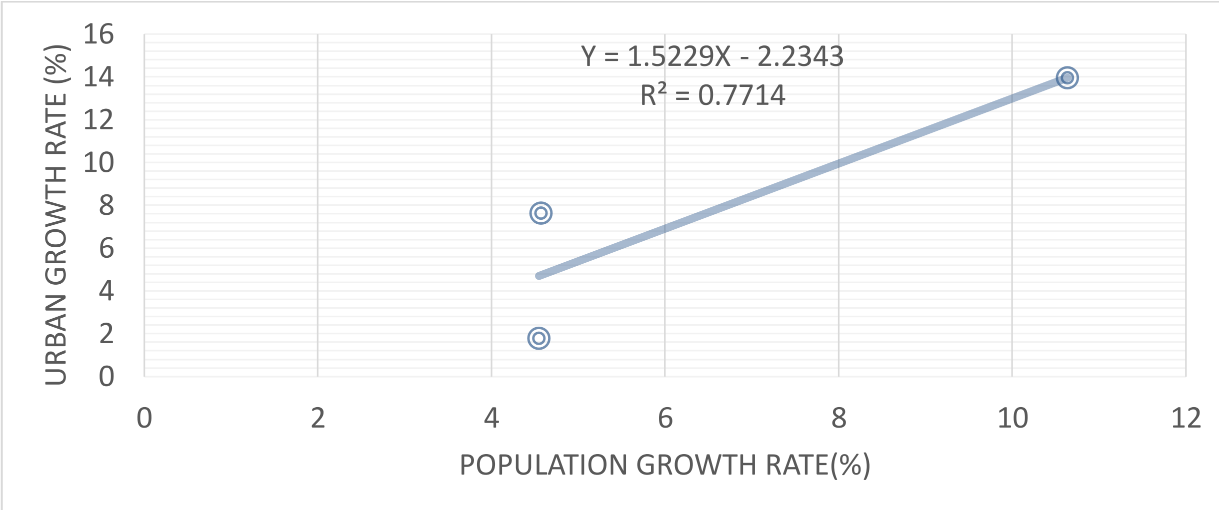


Figure 4. 16: Regression line and equation analysis between urban growth and population growth

## 4.5 Spatial Patterns of Urbanization

The transformation of urbanized areas is generally related to population dynamics (Sudhira et al., 2004) that drives the built-up area to expand. Verburg et al. (2001) related the physical growth of a city directly to its population growth as an increase in population size that encouraged the agglomeration of businesses and new urban development. Moreover, the presence and accessibility of transportation routes force patterns of urban growth. In order to understand the spatial pattern of urbanization of Adama Town eleven spatial metrics at class and landscape level were used. These metrics are discussed below. In class metrics; (NP, PD, PAFRAC, CLUMPY, NLSI, PLAND, COHESION, IJI and AI) and in landscape metrics the LPI and LSI was used.

| NP | N | NE | E | SE | S | SW | W | NW |
|---|---|---|---|---|---|---|---|---|
| 1990 | 69 | 193 | 261 | 125 | 161 | 179 | 195 | 29 |
| 2000 | 47 | 196 | 336 | 139 | 137 | 100 | 130 | 35 |
| 2010 | 235 | 462 | 701 | 259 | 260 | 181 | 206 | 74 |
| 2019 | 577 | 484 | 423 | 450 | 878 | 371 | 704 | 349 |

**A. The number of patches**: NP is a type of metrics that describes the growth of particular patches whether in an aggregated or fragmented growth in the region and also explains the underlying urbanization. It ranges from 0 (Clumpiness) to 100 (fragmented). When the number of patches increases the level of fragmentation will increase.

Table 4. 8: Number of patches (Basu Bhatta) between 1990 and 2019 in eight directions

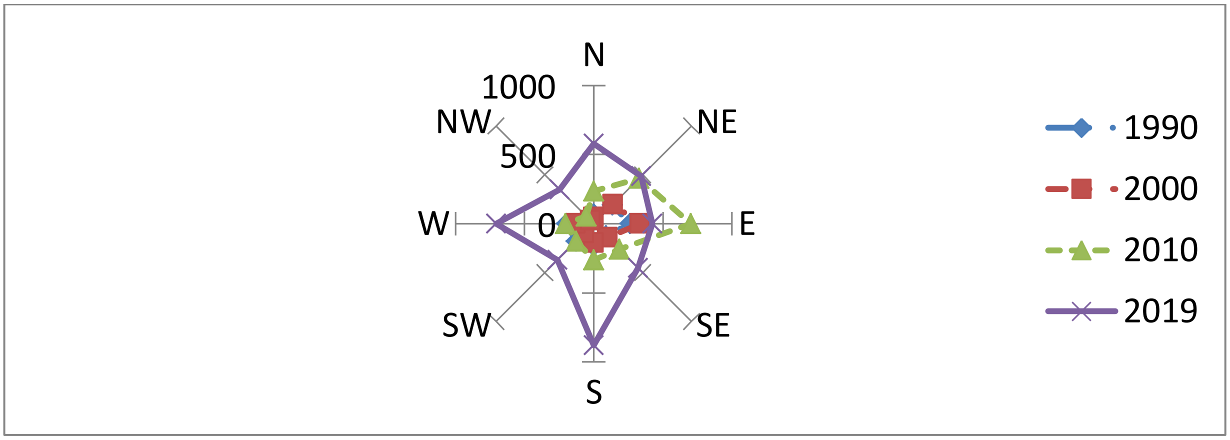


Figure 4. 17: Change in landscape structure described by NP in 8 directions

The number of patches increased between 1990 and 2000 except in the N, S, SW and W direction. While in the second and third period the NP was increased in all directions except during 2019 in E direction. In general, the number of the patches in the study area was increased from 1990 to 2019. Therefore, this shows that the Town is becoming more fragmented.

**B. Patch Density (PD)**: The patch density is quite similar to the number of patch's but gives density about the landscape in analysis as the number patches increase the patch density increases.

Table 4. 9: Patch density (PD) between 1990 and 2019 in eight directions

| Year | N | NE | E | SE | S | SW | W | NW |
|---|---|---|---|---|---|---|---|---|
| 1990 | 1.96 | 5.61 | 6.44 | 3.65 | 3.20 | 4.70 | 4.25 | 1.43 |
| 2000 | 1.34 | 5.69 | 8.30 | 4.06 | 2.72 | 2.63 | 2.83 | 1.73 |
| 2010 | 6.69 | 13.42 | 17.31 | 7.57 | 5.16 | 4.75 | 4.49 | 3.65 |
| 2019 | 16.46 | 14.09 | 10.47 | 13.19 | 17.54 | 9.76 | 15.39 | 17.27 |

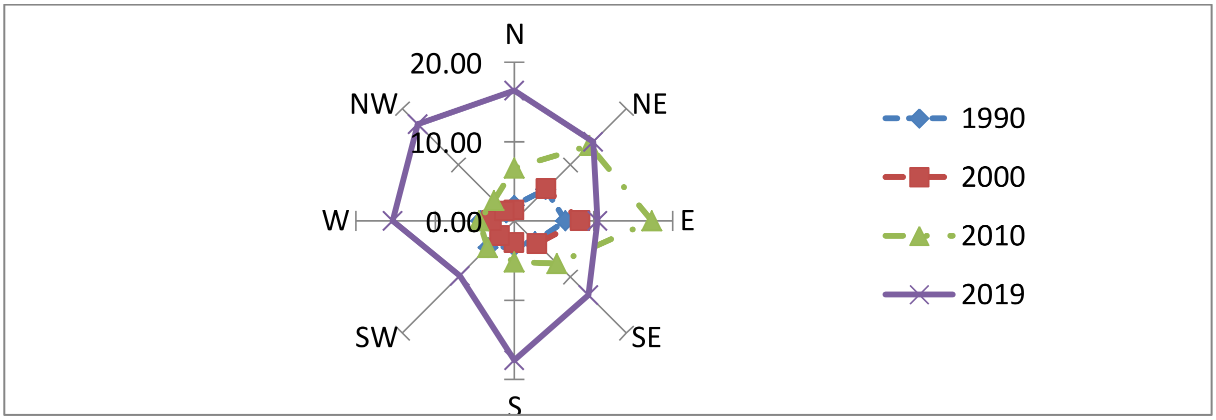


Figure 4.18: Changes in landscape structure described by PD in 8 directions

The results in the Table shows that the PD increased in NE, E and SE directions, while in N, S, SW, and W the PD decreased between 1990 and 2000. During the second period (2000-2010) the PD was increased in all direction. And again, in the third period (2010-2019) the PD increased in all directions. This shows that as the PD increases the level of fragmentation also increases. While during 1990 and 2000 in N and NW directions the PD was minimal means that the patches was clumpy and the study area was less fragmented.

**C. Largest Patch Index (LPI)**: LPI measures the proportion of total landscape area comprised of the largest urban patch at the landscape level. LPI approaches (0) when the largest patch in the landscape is increasingly small. LPI approaches (100) when the entire landscape consists of a single patch; that is, when the largest patch comprises 100 percent of the landscape.

Table 4. 10: Largest patch index (LPI) between 1990 and 2019 in eight directions

| Year/Zone | N | NE | E | SE | S | SW | W | NW |
|---|---|---|---|---|---|---|---|---|
| 1990 | 87.05 | 71.70 | 52.46 | 22.14 | 21.34 | 4.92 | 11.52 | 41.08 |
| 2000 | 87.93 | 65.26 | 54.64 | 25.90 | 53.64 | 50.36 | 32.35 | 80.31 |
| 2010 | 40.79 | 53.86 | 48.59 | 56.96 | 53.63 | 67.00 | 33.82 | 65.29 |
| 2019 | 73.79 | 85.40 | 83.97 | 75.49 | 66.23 | 65.93 | 51.25 | 58.72 |

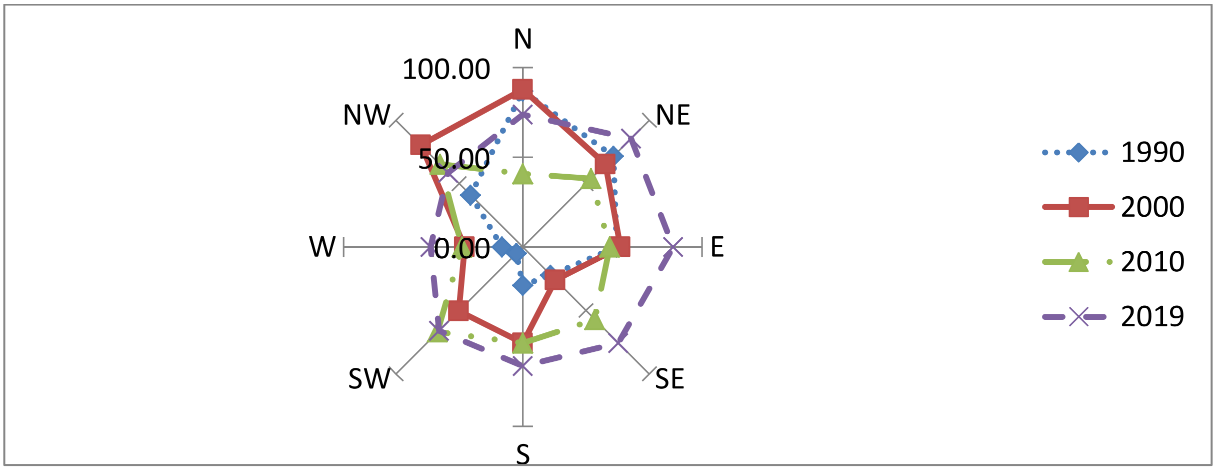


Figure 4.19: Changes in landscape structure described by LP I in 8 directions

The LPI during 1990 and 2000 was maximum especially in N, NE and E directions, while it was minimum in SW and W directions. During 2010 the LPI was increased in all direction except in SW and NW direction. In the third period LPI also increased in all direction except in SW and NW directions indicating considerable growth within the area. However, this tendency changed in the second period, when the size of the LPI decreased. Adama Town has a slower urbanization rate in the second period which is characterized by the appearance of new and dispersed settlements.

**D**. **Landscape Shape Index (LSI**): LSI is one when the landscape consists of a single patch of the corresponding type and is circular (vector) or square (raster); LSI increases without limit as landscape shape becomes more irregular or as the length of edge within the landscape of the corresponding patch type increases or both.

Table 4. 11: landscape shape index (LSI) between 1990 and 2019 in eight directions

| Year/Zone | N | NE | E | SE | S | SW | W | NW |
|---|---|---|---|---|---|---|---|---|
| 1990 | 6.98 | 14.89 | 16.39 | 13.88 | 14.92 | 16.70 | 16.96 | 6.96 |
| 2000 | 9.32 | 16.82 | 22.72 | 15.30 | 15.23 | 13.15 | 15.00 | 5.94 |
| 2010 | 18.04 | 26.08 | 31.99 | 21.43 | 21.46 | 21.68 | 19.29 | 9.36 |
| 2019 | 24.51 | 24.72 | 28.01 | 29.54 | 32.85 | 24.90 | 39.22 | 19.51 |

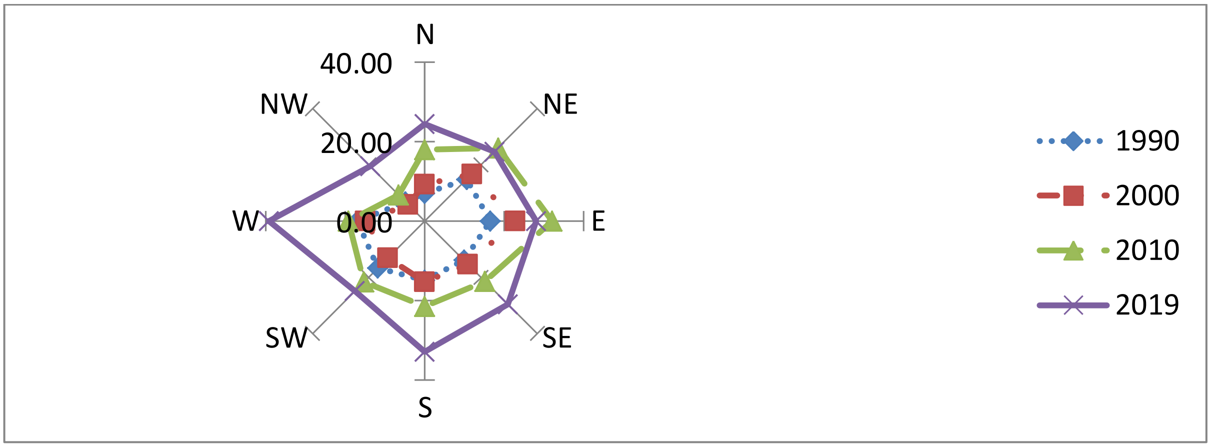


Figure 4. 20: Changes in landscape structure described by LSI in 8 directions

The results in the figure above shows that there were low LSI values in 1990 and 2000 compared to 2010 and 2019 as there were minimal urban areas. However, increasing the value of LSI during 2010 and 2019 in all direction, this suggested that the Town has been experiencing dispersed growth in all direction (the patch type becomes more disaggregated). While in 1990 (N & NW) and in 2000 (NW) was minimal means single square or maximally compact (i.e., almost square).

E. **Perimeter-Area Fractal Dimension (PAFRAC)**: PAFRAC is a patch mosaic provides an index of patch shape complexity across a wide range of spatial scales (i.e., patch sizes) (Fragstats 4.2). PAFRAC approaches 1 for shapes with very simple perimeter such as square (indicating clumping of specific class) and approaches two for shapes with highly convoluted parameters.

Table 4. 12: Perimeter-Area Fractal Dimension (PAFRAC) between 1990 and 2019 in eight directions

| Year/Zone | N | NE | E | SE | S | SW | W | NW |
|---|---|---|---|---|---|---|---|---|
| 1990 | 1.543 | 1.527 | 1.588 | 1.593 | 1.523 | 1.485 | 1.515 | 1.604 |
| 2000 | 1.619 | 1.595 | 1.636 | 1.556 | 1.563 | 1.516 | 1.579 | 1.548 |
| 2010 | 1.585 | 1.589 | 1.591 | 1.624 | 1.529 | 1.562 | 1.564 | 1.441 |
| 2019 | 1.598 | 1.593 | 1.591 | 1.595 | 1.622 | 1.572 | 1.608 | 1.599 |

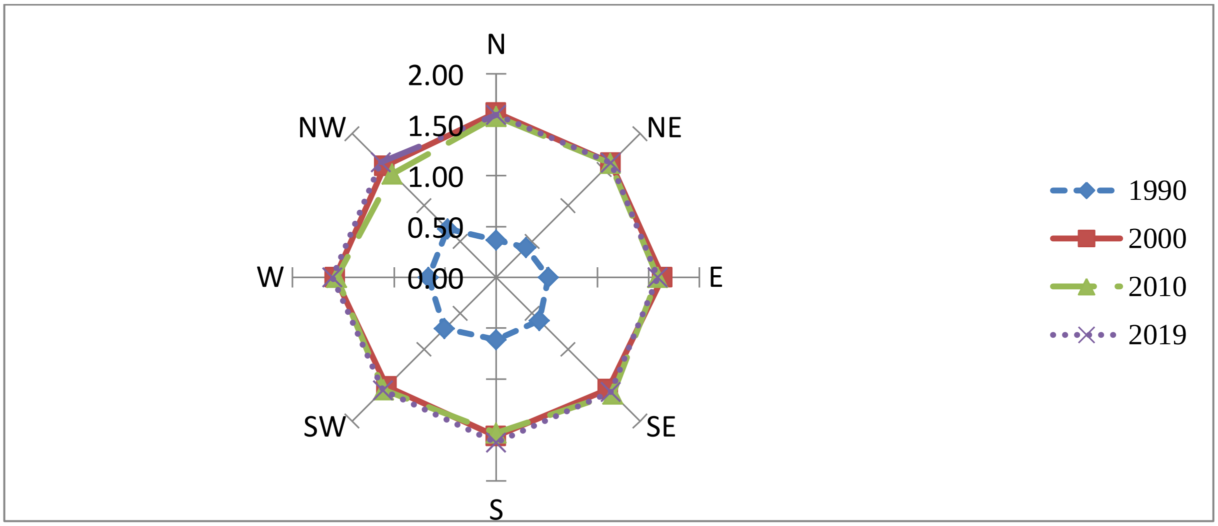


Figure 4.21: Changes in landscape structure described by PAFRAC in 8 directions

The results in the figure below that the shape of the Town was maximum and approach to 2 in all directions during the study period so, according to PAFRAC requirement of definition the shape of the Town was highly convoluted.

**F. Clumpiness Index (CLUMPY)**: Indicates aggregation (when clumpy = 1) or when the patches are distributed randomly (clumpy = 0) of the class in the landscape.

Table 4. 13: Clumpiness index (CLUMPY) between 1990 and 2019 in eight directions

| Year/Zone | N | NE | E | SE | S | SW | W | NW |
|---|---|---|---|---|---|---|---|---|
| 1990 | 0.63 | 0.57 | 0.47 | 0.39 | 0.38 | 0.28 | 0.33 | 0.32 |
| 2000 | 0.63 | 0.49 | 0.46 | 0.47 | 0.51 | 0.46 | 0.39 | 0.50 |
| 2010 | 0.58 | 0.48 | 0.45 | 0.47 | 0.52 | 0.48 | 0.50 | 0.51 |
| 2019 | 0.63 | 0.67 | 0.66 | 0.58 | 0.59 | 0.60 | 0.45 | 0.41 |

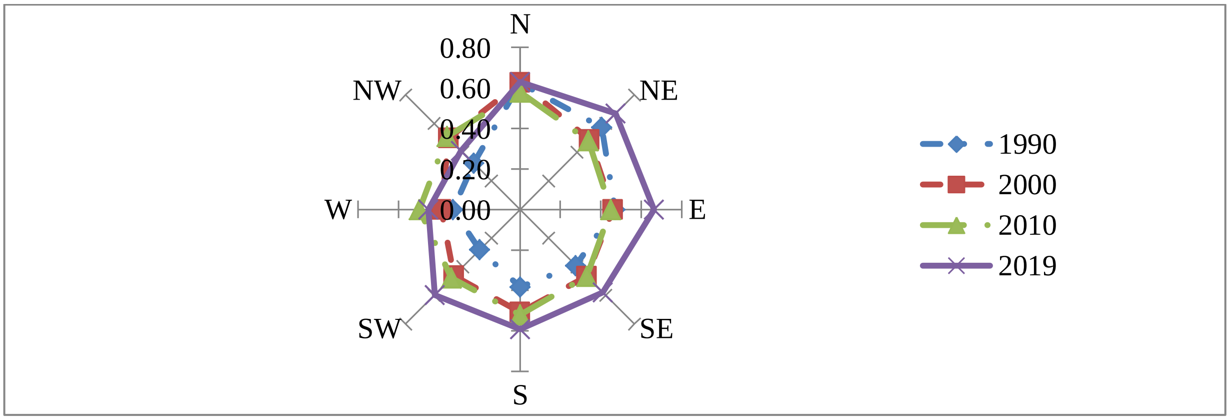


Figure 4.22: Changes in landscape structure described by CLUMPY in 8 directions

Values closer to zero in 1990 in SE, S, SW, N and NW, in 2000 NE, E, SE, SW and W, during 2010 NE, E, SE and SW directions indicates that growth is disaggregated. However, during the 1990's, N and SE, in 2000's N, S and NW, in 2010 N, S, W and NW in all direction in 2019 shows a value close to 1 indicating aggregation.

**G**. **Normalized Shape Index (nLSI):** nLSI is similar to Landscape Shape Index, but this represents the normalized value. nLSI is concerned with the shape and the value ranges from 0 (maximally compact patch) to 1 (disaggregated landscape).

Table 4.14: Normalized Shape Index (nLSI) index between 1990 and 2019 in eight directions

| Year/Zone | N | NE | E | SE | S | SW | W | NW |
|---|---|---|---|---|---|---|---|---|
| 1990 | 0.369 | 0.416 | 0.513 | 0.600 | 0.611 | 0.712 | 0.663 | 0.674 |
| 2000 | 0.368 | 0.500 | 0.517 | 0.521 | 0.488 | 0.533 | 0.605 | 0.498 |
| 2010 | 0.401 | 0.482 | 0.507 | 0.510 | 0.467 | 0.509 | 0.490 | 0.483 |
| 2019 | 0.304 | 0.259 | 0.262 | 0.346 | 0.352 | 0.361 | 0.503 | 0.559 |

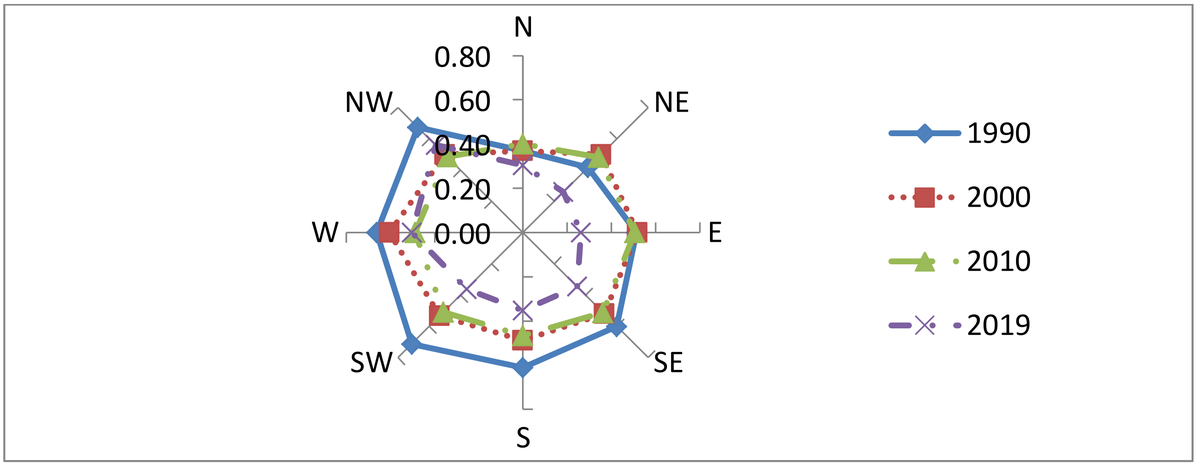


Figure 4. 23: Changes in landscape structure described by nLSI in 8 directions

The result highlights that nLSI values were closer to 1 in all direction except N & NE directions during 1990. nLSI during 2000 there is an increase in all direction. However, nLSI of 2010 and 2019 shows a decreasing value in all direction except E & SW (2010) and W & NW (2019) confirming that these regions are transforming into a compact patch of simple shape.

**H. Proportion of Landscape (PLAND):** PLAND is fundamental measures of landscape composition; specifically, to know how much of the landscape is comprised of a particular patch type. It ranges from 0 to 100 where the value 100 indicates the landscape comprises of a single urban class and zero represents the absence of urban class.

Table 4.15: Proportion of Landscape **(**PLAND) between 1990 and 2019 in eight directions.

| PLAND | N | NE | E | SE | S | SW | W | NW |
|---|---|---|---|---|---|---|---|---|
| 1990 | 1.50 | 2.70 | 2.94 | 1.43 | 0.84 | 0.95 | 1.05 | 0.37 |
| 2000 | 1.43 | 2.52 | 4.10 | 2.10 | 1.21 | 1.03 | 0.95 | 0.56 |
| 2010 | 7.90 | 4.59 | 7.29 | 4.10 | 2.67 | 2.11 | 2.45 | 1.26 |
| 2019 | 17.8 | 21.44 | 22.02 | 17.37 | 13.83 | 10.58 | 8.14 | 5.19 |

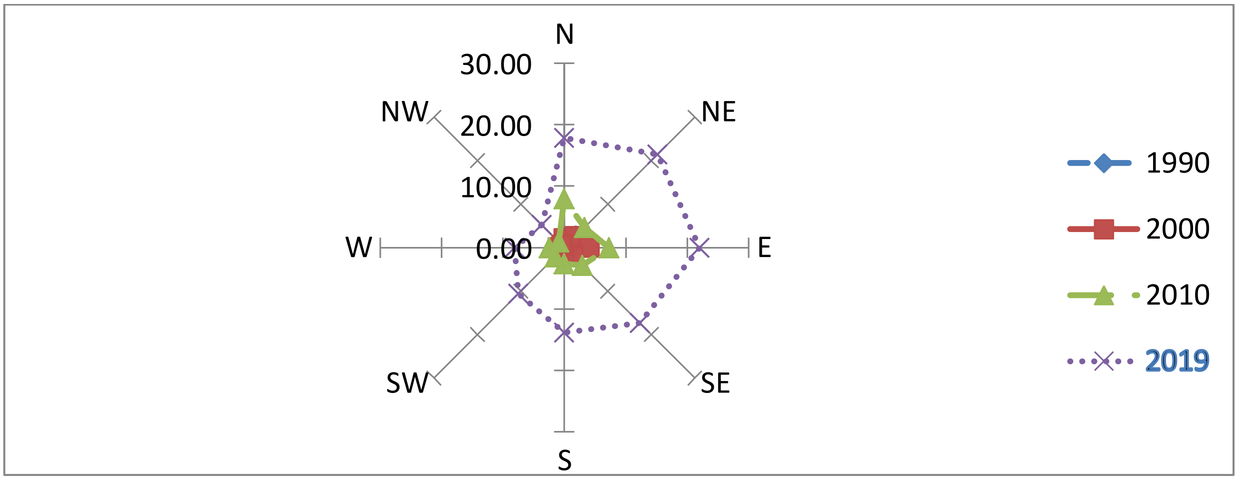


Figure 4. 24: Changes in landscape structure described by PLAND in 8 directions

The results of the analysis are represented in (Fig.4.23), which indicates spurt in urban land use especially during post 2010 in almost all directions except in the W and NW.

**I. Patch Cohesion Index (COHESION):** Cohesion measures the physical connectivity between adjacent patches where the cohesion value 0 indicates disaggregation and no interconnectivity between patches and higher value indicates clumped and connectivity between patches.

Table 4.16: Cohesion index (COHESION) between 1990 and 2019 in eight directions

| Year/Zone | N | NE | E | SE | S | SW | W | NW |
|---|---|---|---|---|---|---|---|---|
| 1990 | 90.39 | 91.46 | 87.95 | 73.92 | 68.70 | 48.45 | 62.50 | 67.27 |
| 2000 | 94.20 | 88.18 | 92.38 | 79.56 | 88.76 | 77.25 | 73.41 | 79.22 |
| 2010 | 90.89 | 93.86 | 92.05 | 92.88 | 92.74 | 85.08 | 86.42 | 77.57 |
| 2019 | 97.79 | 98.54 | 98.57 | 97.94 | 97.12 | 96.12 | 91.53 | 89.16 |

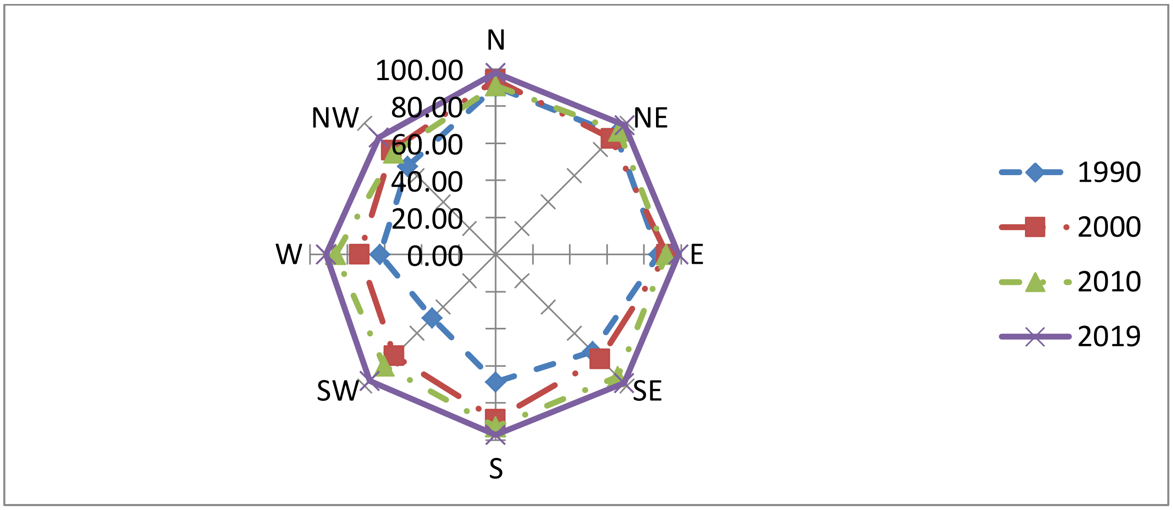


Figure 4.25: Changes in landscape structure described by COHESION in 8 directions

Higher values during post-2000 illustrate of fragmented landscape forming clumped patches in almost all zones (see Fig. 4.13i). While decreasing in the N and NW direction during 2010. Finally, during the study period the town was higher connectivity (clumpy) between patches.

**J. Interspersion and juxtaposition index (IJI).** IJI measures the extents to which patch types are interspersed. Higher values result when the urban patch types are well interspersed (i.e., equally adjacent to each other), whereas lower values characterize landscapes in which the patch types are poorly interspersed i.e., disproportionate distribution of patch type adjacencies (Zhang et al., 2004). IJI approaches 0 when the corresponding patch type is adjacent to only one other patch type and the number of patch types increases. IJI = 100 when the corresponding patch type is equally adjacent to all other patch types (maximally interspersed and juxtaposed to other patch types).

Table 4.17: Interspersion and juxtaposition index (IJI) between 1990 and 2019 in eight directions

| IJI | N | NE | E | SE | S | SW | W | NW |
|---|---|---|---|---|---|---|---|---|
| 1990 | 58.15 | 67.61 | 64.42 | 71.49 | 61.07 | 65.13 | 91.90 | 60.05 |
| 2000 | 51.56 | 63.06 | 54.65 | 66.94 | 51.63 | 65.81 | 83.32 | 74.69 |
| 2010 | 32.94 | 47.64 | 49.60 | 57.75 | 40.05 | 53.83 | 61.49 | 45.99 |
| 2019 | 50.97 | 64.22 | 55.20 | 64.10 | 51.71 | 54.24 | 57.69 | 55.30 |

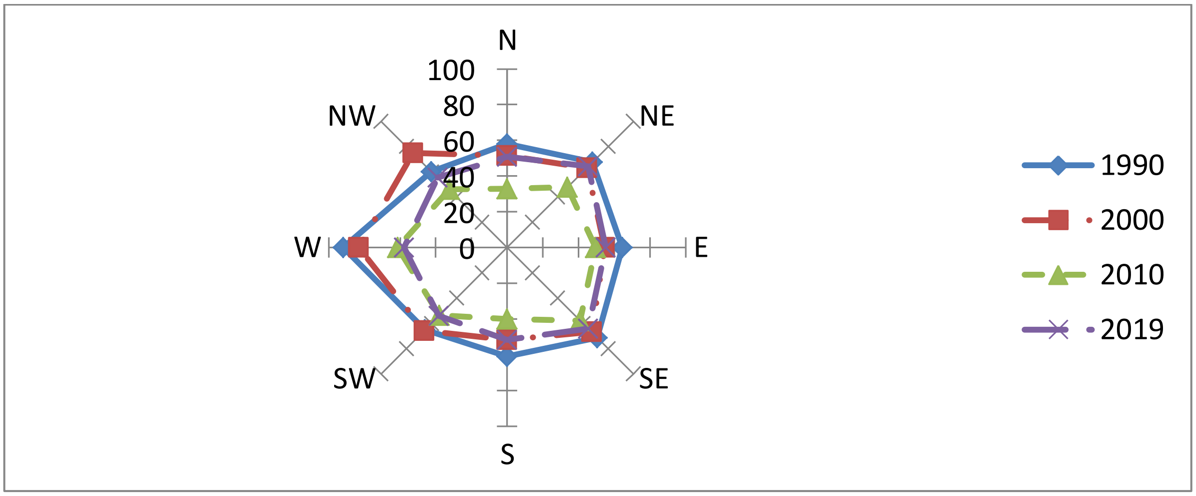


Figure 4. 26:Changes in landscape structure described by IJI in 8 directions

During 1990 and 2000 the town was maximally interspersed in all directions especially in W (91.9), SE (71.48) and W (66.94), NW (74.69) respectively. This shows that the corresponding patch type is equally adjacent to all other patch types (maximally interspersed and juxtaposed to other patch types) compared to other years. The IJI of Adama Town decreased in the second period. This shows that the Town experienced poorly interspersed (disproportionate distribution of patch type adjacencies) while in the third period IJI shows increment.

**K. Aggregation Index (AI)** is a measure of disaggregation or aggregation of a landscape, the metric varies from zero to 100 per cent, values closer to zero indicate disaggregation and values closer to 100 indicate aggregated growth of the urban areas.

Table 4. 18: Aggregation index (AI) between 1990 and 2019 in eight directions

| Year/Zone | N | NE | E | SE | S | SW | W | NW |
|---|---|---|---|---|---|---|---|---|
| 1990 | 63.09 | 58.41 | 48.70 | 39.96 | 38.89 | 28.76 | 33.72 | 32.65 |
| 2000 | 63.16 | 50.03 | 48.27 | 47.95 | 51.23 | 46.75 | 39.48 | 50.22 |
| 2010 | 59.87 | 51.81 | 49.33 | 48.96 | 53.34 | 49.13 | 51.05 | 51.69 |
| 2019 | 69.64 | 74.12 | 73.81 | 65.37 | 64.76 | 63.94 | 49.74 | 44.14 |

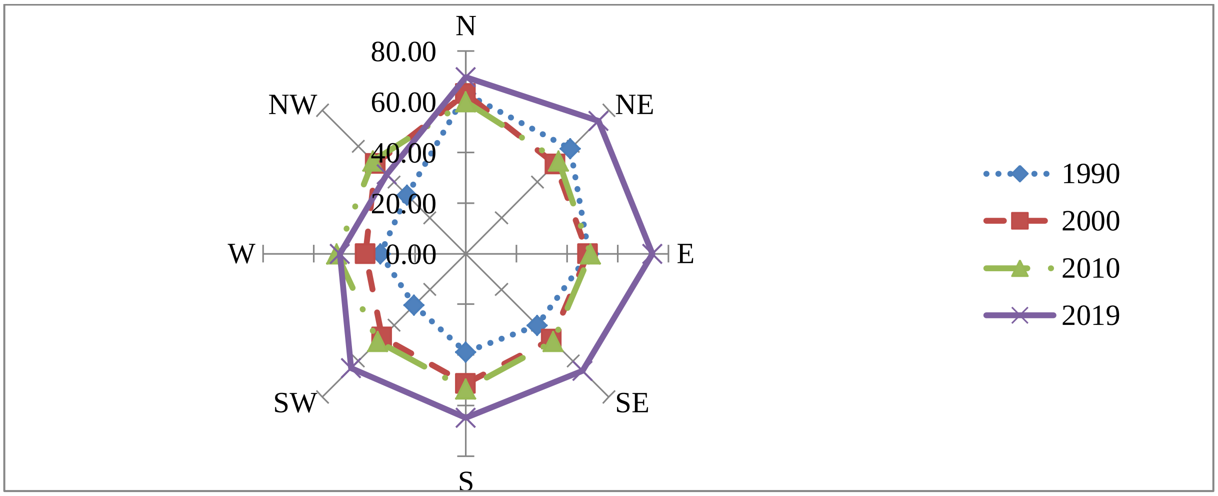


Figure 4. 27: Changes in landscape structure described by AI in 8 directions

Aggregation index indicated that the patches are maximally aggregated between 1900-2010 in N and NE directions and during 2019 in all direction except W and NE. While AI indicated that patches are more dispersed from 1990 to 2010 in all directions except in the N and NE direction. This suggested that the Town is getting more and more compact in the W, NW and N directions (Fig 4.26).

## 4.6. Discussions

### 4.6.1 Land use and land cove dynamics

The findings in the study area shows that a significant decrease in Land cover change occurred from 1990 to 2000 which showed a negative change in almost all of the categories except built up area and fallow land. About 1101.86 ha of vegetation cover has decreased during the first period and it has decreased by 482.7 ha in the second period. While in the third period the vegetation cover showed a positive increase of 1208.20 ha (4.40%, 2.70% and 6.5%) respectively. Bare land, showed a decreasing trend in all the study time period. The expansion rate for built-up area was increased following the development of residential areas for commercial, academic, and business purposes in all the three-time periods from1990 to 2019 105.62 ha (1.80%, and 738.70 ha (7.60%) and 3472.67 ha (14.00%) respectively. Similarly, the fallow land was increased in the first and second period by 4317.89 ha and 1551.63 ha respectively, while in the third period it has decreased by 3143.14 ha. The change in agricultural land was negative during the first and third period by 12.51 ha and 461.82 ha respectively while in the second period the relative change in agricultural land was positive by 192.82 ha.

Similar observations showed a decline in vegetation cover, agricultural land and bare land accompanied by expansion in built-up areas (McGarigal and Marks, 1994; Solomon et al., 2017).

The post-classification comparison result analysis from 1990 to 2019 for change detection revealed that the extent of LULC dynamics occurring in different LULC classes throughout the study time. Adama has experienced substantial increase rates of LULC changes between 1990 and 2019. Most vegetation cover, bare land, and agricultural land from 1990 to 2019 were intensively converted to built-up areas and fallow land.

This study showed that there was a rapid LULC change in study area with vegetation converted to fallow land and bare land to fallow land and built up areas. Our results are in agreement with the findings of numerous studies (Deribew and Wana, 2019)

### 4.6.2. Urban Landscape Structure and Dynamics

The results shown in this study at landscape and class level table in 4.6, Fig 4.4 and Fig 4.5, suggested that the number of patches in the study area was increased from 2538 in 1990 to 4086 in 2019. The highest change of NP was found in bare land areas and increased from 1067 in 1990 to 2023 in 2019 followed by built up area which increased from 159 in 1990 to 715 in 2019 especially in S and E directions. In addition, the patch density was increased from 8.07% in 1990 to 13.02% in 2019. The highest PD was observed for bare land which increased from 3.39% in 1990 to 4.20% in 1990 followed by vegetation areas which increased from 2.50% in 1990 to 2.72% in 2019 especially in the S and SE directions.

The contagion index (CONTAG) increased from 44.48% in 1990 to 50.12% in 2000 and increased to 50.125% in the third period while decreased to 41.07% in 2019.

The largest patch index (LPI) at landscape level significantly increased from 39.21% in 1990 to 57.03% in 2019. The maximum LPI were 75.38 (N) and 70.87 (NW) during 2010 and 2019 respectively. In the bare land, the LPI decreased from 10.21% in 1990 to 3.12% in 2019. The Area-weighted mean fractal dimension index (FRAC_AW) showed a very slight increase in the first period (1900–2000), while a slight decrease in the second period (2000–2010). Similarly, a decrement of value was seen in the third period (2010–2019). This indicates that shape complexity has become more irregular over time and fragmentation processes have strengthened in the first and third period compared to the second period. Human activities, including accelerated urbanization, can result in landscape pattern fragmentation and result in a more complex landscape structure. The larger shape complexity resulted from more complicated spatial configurations in bare land, fallow land and built up areas in all directions. All four vegetated LULC classes had a relatively high shape complexity. The fact that bare land and fallow land influenced the highest value of perimeter-area fractal dimension suggests that the impact of human activities was strong on the pattern of these LULC classes. Shannon's diversity index (SHDI) decreased from 11.11 percent (1.08 to 0.96) between 1990 and 2000, and further 3.1 percent (0.96 to 0.93) between 2000 and 2010. however, SHDI increases 22.6 percent (0.93 to 1.14 between 2010 and 2019. With both of these indices going towards zero, the landscape showed more of aggregation than fragmentation between 1990 and 2000, and 2000 and 2010. SHDI going towards zero while between 2010 and 2019 SHDI was increased. Fragmentation and hence ecological processes in the landscape thus receded between the patch cohesion index (COHESION) showed a slight increment from 1990 to 2000 (0.58), while decreased in the second and third period by 0.01 and 0.13 respectively. The maximum cohesion index for fallow land area from 99.41 in 1990 to 99.73 in 2019. Especially 99.88 (N) in 2010. The overall study reveals that the fallow land comprises the maximum COHESION index in three decades. This showed that the fallow land was more clumped or aggregated in its distribution; hence, more physically connected compared to other classes. The patch cohesion index (COHESION) for the fallow land area was increased from 99.41 in 1990 to 99.80 in 2000, again increased to 99.81 in 2010, while decreased to 99.73 in 2019. The maximum COHESION index for the fallow land area was found to be 99.67(N), 99.83 (W), 99.88 (N) and 99.76 (NW) in 1990, 2000, 2010 and 2019 respectively. The overall study reveals that the fallow land comprises the maximum COHESION index in three decades. This showed that the fallow land was more clumped or aggregated in its distribution; hence, more physically connected compared to other classes.

The increase in landscape pattern metrics shown during the study period were causes of Physical connectivity between patches which resulted in disaggregated or fragmented. Landscape disaggregation processes were supported and increase in shape complexity in the last three decades. This result agrees with the studies performed in china phoenix metropolitan region and in Arizona (Huang et al., 2010).

### 4.6.3. Urban Sprawl Dynamics

Urban sprawl dynamics was analyzed by considering some of the causal factors. The basis behind this is to identify such factors that play a significant role in the urbanization. The causal factors that were considered responsible for sprawl were: population density and urban growth. To identify the sprawl within the study area, a careful comparison of urbanized area expansion and population dynamic using Shannon's entropy were analyzed. The total population within the study area increased by 57.68% in between 1990 and 2000 while urbanized areas increased by 19.61%, in between 2000 and 2010. Population increased by 57.97% and urban growth by 144.60%, between 2010 and 2019 population increased by 64.97% whereas urban growth increased by 251.16%. The comparison clearly indicates that the growth rate of urbanized areas is always higher than the growth rate of population during all the study period except in the first decade.

Adama is experiencing the highest sprawl in all directions during 2019 as entropy values are closer to the threshold value (log 8 = 0.9). Lower entropy values of 0.034(NW), 0.041, 0.045(S & SW) and 0.050 during 1990 and 0.044 (NW), 0.052, 0.051 (W) and 0.056 (S) during 2000 shows an aggregated growth as most of the urbanizations were concentrated at Town Centre. However, the region experienced dispersed growth in 2019 reaching higher values of 0.336 (E), 0.332 (NE), 0.314(N) in 2019. Similar observations also illustrates the extent of influence of drivers of urbanization in various directions (Effat and El Shobaky, 2015; Luck and Wu, 2002). Entropy value has increased from 0.535 in the year 1990 to 0.612 in the year 2000. Further, an increase from 0.612 in the year 2000 to 1.053 in the year 2010 and further increased to 2.203 in 2019. This increase in the value of entropy indicates an increase in dispersion of built-up area, which is an indication of urban sprawl especially during 2019 Adama was faced to urban sprawl compared to other years. The closer to the upper limit of (log n) i.e. 0.9 the more dispersion is the built-up area in the region. A higher value of overall entropy for the whole urban area represents a higher dispersion of impervious area which is a sign of urban sprawl (Sudhira et al., 2004).

### 4.6.4. Spatial Pattern of Urbanization

The present study, has demonstrated that the spatial pattern of urbanization can be quantified using a combination of landscape metrics and zonal analysis.

The number of patches increased between 1990 to 2000 except in N, S, SW and W direction. While in the second and third periods, the NP was increased in all direction except during 2019 in the E direction. In general, the number of the patch in the study area was increased from 1990 to 2019. Therefore, this shows that the Town is becoming more fragmented. The PD was increased in NE, E and SE directions, while in N, S, SW, and W PD was decreased between 1990 and 2000. During the second period i.e. from 2000 to 2010, the PD was increased in all direction and again, in the third period i.e. from 2010 to 2019 the PD was increased in all directions. This showed that as the PD increases, the level of fragmentation also increase. While during 1990 and 2000 in N and NW directions, the PD was minimal showing that the patches were clumpy and the study area was less fragmented.

As the NP and PD were decreased in the Town center it has been seen that spatial pattern of the Town is aggregated around Town centers (Central Business District) while the NP and PD increased in the periphery of the Town this showing an increased level of fragmentation increase. where urbanization and economic activities are more concentrated

The results from table 4.13, showed that in the first period LPI was maximum in the N, NE and E direction while minimum in the SW and W directions. In the second period the LPI was increased from the first period except in the NE direction while in the third period the LPI of the study area was decreased from the second period except SE and S directions.

In the fourth period the LPI was increased in all directions except in SW and NW direction. This shows that LPI of the study area was maximum in N direction during 1990 and 2000 and minimum SW and W direction during 1990. LPI was increased between 1990 and 2000 in all direction except in NE and in the third period LPI was also increased in all directions except in the SW and NW directions indicating a considerable growth within the area. However, this tendency changed in the second period when the size of the LPI decreased except in the SE and SW directions. Although we have a slower urbanization rate in the second period this one is characterized by the appearance of new and dispersed settlements.

LSI during 1990 (N & NW) and 2000 (NW) was low indicating a maximum compactness (i.e., almost square). However, post 2010 especially in NW direction LSI values indicated disaggregated growth. In general, the LSI of Adama Town was increased from 1990 to 2019 in all most all direction except in SW, W and NW direction between (1990 and 2000) this suggested that the Town has been experiencing dispersed growth.

The shape of the Town was maximum and approaches to 2 in all directions during the study period (1990-2019) so, according to PAFRAC requirement of definition the shape of the Town was highly convoluted.

The result highlights that NLSI values were closer to 1 in all direction except N & NE direction during 1990. NLSI during 2000 there is an increase in all direction. However, NLSI of 2010 and 2019 shows a decreasing value in all direction except E & SW (2010) and W & NW (2019) for confirming that these regions are transforming into a compact patch of simple shape.

During 1990 and 2000 the Town was maximally interspersed in all directions especially in W (91.9), SE (71.48) and W (66.94), NW (74.69) respectively. This shows that the corresponding patch type is equally adjacent to all other patch types (maximally interspersed and juxtaposed to other patch types) compared to other years. The IJI of Adama town was decreased in the second period, this shows that the Town was experienced poorly interspersed (disproportionate distribution of patch type adjacencies).

Aggregation index indicated that the patches are maximally aggregated between 1900-2010 in N, NE direction and during 2019 in all direction except W and NEW. While AI indicated that patches are more dispersed from (1990 to 2010) in all direction except N and NE direction. (Aithal and Ramachandra, 2012; Luck and Wu, 2002; Ramachandra et al., 2012).

Urbanization in the Adama Town has resulted in increases in patch density, NP, and landscape shape complexity, sharp decreases in the largest patch and landscape connectivity (Fig 4.5-4.7). The spatial pattern of urbanization revealed here was that the increasingly urbanized landscape became compositionally diverse, geometrically complex, and ecologically more fragmented.

Most previous studies on spatial pattern of urbanization have focused based on the landscape metrics and gradient analysis and have shown the trends towards the center the aggregation and landscape connectivity increase while towards the periphery decreased.

# 5. CONCLUSION AND RECOMMENDATION

## 5.1 Conclusion

- Spatio- temporal data integrated with GIS and RS were used to quantitatively analyze the time series changes of land use and landscape pattern in Adama Town. Four years of data from 1990 to 2019 were interpreted to obtain land-use changes. The Classification results show a reduction in agricultural land in the first and second period while increase with corresponding increases in residential area in between 1990 and 2019. The study has shown that urban land use change has profound impact on urban Landscape especially in the S and E directions during the entire study periods.
- The increase in landscape pattern metrics during the study period was because of the fact that fragmentation of the landscape tended to strengthen and the spatial variability of the landscape increased in Adama Town in the last three decades. Moreover, the landscape pattern structure became more complex, as discerned in the following landscape metric changes from 1990 to 2019. Human activities, including urban expansion and population growth, can result in landscape pattern fragmentation and result in a more complex landscape structure.
- The urban population growth rate has less than the urban growth of Adama Town in the second and third period. The total population within the study area was increased by 57.68% between 1990 and 2000, although urbanized areas increased by 19.61%. In between 2000 and 2010 population increased by 57.97% and urban growth increased by 144.60% and in between 2010 and 2019. Population increased by 64.97% whereas urban growth increased by 251.16%. Urban sprawl is evidenced from the current study that Adama town is maximally sprawl post 2010 especially in E (2010) and S (2019).
- The spatial metrics further confirmed that the phenomenon of dispersed growth was shown at outskirts of the Town while compacted growth at the center especially during 2010 (S) and in 2019 (S) and (W) directions. This is because of urbanization which is attributed to population growth and urban growth.

## 5.2 Recommendations

- Urban land use and planning policy direction should be revised based on the status of Landscape pattern.
- There should be redevelopment activities in the coming decade for improving the urban problems related to sprawling.
- FRAGSTATS is efficient software for calculating landscape metrics.

## REFFERENCES


Aithal, B. H., & Ramachandra, T. (2012). *Modelling the Spatial Patterns of Landscape dynamics: Review*. Retrieved from

Araya, Yikalo H Cabral, Pedro (2010). Analysis and modeling of urban land cover change in Setúbal and Sesimbra, Portugal: Remote Sensing

Ashkenazi, & Frenkel. (2008). Measuring urban sprawl: how can we deal with it? *Environ. Plan*, 56–79.

Bajracharya, Ashim Ratna Rai, Ritu Raj Rana, Shreema (2015). Effects of urbanization on storm water run-off: a case study of Kathmandu Metropolitan City, Nepal. Journal of the Institute of Engineering

Batty, Michael Besussi, Elena Chin, Nancy. (2003). Traffic, urban growth and suburban sprawl

Barnes, Kent B Morgan III, John M Roberge, Martin C Lowe, Shannon (2001). Sprawl development: Its patterns, consequences, and measurement: Towson University, Towson

Belay, T., & Mengistu, D. A. (2019). Land use and land cover dynamics and drivers in the Muga watershed, Upper Blue Nile basin, Ethiopia. *Remote Sensing Applications: Society and Environment, 15*, 100249.

Bhatta, B. (2009). Analysis of urban growth pattern using remote sensing and GIS: a case study of Kolkata, India. *International Journal of Remote Sensing, 30*(18), 4733-4746.

Bhatta, B. (2010). *Analysis of urban growth and sprawl from remote sensing data*: Springer Science & Business Media.

Brockerhoff, M. (2000). *An urbanizing world*: Population Reference Bureau.

Butt, A., Shabbir, R., Ahmad, S. S., & Aziz, N. (2015). Land use change mapping and analysis using Remote Sensing and GIS: A case study of Simly watershed, Islamabad, Pakistan. *The Egyptian Journal of Remote Sensing and Space Science, 18*(2), 251-259.

Calvo-Iglesias, María Silvia, Fra-Paleo, Urbanos Diaz-Varela, Ramón Alberto (2009). Changes in farming system and population as drivers of land cover and landscape dynamics: the case of enclosed and semi-open field systems in Northern Galicia (Spain): Landscape and Urban Planning.

Christiansen, Petter Loftsgarden, Tanja (2011). Drivers behind urban sprawl in Europe:

Dadras, Mohsen Shafri, MohdZulhaidi, Helmi Ahmad, Noordin Pradhan, Biswajeet Safarpour, Sahabeh. (2014). Land use/cover change detection and urban sprawl analysis in Bandar Abbas City, Iran: The Scientific World Journal

Dasgupta, A., Kumar, U., & Ramachandra, T. (2009). *Urban Landscape analysis through spatial metrics.* Paper presented at the Proceedings of International Conference on Infrastructure, Sustainable Transportation and Urban Planning,(CISTUP@ CiSTUP), Indian Institute of Science, Bangalore, India.

De Leeuw, Jan Jia, H Yang, L Liu, X Schmidt, K Skidmore, AK (2006). Comparing accuracy assessments to infer superiority of image classification methods : International Journal of Remote Sensing

de Wit, S. (2016). Sensory landscape experience: Stepping outside the visual landscape of the motorway in the Garden of Birds. *Journal of Landscape Architecture, 11*(3), 20-31.

Deribew, K., & Wana, D. (2019). Land use and forest cover dynamics in the North-eastern Addis Ababa, central highlands of Ethiopia. *Environmental Systems Research, 8*. doi:10.1186/s40068-019-0137-1

Division, U. N. S. (2000). *The World's Women, 2000: Trends and Statistics* (Vol. 16): United Nations Publications.

Duda, R. O., Hart, P. E., & Stork, D. G. (2001). Pattern classification. *International Journal of Computational Intelligence and Applications, 1*, 335-339.

Effat, H. A., & El Shobaky, M. A. (2015). Modeling and mapping of urban sprawl pattern in Cairo using multi-temporal landsat images, and Shannon's entropy. *Advances in Remote Sensing, 4*(04), 303.

Fenta, A. A., Yasuda, H., Haregeweyn, N., Belay, A. S., Hadush, Z., Gebremedhin, M. A., & Mekonnen, G. (2017). The dynamics of urban expansion and land use/land cover changes using remote sensing and spatial metrics: the case of Mekelle City of northern Ethiopia. *International Journal of Remote Sensing, 38*(14), 4107-4129.

Frenkel, A., & Ashkenazi, M. (2008). Measuring urban sprawl: how can we deal with it? *Environment and Planning B: Planning and Design, 35*(1), 56-79.

Galster, George Hanson, Royce Ratcliffe, Michael R Wolman, Harold Coleman, Stephen Freihage, Jason (2001). Wrestling sprawl to the ground: defining and measuring an elusive concept: Housing policy debate

Gebregergis, Weldegebriel Mebrahtu Gebre, Habtamu Atelaw Badesso, Barana Babiso. (2016). Dynamics of Land Use Land Cover Change and Urbanization in Jigjiga Town, Ethiopian Somali Regional State, Eastern Ethiopia

Gustafson, E. J. (1998). Quantifying landscape spatial pattern: what is the state of the art? *Ecosystems, 1*(2), 143-156.

Haregewoin, B. (2005). Urbanization and Urban sprawl.

Herold, M., Couclelis, H., & Clarke, K. C. (2005). The role of spatial metrics in the analysis and modeling of urban land use change. *Computers, environment and urban systems, 29*(4), 369-399.

Houet, T., Verburg, P. H., & Loveland, T. R. (2010). Monitoring and modelling landscape dynamics. *Landscape ecology, 25*(2), 163-167.

Huang, J., Lin, J., & Tu, Z. (2010). Detecting spatiotemporal change of land use and landscape pattern in a coastal gulf region, southeast of China. *Environment, development and sustainability, 12*(1), 35-48.

Inostroza, L., Baur, R., & Csaplovics, E. (2013). Urban sprawl and fragmentation in Latin America: A dynamic quantification and characterization of spatial patterns. *Journal of environmental management, 115*, 87-97.

Jaeger, Jochen AG. (2000). Landscape division, splitting index, and effective mesh size: new measures of landscape fragmentation: Landscape ecology

Jat, M. K., Garg, P. K., & Khare, D. (2008). Monitoring and modelling of urban sprawl using remote sensing and GIS techniques. *International journal of Applied earth Observation and Geoinformation, 10*(1), 26-43.

Jansen, Louisa JM Di Gregorio, Antonio (2002). Parametric land cover and land-use classifications as tools for environmental change detection: Agriculture, Ecosystems & Environment

Kaeli, David R Mistry, Perhaad Schaa, Dana Zhang, Dong Ping (2015). Heterogeneous computing with OpenCL 2.0

Kumar, Mukesh Denis, Derrick M Singh, Sudhir Kumar Szabó, Szilárd Suryavanshi, Shakti. (2018). Landscape metrics for assessment of land cover change and fragmentation of a heterogeneous watershed: Remote Sensing Applications: Society and Environment

Lamine, S., Petropoulos, G. P., Singh, S. K., Szabó, S., Bachari, N. E. I., Srivastava, P. K., & Suman, S. (2018). Quantifying land use/land cover spatio-temporal landscape pattern dynamics from Hyperion using SVMs classifier and FRAGSTATS®. *Geocarto international*, *33*(8), 862-878.

Luck, M., & Wu, J. (2002). A gradient analysis of urban landscape pattern: a case study from the Phoenix metropolitan region, Arizona, USA. *Landscape ecology, 17*(4), 327-339.

MacLean, Meghan Graham Congalton, Russell G. (2015). A comparison of landscape fragmentation analysis programs for identifying possible invasive plant species locations in forest edge: Landscape ecology

Mahamud, M. A., Samat, N., & Noor, N. M. (2016). Identifying factors influencing urban spatial growth for the George Town Conurbation. *PLANNING MALAYSIA JOURNAL, 14*(5).

McGarigal, K. (2002). FRAGSTATS: Spatial Pattern Analysis Program for Categorical Maps. Computer software program produced by the authors at the University of Massachusetts, Amherst. *http://www. umass. edu/landeco/research/fragstats/fragstats. html*.

McGarigal, K., & Marks, B. J. (1994). FRAGSTATS. Spatial pattern analysis program for quantifying landscape structure. Version 2.0. *Forest Science Department, Oregon State University, Corvallis, 67*.

McGarigal, K., & Marks, B. J. (1995). FRAGSTATS: spatial pattern analysis program for quantifying landscape structure. *Gen. Tech. Rep. PNW-GTR-351. Portland, OR: US Department of Agriculture, Forest Service, Pacific Northwest Research Station. 122 p, 351*.

Meinel, Gotthard Lippold, Regin Netzband, Maik (1997). The potential use of new high-resolution satellite data for urban and regional planning

Mdemu, M., Kashaigili, J., Lupala, J., Levira, P., Liwenga, E., Nduganda, A., & Mwakapuja, F. (2012). *Dynamics of land use and land cover changes in the Pugu and Kazimzumbwi Forest Reserves*. Retrieved from

O'neill, R., Krummel, J., Gardner, R. e. a., Sugihara, G., Jackson, B., DeAngelis, D., . . . Christensen, S. (1988). Indices of landscape pattern. *Landscape ecology*, *1*(3), 153-162.

Puyravaud, Jean-Philipp Dufour, Céline Aravajy, Subramanian (2003). Rain forest expansion mediated by successional processes in vegetation thickets in the Western Ghats of India

Ramachandra, T., Aithal, B. H., & Sreekantha, S. (2012). Spatial metrics based landscape structure and dynamics assessment for an emerging Indian megalopolis. *facilities, 1*(1).

Ramachandra, T., Bharath, H., & Sowmyashree, M. (2013). Analysis of spatial patterns of urbanisation using geoinformatics and spatial metrics. *Theoretical and Empirical Researches in Urban Management*, *8*(4), 5-24.

Rai, Raju Zhang, Yili Paudel, Basanta Acharya, Bipin Basnet, Laxmi. (2018). Land use and land cover dynamics and assessing the ecosystem service values in the trans-boundary Gandaki River Basin, Central Himalayas: Sustainability

Riitters, K. H., O'neill, R., & Jones, K. (1997). Assessing habitat suitability at multiple scales: a landscape-level approach. *Biological Conservation*, *81*(1-2), 191-202.

Serneels, S., & Lambin, E. F. (2001). Proximate causes of land-use change in Narok District, Kenya: a spatial statistical model. *Agriculture, Ecosystems & Environment, 85*(1-3), 65-81.

Singh, S. K., Srivastava, P. K., Szabó, S., Petropoulos, G. P., Gupta, M., & Islam, T. (2017). Landscape transform and spatial metrics for mapping spatiotemporal land cover dynamics using Earth Observation data-sets. *Geocarto international*, *32*(2), 113-127.

Solomon, N., Birhane, E., Tadesse, T., Treydte, A. C., & Meles, K. (2017). Carbon stocks and sequestration potential of dry forests under community management in Tigray, Ethiopia. *Ecological processes, 6*(1), 20.

Srivastava, P. K., Han, D., Rico-Ramirez, M. A., Bray, M., & Islam, T. (2012). Selection of classification techniques for land use/land cover change investigation. *Advances in Space Research*, *50*(9), 1250-1265.

Sudhira, H., Ramachandra, T., & Jagadish, K. (2004). Urban sprawl: metrics, dynamics and modelling using GIS. *International journal of Applied earth Observation and Geoinformation*, *5*(1), 29-39.

Tewolde, M. G., & Cabral, P. (2011). Urban sprawl analysis and modeling in Asmara, Eritrea. *Remote Sensing, 3*(10), 2148-2165.

Verburg, PH (2001). The conversion of land use and its effects (CLUE): An assessment for China

Walz, Ulrich (2011). Landscape structure, landscape metrics and biodiversity: Living reviews in landscape research

Weijers, D. (2012). The suitability of GIS methods for analyzing urban sprawl, and the influence of scale:

Wu, J., Jenerette, G. D., Buyantuyev, A., & Redman, C. L. (2011). Quantifying spatiotemporal patterns of urbanization: The case of the two fastest growing metropolitan regions in the United States. *Ecological Complexity, 8*(1), 1-8.

Zhang, L., Wu, J., Zhen, Y., & Shu, J. (2004). RETRACTED: A GIS-based gradient analysis of urban landscape pattern of Shanghai metropolitan area, China: Elsevier.

Zhou, W., Pickett, S. T., & Cadenasso, M. L. (2017). Shifting concepts of urban spatial heterogeneity and their implications for sustainability. *Landscape ecology, 32*(1), 15-30.

Zipperer, W. C., Wu, J., Pouyat, R. V., & Pickett, S. T. (2000). The application of ecological principles to urban and urbanizing landscapes. *Ecological applications, 10*(3), 685-688.

**ANNEX A1. Overall change of land use land cover with 2 km buffer**

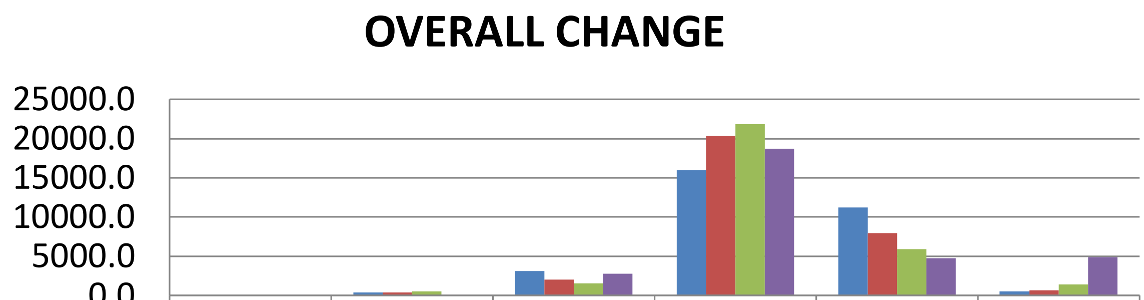


| | Water | Agriculture | Vegetation | Fallow Land | Bare Land | Built UP |
|---|---|---|---|---|---|---|
| Area 1990 | 83.8 | 365.8 | 3113.2 | 15993.3 | 11209.3 | 538.7 |
| Area 2000 | 57.1 | 353.3 | 2011.3 | 20311.2 | 7926.8 | 644.3 |
| Area 2010 | 103.9 | 546.1 | 1528.6 | 21862.8 | 5879.9 | 1382.7 |
| Area 2019 | 135.8 | 84.3 | 2736.8 | 18719.7 | 4772.1 | 4855.3 |

**ANNEX A2. Stratified random sampling for LULC**

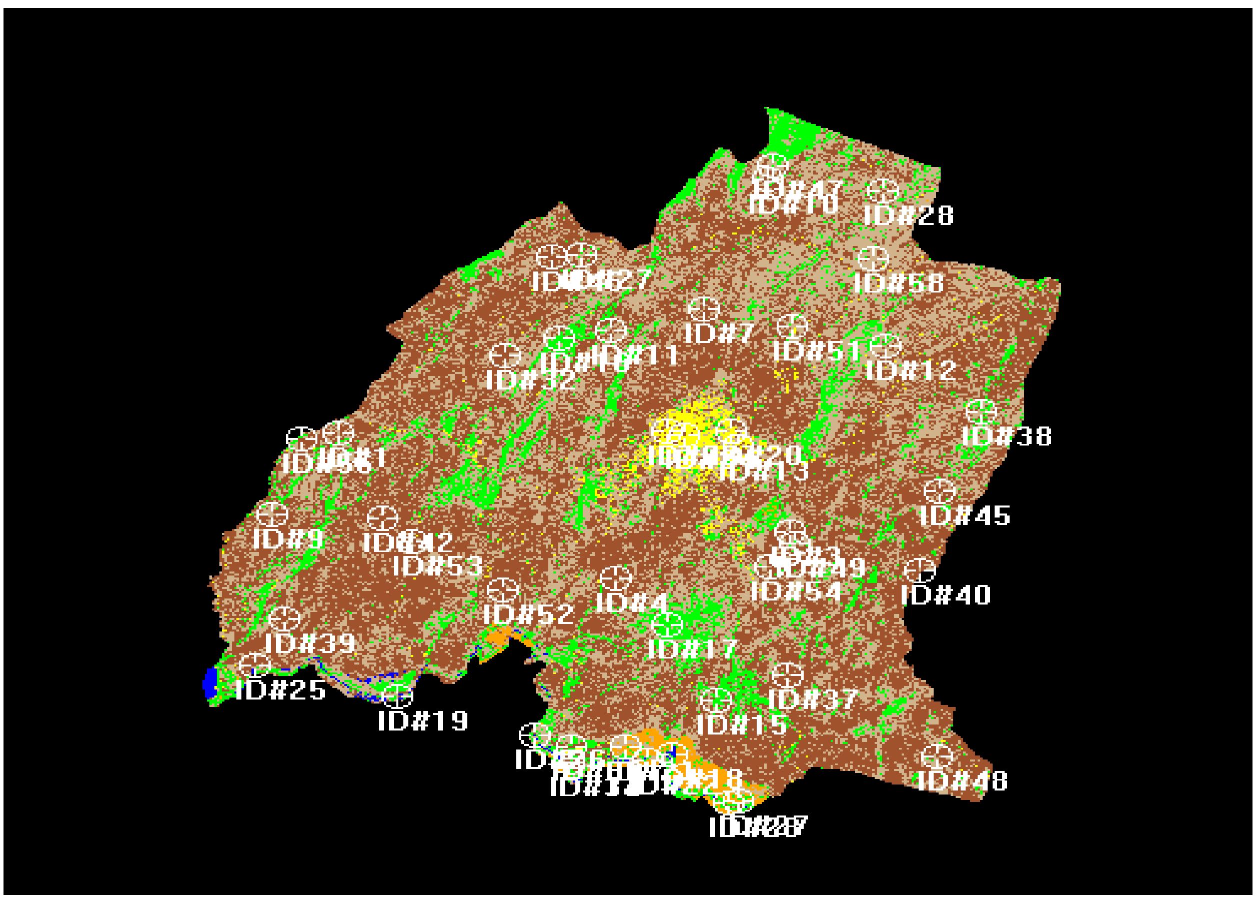

**ANNEX A3. Cardinal direction**

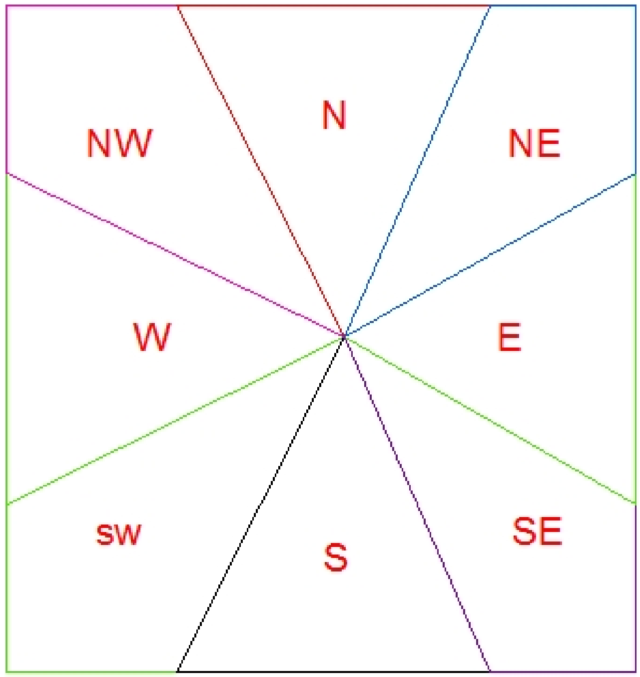


**ANNEX 5. Urban sprawl with 2 km buffer**

| Zone | urban area in km^2 | | | | Area of districts | urban density with 2km buffer | | | | pi logepi | | | |
|---|---|---|---|---|---|---|---|---|---|---|---|---|---|
| | 1990 | 2000 | 2010 | 2019 | km^2 | 1990 | 2000 | 2010 | 2019 | 1990 | 2000 | 2010 | 2019 |
| N | 0.82 | 0.80 | 2.01 | 7.83 | 63.25 | 0.01 | 0.01 | 0.03 | 0.12 | 0.06 | 0.06 | 0.11 | 0.26 |
| NE | 1.46 | 1.24 | 3.19 | 8.62 | 58.16 | 0.03 | 0.02 | 0.05 | 0.15 | 0.09 | 0.08 | 0.16 | 0.28 |
| NW | 0.14 | 0.25 | 0.40 | 1.50 | 36.22 | 0.00 | 0.01 | 0.01 | 0.04 | 0.02 | 0.03 | 0.05 | 0.13 |
| S | 0.80 | 1.00 | 1.76 | 8.45 | 78.86 | 0.01 | 0.01 | 0.02 | 0.11 | 0.05 | 0.06 | 0.08 | 0.24 |
| SE | 0.70 | 0.96 | 1.80 | 7.15 | 57.34 | 0.01 | 0.02 | 0.03 | 0.12 | 0.05 | 0.07 | 0.11 | 0.26 |
| SW | 0.64 | 0.74 | 1.26 | 5.73 | 67.62 | 0.01 | 0.01 | 0.02 | 0.08 | 0.04 | 0.05 | 0.07 | 0.21 |
| E | 1.49 | 1.85 | 3.83 | 10.12 | 65.02 | 0.02 | 0.03 | 0.06 | 0.16 | 0.09 | 0.10 | 0.17 | 0.29 |
| W | 0.61 | 0.55 | 1.35 | 7.19 | 72.82 | 0.01 | 0.01 | 0.02 | 0.10 | 0.04 | 0.04 | 0.07 | 0.23 |

# ANNEX 6. Google Earth Image